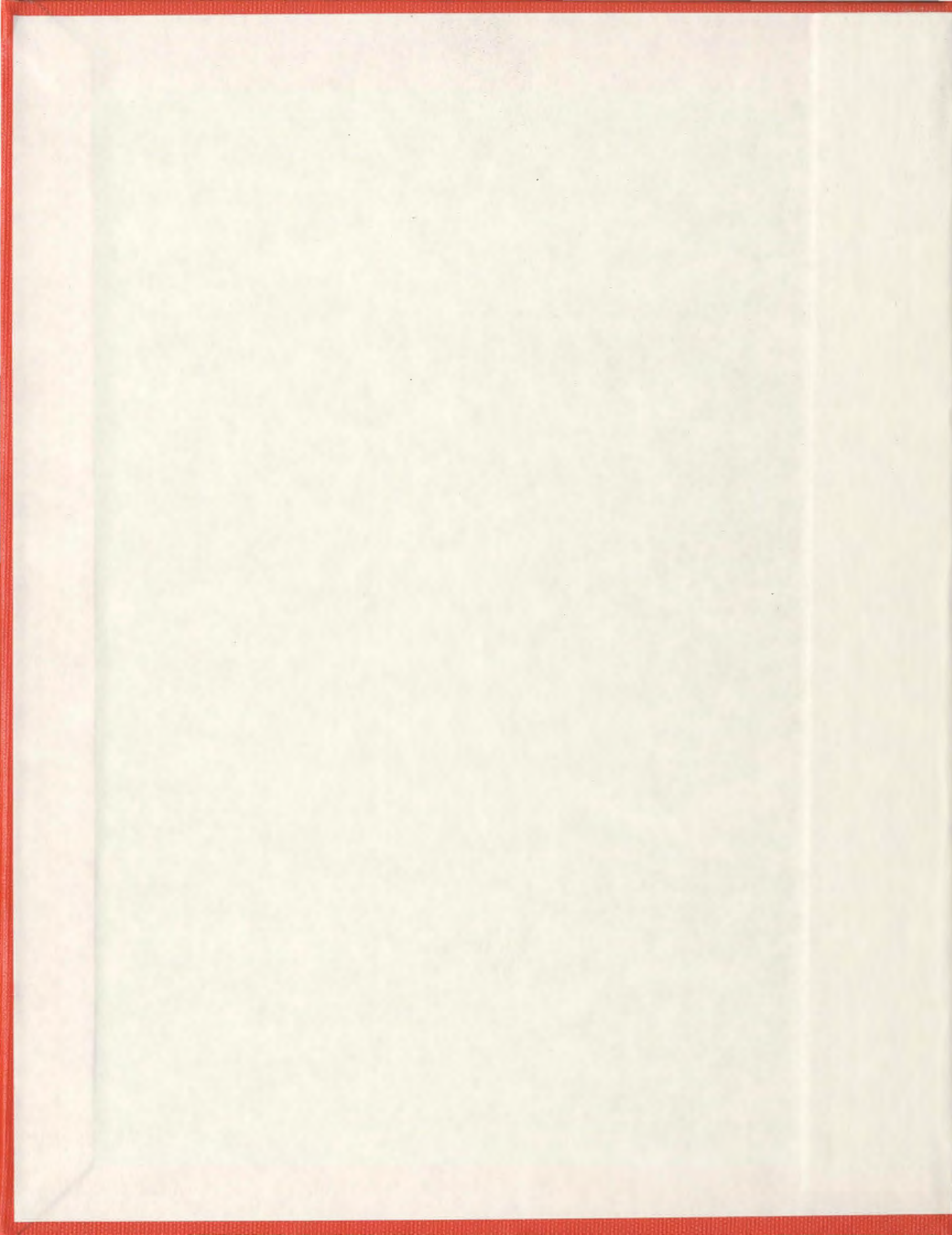


**METHODS FOR IMPROVING POWER SYSTEM  
TRANSIENT STABILITY PERFORMANCE**

**XIDUAN LU**







# **Methods for Improving Power System Transient Stability Performance**

by

© Xijuan Lu, B. Eng.

A Thesis submitted to the School of Graduate Studies

in partial fulfillment of the requirements

for the degree of Master of Engineering

**Faculty of Engineering and Applied Science**

Memorial University of Newfoundland

**March 2013**

St. John's

Newfoundland

Canada

# Abstract

As the power system operation safety and continuity are emphasized by electric power utilities, the transient stability performance of power systems becomes a common topic studied by many researchers. This thesis focuses on three different methods on power system transient stability enhancement. Different systems and fault scenarios are simulated and discussed to support the conclusions. First, the concepts of “power system stability” and “power system transient stability” are introduced. And then, the methods of fast fault clearing, high speed excitation systems, and the Static VAR Compensator (SVC) reactive power support are explained in details with a series of case studies. Finally, an SVC allocation method based on simplified sensitivity analysis is also presented, which validates the effect from SVCs on the power system transient stability improvement and the transient bus voltage sag problem. The thesis also presents the optimized allocation of SVCs based on the transient voltage sags.

# Acknowledgements

I would like to extend my sincere immense gratitude and appreciation to my supervisor Dr. Benjamin Jeyasurya for his useful suggestions and guidance on my research and the thesis writing. I am deeply grateful for his help during my graduate program to pursue my M.Eng Degree.

I express my great gratitude to my father, mother, and grandparents for their love and support. Also, I take this opportunity to thank all my friends in Canada and China for their encouragement and help. All these supports help to turn this work into reality.

Finally, I owe a special gratitude to Memorial University of Newfoundland and NSERC for the financial support, which enables the research to be completed. Many thanks are also given to the Faculty of Engineering and Applied Science and the Elizabeth II Library for the research resource provided.

# Contents

<b>Abstract.....</b>	<b>i</b>
<b>Acknowledgements .....</b>	<b>ii</b>
<b>List of Figures.....</b>	<b>ix</b>
<b>List of Tables .....</b>	<b>xv</b>
<b>List of Abbreviations and Symbols .....</b>	<b>xvii</b>
<b>1 Introduction.....</b>	<b>1</b>
1.1 Objective of Research .....	2
1.2 Organization of Thesis .....	2
<b>2 Power System Stability and Transient Stability .....</b>	<b>5</b>
2.1 Introduction.....	5
2.2 Overview of Power System Transient Stability Concept and System Operation requirements.....	5
2.3 Definition and Classification of Power System Stability .....	7

2.4	Power System Transient Stability.....	9
2.5	System Protection and Assessment of System Transient Stability.....	11
2.6	Transient Stability Simulation Software.....	12
2.7	Conclusion.....	14
<b>3</b>	<b>Transient Stability Enhancement through Fast Fault Clearing.....</b>	<b>15</b>
3.1	Introduction.....	15
3.2	The Swing Equations.....	16
3.3	The Equal-Area Criterion.....	22
3.4	Clearing Time Control.....	28
3.5	Generator Model Introduction.....	29
3.5.1	Classical (GENCL) Model.....	29
3.5.2	GENROU Model.....	31
3.6	Case Studies.....	33
3.6.1	Three-Bus System (One Machine to Infinite Bus System).....	34
3.6.2	Nine-Bus System.....	36

3.6.3	37 - Bus System .....	38
3.7	Conclusion .....	42
<b>4</b>	<b>Transient Stability Enhancement through High Speed Excitation.....</b>	<b>43</b>
4.1	Introduction.....	43
4.2	Typical Excitation System .....	44
4.3	Classification of the Excitation Systems and Auxiliary Systems .....	50
4.4	Fast Acting Excitations' Contribution to Transient Stability .....	54
4.5	Power System Stabilizer (PSS).....	56
4.6	Case studies.....	58
4.6.1	One Generator Connected to an Infinite Bus System .....	58
4.6.2	Nine-Bus System .....	63
4.7	Conclusion .....	66
<b>5</b>	<b>Static VAR Compensator and its Contribution to Transient Stability</b>	
	<b>Improvement.....</b>	<b>68</b>
5.1	Introduction.....	68

5.2	Flexible AC Transmission System.....	69
5.3	Static VAR Compensator (SVC) .....	71
5.3.1	Definition and Significance of SVC .....	71
5.3.2	Configurations and Characteristics of SVC .....	72
5.3.3	SVC Model .....	75
5.3.4	Effects of SVC .....	78
5.4	Case study: Transient Stability Enhancement with SVC.....	79
5.5	Case Study: Transient Stability Enhancement Evaluation in a Two Area Power System.....	83
5.6	Conclusion .....	88

<b>6</b>	<b>Static VAR Compensator (SVC) Allocation and its Influence on Transient Stability Improvement .....</b>	<b>89</b>
6.1	Introduction.....	89
6.2	Transient Stability Improvement Function of SVC .....	90
6.3	SVC Allocation .....	93
6.4	Allocation of SVCs by Sensitivity Analysis.....	94

6.4.1	Sensitivity Analysis and its Simplification .....	94
6.4.2	Calculation of Sensitivity Index.....	96
6.4.3	Algorithm of the Fast SVC Allocation Method based on Simplified Sensitivity Analysis .....	98
6.5	Case Study: New – England 39 - Bus System .....	100
6.5.1	Contingency close to Bus 16 at Line 16-17 .....	101
6.5.2	Contingency close to Bus 21 at Line 21-22 .....	108
6.5.3	Other Severe Contingencies.....	114
6.5.4	Summary .....	116
6.6	Conclusion .....	116
<b>7</b>	<b>Conclusions and Future Work.....</b>	<b>118</b>
7.1	Summary of the Thesis and Application of the Research.....	118
7.2	Future Work .....	119
	<b>References .....</b>	<b>121</b>
	<b>Appendix A: One Generation Station towards Infinite Bus System Data.....</b>	<b>127</b>

<b>Appendix B: Nine - Bus System Data.....</b>	<b>128</b>
<b>Appendix C: 500 kV Transmission System with Two Generation Units Data ..</b>	<b>129</b>
<b>Appendix D: Two - Area with Added Load Area System Data.....</b>	<b>130</b>
<b>Appendix E: New England 39 - Bus System Data.....</b>	<b>131</b>
<b>Research Papers Presented during the M.Eng. Program .....</b>	<b>132</b>

# List of Figures

Figure 2.1 Classification of Power System Stability .....	9
Figure 2.2 A Classical Mechanical Analogy to the Transient Stability Problem .....	10
Figure 3.1 System Diagram of a Three-bus System .....	18
Figure 3.2 System Network during the Fault of Three Bus System .....	19
Figure 3.3 System Network after the Fault Clearance of Three Bus System .....	19
Figure 3.4 Solutions of Swing Equations: Rotor Angles v.s. Time for the Three Bus System.....	21
Figure 3.5 Different Fault Clearing Time Comparison in Stable Scenario for Three Bus System.....	22
Figure 3.6 Single Generator towards Infinite Bus System Example .....	23
Figure 3.7 Power Curve for a Typical Synchronous Machine.....	24
Figure 3.8 Normal Operation Point for a Typical Synchronous Machine .....	24
Figure 3.9 Equal Area Criteria for a Typical Synchronous Machine .....	26
Figure 3.10 Stability Margin for a Typical Synchronous Machine .....	27
Figure 3.11 Classical Generator Model .....	29
Figure 3.12 Flux Paths regarding to Generator Direct Axis .....	30
Figure 3.13 Fundamental Frequency Component of Armature Current.....	31

Figure 3.14 GENROU Direct Axis Model .....	32
Figure 3.15 Three-Bus System Generator Rotor Angle Variations with a Fault at Bus 3 and Clearing Time 0.1 s .....	34
Figure 3.16 Bus 1 Voltage Variation in Three-Bus System .....	35
Figure 3.17 Three-Bus System Generator Rotor Angle Variations with a Fault at Bus 3 and Clearing Time 0.4 s .....	35
Figure 3.18 Single Line Diagram of a Nine-Bus System .....	36
Figure 3.19 Nine-Bus System Generator Rotor Angle Variations with a Fault at Line 6-9 and Clearing Time 0.1 s .....	37
Figure 3.20 Nine-Bus System Generator Rotor Angle Variations with a Fault at Line 6-9 and Clearing Time 0.3 s .....	38
Figure 3.21 Single Line Diagram of a 37 Bus System .....	39
Figure 3.22 37 - Bus System Bus Jo Generator Rotor Angle Variation regarding to the Slack Bus Generator with a Fault at Line Slack 345- Jo 345 and CT = 0.1 s .....	40
Figure 3.23 37 - Bus System Bus Jo Generator Rotor Angle Variation regarding to the Slack Bus Generator with a Fault at Line Slack 345- Jo 345 and CT = 0.6 s .....	40

Figure 3.24 37 - Bus System Bus Jo Generator Rotor Angle Variation regarding to the  
 Slack Bus Generator with a Fault at Line Slack 345- Jo 345 and  $CT = 2$  s 41

Figure 4.1 Excitation Control .....	44
Figure 4.2 Block Diagram of Type I Excitation System and Generator.....	46
Figure 4.3 High Speed Excitation's Contribution.....	49
Figure 4.4 DC Excitation System with Voltage Regulator.....	50
Figure 4.5 AC Alternator - Type Excitation System .....	51
Figure 4.6 AC Static- Type Excitation Systems .....	52
Figure 4.7 Control System of PSS .....	56
Figure 4.8 Connected Power System Stabilizer.....	57
Figure 4.9 System Diagram of a Generation Station towards an Infinite Bus System	58
Figure 4.10 Three Scenarios of Rotor Angle Responses for One Generation Station towards an Infinite Bus System with a Fault Clearing Time 0.066 Seconds .....	60
Figure 4.11 Three Scenarios of Terminal Voltages for One Generation Station towards an Infinite Bus System with a Fault Clearing Time 0.066 Seconds .....	61
Figure 4.12 Single Line Diagram of a Nine-Bus System .....	63
Figure 4.13 Three Scenarios of Generator Two Rotor Angle Responses for Nine-Bus System with a Fault Clearing Time 0.1 Seconds .....	64

Figure 4.14 Three scenarios of Generator Two Voltage for Nine-Bus System with a Fault Clearing Time 0.1 Seconds .....	64
Figure 5.1 Typical Configurations of SVCs .....	72
Figure 5.2 Thyristor Controlled Reactor .....	74
Figure 5.3 TSC-TCR SVC and Its Total VAR Demand versus VAR Output .....	74
Figure 5.4 V-I Characteristic of SVC .....	75
Figure 5.5 SVC and Simplified Control System Block Diagram (Phasor Type) .....	77
Figure 5.6 SVC Model Block Diagram in Power System Toolbox.....	78
Figure 5.7 500 kV Two Generation Units Power Transmission System Diagram .....	79
Figure 5.8 Generator One Rotor Angle Differences for 500 kV Two Generation Units Power Transmission System with a Fault Clearing Time 0.09 Seconds ...	80
Figure 5.9 Generator One Terminal Voltages for 500 kV Two Generation Units Power Transmission System with a Fault Clearing Time 0.09 Seconds.....	81
Figure 5.10 Critical Fault Clearing Cycles versus SVC VAR Ratings for 500 kV Two Generation Units Power Transmission System.....	82
Figure 5.11 Single Line Diagram of a Two-Area with Added Load Area System .....	83
Figure 5.12 Rotating Speed Deviation between Generator 4 and Generator 5 for Two- Area with Added Load Area System with a Fault on the line 25-3 and Fault Clearing Time 0.07 Seconds .....	84

Figure 5.13 Voltage Variations at Bus 25 for Two-Area with Added Load Area System with a Fault on the Line 25-3 and Fault Clearing Time 0.07 Seconds .....	86
Figure 6.1 Transient Voltage Dip Definition for WECC Criteria .....	91
Figure 6.2 Voltage Sag Duration in Slow Recovery Case.....	96
Figure 6.3 Flowchart of SVC Allocation Analysis.....	99
Figure 6.4 Single Line Diagram of the New England 39 Bus System.....	100
Figure 6.5 New England System without SVC Bus Voltage Sags with a Fault in Line 16- 17 and Clearing Time 0.1 Seconds .....	101
Figure 6.6 New England System Sensitive Buses with Sensitivity Indices for Fault on Line 16-17.....	105
Figure 6.7 New England System with a SVC (at Bus 20) Bus Voltage Sags with a Fault in Line 16-17 and Clearing Time 0.1 Seconds.....	106
Figure 6.8 New England System with SVCs (at Bus 20 and 15) Bus Voltage Sags with a Fault in Line 16-17 and Clearing Time 0.1 Seconds .....	108
Figure 6.9 New England System without SVC Bus Voltage Sags with a Fault in Line 21- 22 and Clearing Time 0.1 Seconds .....	109
Figure 6.10 New England System Sensitive Buses with Sensitivity Indices for Fault in Line 21-22.....	110
Figure 6.11 New England System Largest Bus Voltage Sag Rates with SVC at Bus 23	112

Figure 6.12 New England System Largest Bus Voltage Sag Time Durations with SVC at

Bus 23 (Contingency in Line 21-22, Fault Clearing Time 0.1 Seconds) 113

Figure 6.13 New England System with an SVC (at Bus 23) Bus Voltage Sags with a Fault

in Line 21-22 and Clearing Time 0.1 Seconds..... 113

# List of Tables

Table 3.1 Summary of the Nine-Bus System Case Information.....	37
Table 3.2 Summary of the 37 Bus Case Information.....	39
Table 4.1 Summary of the One Generator Connected to an Infinite Bus System .....	59
Table 4.2 Critical Clearing Time and Cycle of Different Scenarios for One Generation Station towards Infinite Bus System.....	62
Table 4.3 Critical Clearing Time (Cycle) of Different Scenarios for Nine-Bus System	65
Table 5.1 Critical Clearing Time (Cycle) Summary for 500 kV Two Generation Units Power Transmission System .....	82
Table 5.2 Critical Clearing Time Summary for Two-Area with Added Load Area System .....	87
Table 5.3 Summary of SVC parameters at Bus 21 for Two-Area with Added Load Area System.....	88
Table 6.1 New England System Voltage Sag and Sensitivity Index Summary.....	102
Table 6.2 Summary of SVC Allocation Plan I for the New England System with a fault on line 16-17: One SVC at Bus 20.....	105
Table 6.3 Summary of SVC Allocation Plan II for the New England System with a Fault in Line 16-17 and Clearing Time 0.1 Seconds: Two SVCs at Bus 20 and 22	107

Table 6.4 New England System Voltage Sag and Sensitivity Index Summary.....	109
Table 6.5 Summary of SVC Allocation Plan for the New England System with a Fault in Line 21-22 and Clearing Time 0.1 Seconds: an SVC at Bus 23.....	111
Table 6.6 Other Contingencies Threatening the New England System.....	114
Table 6.7 Summary of SVC Allocation Plan for a Fault close to Bus 1.....	115

## List of Abbreviations and Symbols

$\delta$	:	Generator rotor angle
$\omega$	:	Generator rotor rotating speed
$\theta_m$	:	Rotor angular position regarding the initial angular position
$J$	:	The moment of inertia
$\alpha_m$	:	Angular acceleration
$T_m$	:	Mechanical torque
$T_e$	:	Electrical torque
$H$	:	Rated kinetic energy from generators under synchronous speed
$D$	:	Coefficient for the generator damping torque
$E'$	:	Generator inner voltage
$X_d$	:	Generator synchronous d-axis reactances regarding to the steady-state process
$X_q$	:	Generator synchronous q-axis reactances regarding to the steady-state process
$X_d'$	:	Generator d - axis transient reactance
$X_q'$	:	Generator q - axis transient reactance
$X_d''$	:	Generator d - axis subtransient reactance
$X_q''$	:	Generator q - axis subtransient reactance
$V$	:	Voltage
$P_e$	:	Electric power
$P_m$	:	Mechanical power
$X_{eq}$	:	Equivalent reactance
$\delta_c$	:	Generator critical clearing angle

$X_{ad}$	:	The mutual flux reactance between the generator stator and the rotor d-axis
$X_l$	:	The generator armature leakage reactance
$X_{fd}$	:	The leakage reactance in the generator field
$X_{pl}$	:	The mutual reactance between generator d-axis damper and the field
$X''$	:	Generator subtransient inner reactance
$X'$	:	Generator transient inner reactance
$X_s$	:	Generator steady state inner reactance
$\phi_l$	:	Generator armature leakage flux
$\phi_{1d}$	:	Generator damper leakage flux
$\phi_{fd}$	:	Generator field leakage flux
$\phi_{pl}$	:	Generator mutual flux between damper and field
$\phi_{ad}$	:	Generator mutual flux between the armature and the direct axis
$T'_{d0}$	:	Generator d-axis transient open circuit time constant
$T'_{q0}$	:	Generator q-axis transient open circuit time constant
$T''_{d0}$	:	Generator d-axis subtransient open circuit time constant
$T''_{q0}$	:	Generator q-axis subtransient open circuit time constant
p.u.	:	Per unit
CT	:	Fault clearing time
CCT	:	Critical fault clearing time
DC	:	Direct current
AC	:	Alternating current
AVR	:	Automatic voltage regulator
$R_e$	:	Generator exciter field resistance

$L_e$	:	Exciter field inductance
$E_{fd}$	:	Generator exciter field voltage
$V_{ref}$	:	Reference voltage
$i_e$	:	Generator excitation current
PPT	:	Power potential transformer
SCT	:	Saturable-current transformer
PSS	:	Power system stabilizer
P	:	Real Power
Q	:	Reactive Power
FACTS	:	Flexible AC Transmission System
SVC	:	Static VAR Compensators
TCSC	:	Thyristor Controlled Series Capacitor
STATCOM	:	Static Condenser
TCR	:	Thyristor-controlled reactor
TSC	:	Thyristor-switched capacitor
MSC	:	Mechanically switched capacitor
FC	:	Fixed capacitor
$\alpha$	:	Tyristor firing angles
$B$	:	Susceptance
$I_{LF}$	:	The variable current in the controllable reactor of SVC
$I_{cn}$	:	The current flowing though the connected capacitors of SVC
WECC	:	Western Electricity Coordinating Council
NERC	:	North American Electric Reliability Corporation
$t_{sag}$	:	Sag time duration

$V_{msag}$	:	The maximum transient voltage dip/sag
$S_t$	:	The voltage sag time duration sensitivity index
$S_V$	:	The voltage sag sensitivity index
$S$	:	Sensitivity index

# Chapter 1

## Introduction

In today's power systems, the most important operation requirements are safety and reliability. Since the power supply is needed in daily life, any electric power outage or blackout may bring economic losses and inconvenience.

Power system transient stability has been significantly considered in electric power industry for a long time especially in the power system blackouts prevention [1]-[4]. Transient stability problems bring electric power utilities great challenges and a series of negative consequences: the losses of generation units, power system components, or loads. In the worst case, the whole system may lose control and collapse, leading to blackouts in large areas. In order to ensure a safe, reliable, continuous power supply, the power utilities should consider the power system transient stability performance.

## **1.1 Objective of Research**

This research aims at exploring the nature of power system transient stability and discussing three main methods of improving the power system performance with respect to transient stability: decreasing fault clearing times, employing high speed excitation systems, and the assistance from Static Var Compensators (SVC). It also aims at exploring an improved method to allocate SVCs in order to better enhance the system transient voltage performance. This research verifies and studies those methods by case studies. Different types of excitation systems and different allocations of SVCs are evaluated.

This research indicates that, by strengthening the power system transient stability performance, power grids can transmit more electric power with less potential safety hazards. With better stability performance, the power supply becomes more reliable and safer, which benefits the whole society and people's daily life.

## **1.2 Organization of Thesis**

In this research, the theory of transient stability enhancements are first presented and explained, and, then, it is illustrated and verified by case studies. Comparisons are

conducted to clearly demonstrate how the generator rotor angle performances and transient voltage performances are improved by those measures and devices. The results obtained show that the effects of those measures and devices indeed contribute to the power system transient stability enhancement.

This thesis is organized as follows:

Chapter 2 discusses the concept of the power system stability and introduces the term of “power system transient stability” in detail. The method of evaluating the power system transient stability is also introduced, and this chapter serves as the fundamental of the following transient stability improvement analysis.

Chapter 3 focuses on the transient stability enhancement by decreasing the fault clearing time in systems. The swing equations and the equal area criteria help to explore the nature of the rotor angle stability problems. Three power systems are simulated and analyzed in PowerWorld Simulator [5] to demonstrate the effect of fast fault clearing method on the power system transient stability enhancement.

Chapter 4 shows how the high speed excitation systems benefit the transient stability enhancement in the power system. Typical excitation systems and their control diagrams are introduced in detail. Their contributions on power system transient stability enhancement are also illustrated for three different power systems.

Chapter 5 introduces the basic theory on the Flexible AC Transmission System and the Static Var Compensators (SVC). The classification and functions of SVCs are emphasized, especially the effects on the power system transient stability enhancement. Two case studies are presented to illustrate the role of SVC in the power system transient voltage improvement and the transient stability improvement. The MATLAB Simulink [6] and Power System Toolbox (PST) [7] based on MATLAB are employed to conduct simulations.

Chapter 6 further explores how the allocation of SVCs influences the power system transient stability and bus transient voltage sags. Different SVC positions lead to different effects. Contingency analysis is used to detect weak areas in various power systems, and then, the trial and error method or a simplified sensitivity analysis can be further applied to decide specific SVC allocation schemes. The Power system Toolbox (PST) based on MATLAB is used.

Chapter 7 summarizes the thesis and draws conclusions. Contributions of this research to real power systems are discussed. Possible future work on this topic is presented.

# **Chapter 2**

## **Power System Stability and Transient Stability**

### **2.1 Introduction**

In order to discuss the power system transient stability in detail, the concepts of power system stability and the transient stability should be introduced. The definition of these two terms is discussed in this chapter, and two simulation tools used in this thesis are presented as well.

### **2.2 Overview of Power System Transient Stability Concept and System Operation requirements**

In modern power systems, system stability issues are known as significant aspects. In order to operate a system in a safe, reliable state, ensuring its stability is essential and crucial.

The stable parallel operation of AC generators and the power system stability concepts were proposed by experts for the first time in the early decades of the 20th century [1]-[3]. However, since power systems developed quickly during the 20th century, the ideas and concepts presented in the past are not appropriate for modern systems. Realizing this, reference [3] systematically introduces the power system stability definition and classification from a modern point of view. In addition, [3] also discusses the close relationship between reliability, security and stability: maintaining the stability of a system helps to ensure its reliability; a secure system is always founded on its reliable operations.

Many power system blackouts begin with the loss of stability. Reference [4] focuses on the causes of those blackouts, and the recommendations regarding system security enhancements. Experts started to learn from those blackouts that in order to maintain power systems in a safe, reliable state, the power system operation should emphasize on the improvement of the system stability through various strategies, with investments also considered.

In summary, the “stability” serves as an important concept for the world’s electric power generation and distribution systems. The operation of power systems cannot be conducted without considering it.

### 2.3 Definition and Classification of Power System Stability

According to references [3] and [8], a definition of power system stability can be proposed:

*Power system stability refers to the ability that all the synchronous machines in a power system have to return to the previous equilibrium states, or move to new steady states, if there is a disturbance. The integrality of the systems is maintained and the significant variables are bounded.*

It is known that disturbances serve as a key factor in triggering destabilizations in the systems, and may cause big problems. However, since many power supply devices, such as transmission lines, are exposed to the natural changing environment directly, large and small disturbances from the environment are inevitable. Short circuits and sudden loss of power grid elements may happen. These are event-type disturbances [3]. The continuous variation of loads can also affect the operation and the control of generators, but they are referred to as the “norm-type” disturbances, a contrast to the aforementioned sudden event-type disturbances [3]. Therefore, in practice, the stability of power systems experiences many disturbing tests every time, as the environment keeps varying. If the system is not properly designed or operated, a single, small disturbance may lead to a large, severe power outage.

For the analysis of power system stability problems, the following two points are significant. First, in order to simplify the process of researching on system stability issues, such as the normal analysis and simulations, a common valid assumption is employed, in which the system is at a true steady-state operation point before suffering a disturbance. Second, in order to ensure the system security by scientific design, and to control the investment, power engineers should consider both the system security margin and the budget. For an efficient and economical design, some significant possible contingencies are carefully selected and considered; while others are ignored due to the budget limit. This point is applied in the case studies in Chapter 6 of this thesis that only significant contingencies are studied. However, the finite regions of attraction obtained by the contingency selection should be as large as possible [3].

The classification of the power system stability is illustrated in Figure 2.1. The power system stability mainly contains three parts: rotor angle stability, frequency stability, and voltage stability. The transient stability is included in the rotor angle stability.

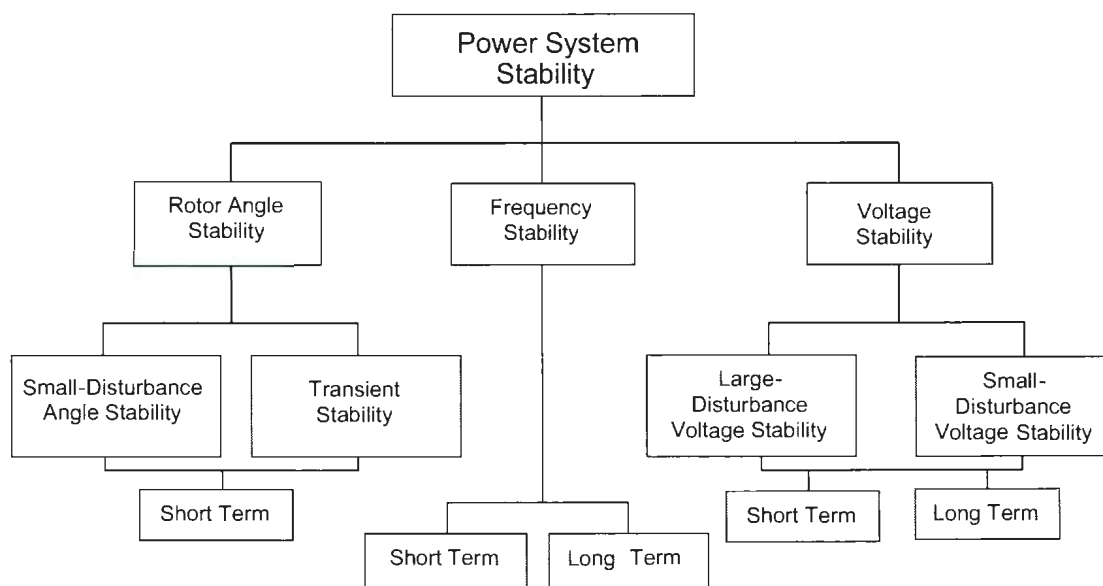


Figure 2.1 Classification of Power System Stability [3]

Figure 2.1 and reference [3] also point out the time frame for each stability type. Though divided into three forms, during a contingency, several types of instability may occur at the same time. One form of instability may also trigger others. Usually, large disturbances are those sudden severe changes in the power system, such as the loss of generators, transmission lines, or transformers. By contrast, small disturbances are less obvious ones, such as low frequency oscillations.

## 2.4 Power System Transient Stability

As Fig.2.1 shows, the power system transient stability belongs to the rotor angle stability. It refers to the ability of the generators in a power system to maintain

synchronism after a large sudden disturbance that leads to great excursions of angle  $\delta$  – the rotor angular differences between the system’s synchronous position and the actual position of the rotor - and frequency deviations [3][9]. If the generators’ rotor angles in a system can return to the previous equilibrium states, or successfully reach a new steady state, this system is stable. Otherwise, the system will oscillate severely, become unstable and the generators will lose synchronism.

Reference [10] provides a classical mechanical analogy to describe the transient stability problem shown in Figure 2.2. It explains this concept using a model consisting of strings and several balls. The breaking of one string disturbs the static state of the balls, causing an oscillation. Finally, a new steady state can be reached, or instability irreversibly occurs. Such a process is similar to the power system transient stability problem.

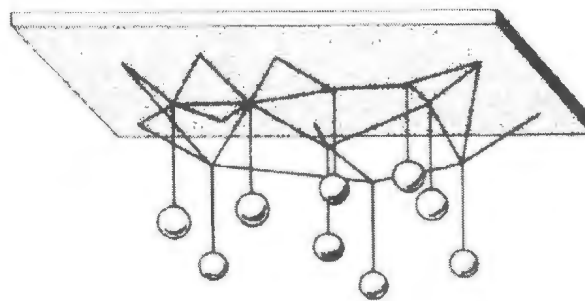


Figure 2.2 A Classical Mechanical Analogy to the Transient Stability Problem [9][10]

The power systems in the world are mainly connected in an interconnected way. The natural energy resources in remote regions can be utilized to generate power efficiently, and the power can be transferred to the load center thousands miles away by transmission lines. Different parts of a power grid can also support each other to improve security margins and power qualities. However, in such big systems with many synchronous machines interconnected, a single local disturbance in the system without proper controls may cause a wide area problem, even lead to a severe blackout in the whole grid, especially when the system is under stress with heavy loads. Reference [11] focuses on the protection strategies and control methods to help enhance the large power system transient stability following severe system oscillations: effective controllers are essential to prevent instabilities; proper circuit breakers and appropriate isolations are also considered as oscillations occur.

## **2.5 System Protection and Assessment of System Transient Stability**

According to the power system operation theory, after large disturbances, specific relays will operate swiftly, forcing a series switches to open as well as minimizing the isolated area. In the power system networks, switches are set related to both primary protections and backup protections. These two kinds of protections should coordinate

with each other very well by proper time intervals. The backup protections operate more slowly after the primary ones with certain time delays, in case of the failure of the primary protections.

The influence that disturbances impose on the whole system varies with cases. Various system configurations, operation conditions, protection designs, or characters of the disturbances may lead to diverse system transient states. The time period for the power system transient stability assessment is 3-5 seconds after the sudden large disturbance for small systems, and 10-20 seconds for large systems [3]. For large-scale power system transient stability studies, digital computer programs play significant roles. The Real-Time Dynamic Security Assessment (DSA) is realized in the power system operation. In reference [12], DSA Models and operation processes are introduced in detail. Reference [13] also serves as an example to illustrate the application of the digital computer programs in the power system transient stability assessment.

## **2.6 Transient Stability Simulation Software**

Software can be employed to evaluate power system transient stability, such as PowerWorld Simulator, PSCAD [14], PSAT [15], MATLAB Simulink and Power

System Toolbox in MATLAB. In this thesis, two types of software are mainly used: PowerWorld Simulator (Version 15) and the Power System Toolbox in MATLAB.

The PowerWorld Simulator, developed by the PowerWorld Corporation, is power system simulation software with strong capabilities of power system studies, basic power flow calculations, optimal power flow analysis, and contingency analysis [5]. The transient stability (TS) analysis package in this software can simulate various transient states, helping to give a thorough interpretation of different contingency situations and transient stability problems. The software is user friendly with easy operation procedures and nice presented figures. Some of the results, such as the bus admittance matrix tables, from the PowerWorld Simulator are compatible with the MATLAB software. In summary, it is a powerful tool to analyze power system transient stability.

The Power System Toolbox is an analysis software package based on the well-known MATLAB software. Since the PowerWorld Simulator software cannot model the SVCs, the Power System Toolbox based on MATLAB is adopted to conduct all the simulations regarding SVCs. The original paper about it was written by Dr. Kwok W. Cheung and Prof. Joe Chow, and the software was modified and improved by Graham Rogers later [16]. The whole package contains MATLAB function files to solve power flows and various dynamic processes, as well as typical power system data files. New

data files can be created and called by those functions files, and all the MATLAB files can be modified according to specific requirements.

## **2.7 Conclusion**

In this chapter, the basic ideas of the power system stability and the transient stability are discussed. In order to evaluate and analyze the stability problems scientifically and in time, digital computer programming and simulations are necessary. PowerWorld Simulator and the Power System Toolbox in MATLAB are used in this research.

## **Chapter 3**

# **Transient Stability Enhancement through Fast Fault Clearing**

### **3.1 Introduction**

The power system transient stability is a complex problem to analyze. A single small contingency without proper measures to deal with may lead to a large system collapse. In this chapter, single synchronous machine stability is thoroughly studied by introducing its swing equations, which is a fundamental of the power system transient stability. In addition, the equal area criteria also illustrate the stability issues regarding a single machine towards the infinite bus system. Then, a basic method of improving the transient stability - fault clearing time control - is proposed and explained. Several case studies are done based on various power systems with diverse fault clearing times.

### 3.2 The Swing Equations [9][17]

In order to estimate the system transient stability, the rotor angle  $\delta$  needs to be introduced first. It is defined that  $\theta_m(t) = \omega_{msyn}t + \delta_m(t)$ .  $\omega_{msyn}$  is the synchronous rotating speed of the rotor from the system, a reference speed.  $\theta_m(t)$  is the rotor angular position regarding the initial angular position.  $\delta_m(t)$  is the rotor angular position difference between the system's synchronous position and the actual position of the rotor, a corrective variable.

According to Newton's second law, the following formula can be derived:

$$J\alpha_m = J \frac{d^2\theta_m(t)}{dt^2} = J \frac{d^2\delta_m(t)}{dt^2} = T_m(t) - T_e(t) = T_a(t); \quad (3.1)$$

$T_m$  represents the mechanical torque which equals to the electrical torque, obtained by subtracting the torque loss from the prime mover.  $T_e$  represents the electrical torque from the power system.  $\alpha_m$  is the angular acceleration, and  $J$  is the moment of inertia. The sudden significant changes from  $T_m$  or  $T_e$  serve as disturbances, breaking the initial equilibrium state.

The problem can be simplified by transferring those torques to powers, and using per-unit values. Under this circumstance, an  $H$  constant is defined as the rated kinetic energy from generators under synchronous speed, respective to the generators' VA rating

$S_{msyn}$ :

$$H = \frac{\frac{1}{2}J\omega_{msyn}^2}{S_{msyn}} \text{ (J/V A)}; \quad (3.2)$$

The typical value for  $H$  is between 1 and 10.

In addition, considering the generator with  $P$  poles and damping torque,  $\delta$ ,  $\omega$ ,  $\omega_{syn}$  and  $\alpha$  are defined as the power angle, electrical radian frequency, synchronous electrical radian frequency, and electrical angular acceleration.  $\alpha(t) = \frac{P}{2}\alpha_m(t)$ ,  $\omega(t) = \frac{P}{2}\omega_m(t)$ ,  $\omega_{syn}(t) = \frac{P}{2}\omega_{msyn}(t)$  and  $\delta(t) = \frac{P}{2}\delta_m(t)$ . The following per-unit swing equation can be derived:

$$\frac{2H}{\omega_{syn}}\omega_{p.u.}(t)\frac{d^2\delta(t)}{dt^2} = p_{mp.u.}(t) - p_{ep.u.}(t) - \frac{D}{\omega_{syn}}\left(\frac{d\delta(t)}{dt}\right) = p_{ap.u.}(t); \quad (3.3)$$

$D$  is the coefficient for the damping torque, with a typical value between 0 and 2.

If we write the equations in the space-state form, the following equations are obtained:

$$\frac{d\delta(t)}{dt} = \omega(t) - \omega_{syn} = \Delta\omega(t) = \omega_{syn}(\Delta\omega_{p.u.}); \quad (3.4)$$

$$\frac{d\omega(t)}{dt} = \frac{d\Delta\omega(t)}{dt} = \frac{\omega_{syn}}{2H\omega_{p.u.}(t)} \left[ p_{mp.u.}(t) - p_{ep.u.}(t) - \frac{D}{\omega_{syn}}\left(\frac{d\delta(t)}{dt}\right) \right]; \quad (3.5)$$

The per-unit swing equation is a foundation for the power system transient stability analysis. The  $\delta(t)$  curve reflects the operating conditions for the individual synchronous machines, as well as the whole power systems. They are non-linear equations with non-linear  $p_e(t)$  and  $\omega_{p.u.}(t)$ . Usually, we assume that  $\omega_{p.u.}(t) \approx 1$  in our calculations, since this per unit value does not change significantly during the transient processes. Reference

[17] mainly introduces four integration approaches to solve these nonlinear differential equations, including three explicit integration methods and one implicit integration method. The advantages and limitations regarding each method are also given. Reference [9] focuses on the modified Euler's method, illustrating the solution process of the swing equations in detail.

In order to explain how the swing equations reflect the performance of the transient stability, a simple small system from reference [9] with three buses is studied. The system diagram is as below:

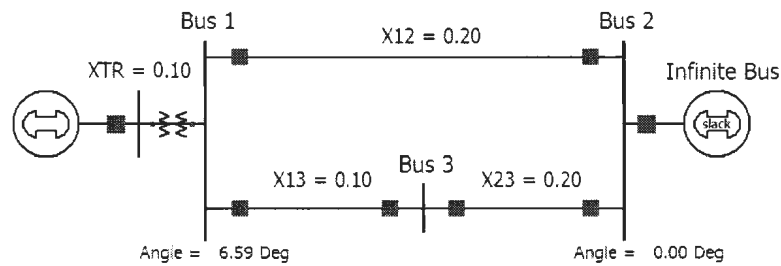


Figure 3.1 System Diagram of a Three-bus System

A synchronous generator is connected through a step-up transformer and two transmission lines to a large power system (infinite bus).  $H = 3$  is employed, and the system can first be solved through basic power flow calculations, obtaining generator inner voltage  $E' = 1.2812 \angle 23.95^\circ$  in per unit. The real power injected to the infinite bus through Bus 2 is 100 MW, and the reactive power going to the system through Bus 2 is

32.86 MVar. Assume that a three-phase-to-ground fault occurs in Bus 3, with the equivalent network changed immediately at that instant,  $X_{13}$  and  $X_{23}$  are connected to the ground directly.

After a short time period, the fault is cleared by isolating the fault area, with the two switches open at both ends of the branch between Bus 1 and Bus 2. The system network diagrams during the fault and after the fault are showed as Figure 3.2 and Figure 3.3.

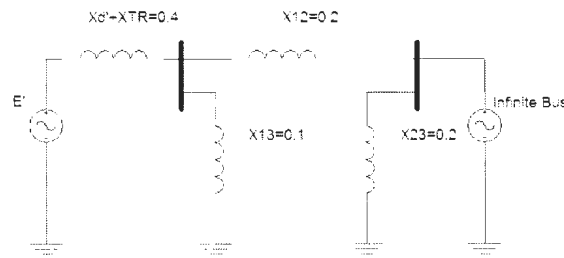


Figure 3.2 System Network during the Fault of Three Bus System

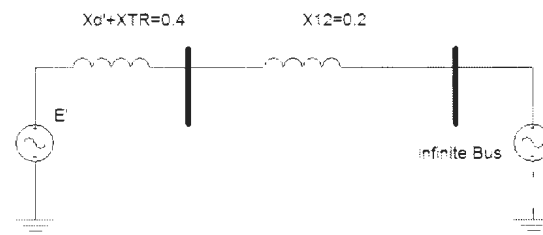


Figure 3.3 System Network after the Fault Clearance of Three Bus System

With the direct axis transient reactance  $X_d'$  for the generator model 0.3, we can easily obtain the Thevenin equivalent circuits seen from the generator ends for the faulted circuit and the post fault circuit.  $X_{Th}$  is the Thevenin equivalent reactance, and  $V_{Th}$  is the Thevenin equivalent voltage.

For the fault circuit,

$$X_{Th} = 0.3 + 0.1 + 0.2 \parallel 0.1 = 0.46667.$$

$$V_{Th} = \frac{0.1}{0.1 + 0.2} \times 1 \angle 0^\circ = 0.3333 \angle 0^\circ.$$

For the post fault circuit,

$$X_{Th} = 0.3 + 0.1 + 0.2 = 0.6.$$

$$V_{Th} = 1 \angle 0^\circ.$$

Providing  $D = 1.5, P_m = 1$ , the swing equations can be written as:

$$\frac{d\delta(t)}{dt} = \Delta\omega(t); \quad (3.6)$$

$$\frac{d\Delta\omega(t)}{dt} = \frac{\pi \times 60}{3} \left[ P_m - \frac{E' V_{Th} \sin \delta}{X_{Th}} - \frac{1.5 \times \frac{d\delta(t)}{dt}}{2\pi \times 60} \right]; \quad (3.7)$$

The solutions of the above two equations can be obtained by MATLAB. Choosing different fault clearing time, the rotor angle variations with time are shown in the following figure. Within a short period of time - 1.5 seconds after the fault, the generator

rotor angle may vary within a bound, or increase boundlessly, depending on different fault clearing times. From the aforementioned stability definitions, the stable and unstable scenarios are distinguished by whether the rotor angle will go to the pre-fault value or a new stable value. Therefore, as Figure 3.4 shows, the line which consists of stars represents a stable case with a fault clearing time 0.3 seconds after the fault; while the solid one stands for an unstable case with the fault clearing time 0.4 seconds.

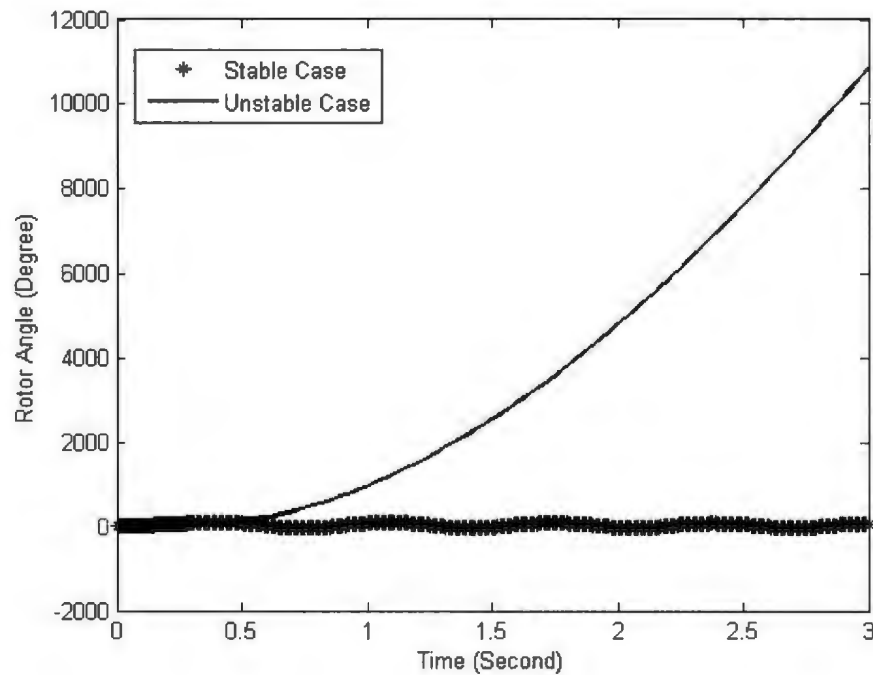


Figure 3.4 Solutions of Swing Equations: Rotor Angles v.s. Time for the Three Bus System

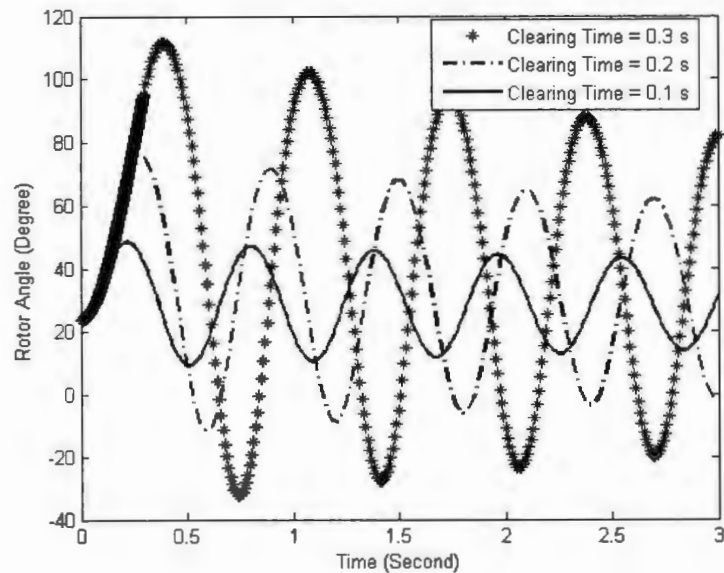


Figure 3.5 Different Fault Clearing Time Comparison in Stable Scenario for Three Bus System

Different fault clearing times are checked and as the fault clearing times vary from 0.1 to 0.3, the rotor angle solutions of the swing equations are presented in Figure 3.5. It clearly indicates that the less clearing time is employed; the rotor angle deviation becomes smaller. The oscillation magnitude decreases with time due to the damping torque.

### 3.3 The Equal-Area Criterion

The Equal-Area Criterion provides another sight into the power system transient stability problem.

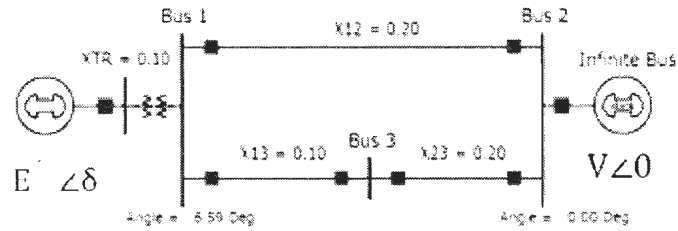


Figure 3.6 Single Generator towards Infinite Bus System Example

Adopting a simplified model for synchronous machine, the electrical power sent from the generator towards the system is  $P_e = \frac{E'V\sin\delta}{X_{eq}}$ , with  $E'$  representing the generator's internal voltage,  $V$  representing the system bus voltage, and  $X_{eq}$  standing for the sum of generator direct axis transient reactance  $X'_d$  and all the external equivalent reactance. Here,  $\delta$  refers to the power angle: the angle difference between the internal voltage  $E'$  and the system (Infinite Bus) voltage  $V$ . Figure 3.6 illustrates the power angle  $\delta$  curve.

In order to simplify the analysis, the voltages  $E'$  and  $V$  can be treated constant at the moment when a disturbance occurs. The relationship between the power angle  $\delta$  and the per unit electrical power  $p_e$  is a sinusoidal curve, shown as Figure 3.7.

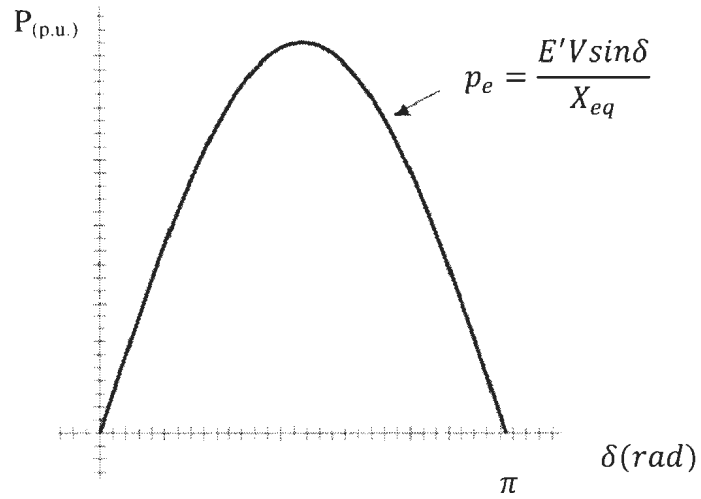


Figure 3.7 Power Curve for a Typical Synchronous Machine

In the equilibrium state, the net mechanical power which excludes the energy loss equals to the electrical power requirement from the system. In Figure 3.8, the steady state operation point is at the intersection of the electrical power curve and the mechanical power straight line.

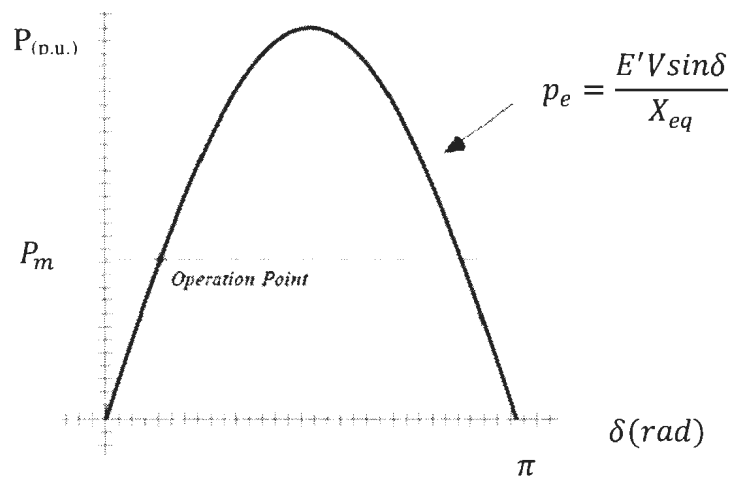


Figure 3.8 Normal Operation Point for a Typical Synchronous Machine

As a disturbance occurs, the operation point moves because the energy supply or the energy consumption conditions change. Consider a three-phase-to-ground short circuit fault at Bus 3 in the 3-bus system as an example. As long as the short circuit occurs, the electrical power transmitted from the generator to the system suddenly drops to a very low level, close to zero. However, because of the inertia of the prime mover and the generator, the mechanical power stays at the same level as the initial equilibrium state. A gap between these two occurs, leading to acceleration. The rotor angle begins to increase from  $\delta_0$  along the during-fault power curve  $p_e = \frac{E'V\sin\delta}{X_{eq, fault}}$ , with the rotor rotating speed growing up.

At some point in time, the fault is cleared from the system. The rotor angle has moved to a new value  $\delta_c$ , reflecting a new electrical power point  $p_{ec} = \frac{E'V\sin\delta_c}{X_{eq}}$  at the original power curve. However, with an almost constant mechanical power, the electrical power requirement is larger than the mechanical power at this time. A deceleration process occurs. Though the angle  $\delta$  keeps increasing due to the inertia, the increasing rate of  $\delta$  drops, and it also jumps to the over-fault power curve, with  $X_{eq} = X_{12} = 0.2$ . Finally, if  $\delta$  can stop increasing at a point  $\delta_{max}$  before reaching the maximum limit  $\delta_m$  (the other intersection point), and begin to move back, the machine stability is maintained:  $\delta$  can finally move back to the initial operation point or a new steady point with the help

of the damping factor. Otherwise, if  $\delta$  cannot stop increasing before reaching  $\delta_m$ , it can never move back by itself, and the unstable situation will occur.

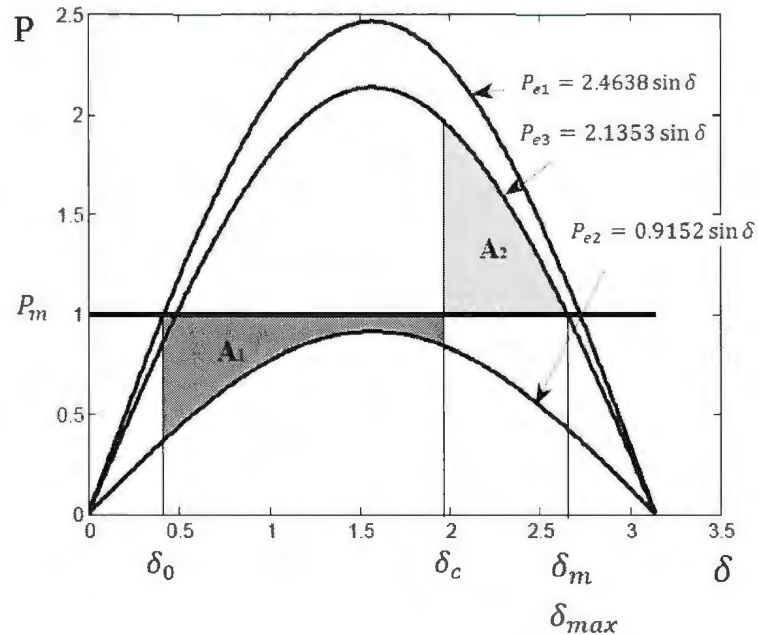


Figure 3.9 Equal Area Criteria for a Typical Synchronous Machine

Considering Figure 3.9, the area in which the mechanical power is larger than the electrical power during the fault time is an acceleration area, named  $A_1$ . The area in which the electrical power exceeds the mechanical power after the fault clearance is a deceleration area, named  $A_2$ . The equal area criteria is that the area of  $A_2$  should be equal or larger than that of  $A_1$  to maintain the transient stability. Otherwise the generator will lose synchronism, because  $\delta$  cannot move back once it goes beyond  $\delta_m$ . If the fault is cleared before  $\delta$  reaches the critical clearing angle and the maximum power angle  $\delta_{max}$  is

less than  $\delta_m$ , the rest of the acceleration area serves as the “stability margin”, shown by Figure 3.10. The more stability margin obtained the more capability a generator has to resist the disturbances, and remain stable. The unit of angle  $\delta$  is radian.

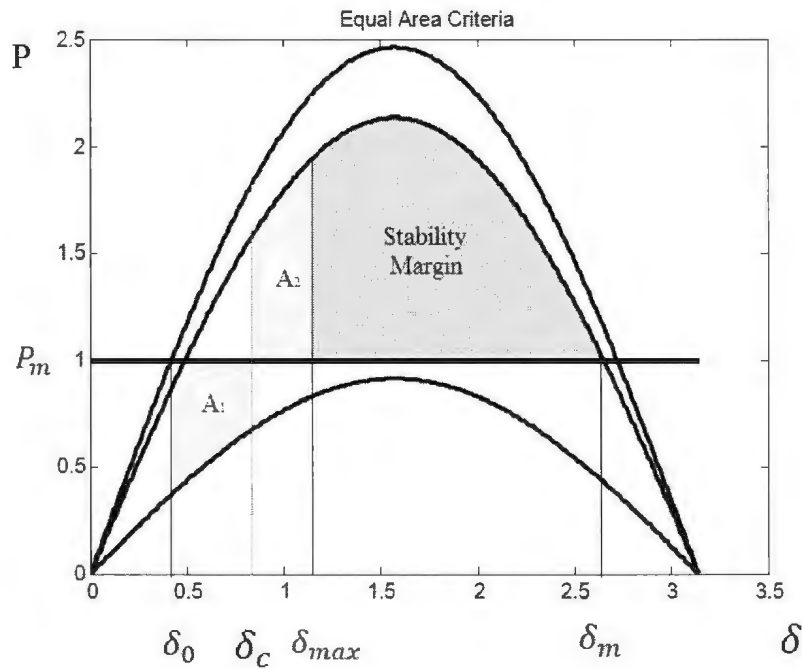


Figure 3.10 Stability Margin for a Typical Synchronous Machine

The above figure shows that the nature of the transient stability enhancement is increasing the deceleration area, limiting the acceleration area, and enlarging the stability margin. A direct method is controlling the Clearing Time. The faster a fault is cleared, the less acceleration area it creates, the more margins for the deceleration exist, and the less instability threatens a system faces.

### 3.4 Clearing Time Control

According to Section 3.3, if a fault is cleared fast enough, the system may have good transient stability performance after a disturbance. However, the clearing time cannot be decreased without limit. The fault detection by the relays takes time; the fault analysis and decision making require time; and the reactions of the switches also take time. In practice, this time value cannot be reduced randomly. In power system transmission line, a typical fault clearing time requirement is 6 – 10 cycles after a fault, which is around 0.1 – 0.167 seconds, assuming the speed of generator unchanged. The higher voltage level the system has, the smaller fault clearing time is desired.

The Critical Clearing Time (CCT) is defined as the longest time after which a fault is cleared to maintain the transient stability, without causing transient instability. In Figure 3.9, the clearing angle  $\delta_c$  is a critical clearing angle, since it critically allows  $A_1 = A_2$ . A fault cleared after  $\delta$  which goes beyond  $\delta_c$  will cause instability in this system. Therefore, CCT is the time after which a fault is cleared and enables the acceleration area equal to the deceleration area. If the fault clearing time is larger than CCT, the synchronous machine will go out of step and lose synchronism with the system.

### 3.5 Generator Model Introduction

In the power system transient stability studies, the modeling of generators are important. After large disturbances or faults, generators respond through a series of protective reaction. Therefore, during transient studies, the power system admittance matrix need to be modified to include the generator synchronous impedances. In addition, complex generator models should also be considered when more accurate estimations of transient stabilities are required. Two generator models which are employed in this thesis are introduced in the following sections.

#### 3.5.1 Classical (GENCL) Model

The Classical Model or GENCL Model consists of the Thevenin voltage of the generator plus a transient direct axis transient reactance  $X'_d$  as Figure 3.11 shows.

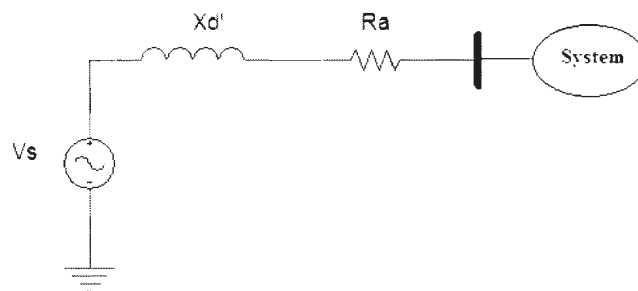


Figure 3.11 Classical Generator Model

$R_a$  represents the resistor of the armature winding in the generator. For the generator part, this model also consider the H constant ( $H = \frac{1}{2} \frac{J \omega_{msyn}^2}{S_{msyn}}$ ) and the damping torque coefficient  $D$ , which are significant parameters for transient studies. The transient reactance  $X'_d$  is the generator direct axis equivalent reactance during the transient process of a disturbance.

According to [17],

$$X'_d = X_l + \frac{1}{\frac{1}{X_{ad}} + \frac{1}{X_{fd} + X_{pl}}} \quad (3.8)$$

$X_{ad}$  reflects the mutual flux linkage between the stator and the rotor d-axis.  $X_l$  is the armature leakage reactance.  $X_{fd}$  stands for the leakage flux in the field, and  $X_{pl}$  represents the effect of the mutual flux between d-axis damper and the field. The corresponding generator flux paths are showed as Figure 3.12.

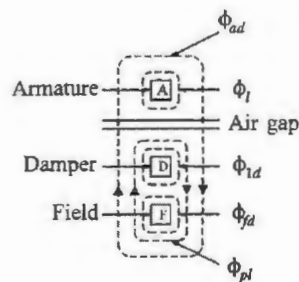


Figure 3.12 Flux Paths regarding to Generator Direct Axis [17]

In common transient stability analysis, after a disturbance, the generator armature current component firstly experiences a subtransient period, and then a transient period, finally a steady-state period as Figure 3.13 shows, reflecting different inner reactances  $X''$ ,  $X'$ , and  $X_s$  correspondingly.

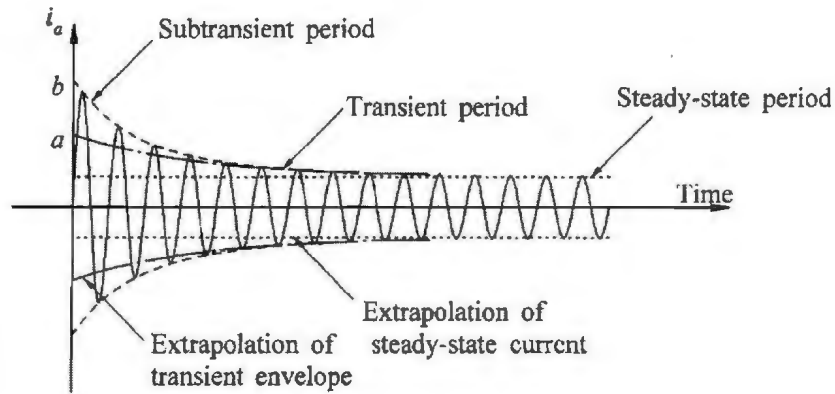


Figure 3.13 Fundamental Frequency Component of Armature Current [17]

For a simple model, it can be assumed that  $X'' = X_d'' = X_q''$ , and  $X' = X_d' = X_q'$  [17].

For this Classical (GENCL) Model, the damper leakage flux  $\phi_{1d}$  is ignored because it decays fast in a few cycles following a disturbance.  $\phi_{1d}$  is only considered to exist in the subtransient period. This simplified classical model is commonly used in many studies for which rigid requirements are not essential. However, for the GENROU Model explained in Section 3.5.2, the armature leakage flux  $\phi_l$ , the damper leakage flux  $\phi_{1d}$ , the field leakage flux  $\phi_{fd}$ , the mutual flux between damper and field  $\phi_{pl}$ , and the mutual flux between the armature and the direct axis  $\phi_{ad}$  in Figure 3.12 are all considered.

### 3.5.2 GENROU Model

The GENROU Model is an advanced generator model compared to the classical one, in which the subtransient process after a fault is considered. In the case study in Section 3.6,

this GENROU Model is adopted instead of the GENCL Model. The direct axis model diagram is shown in Figure 3.14.

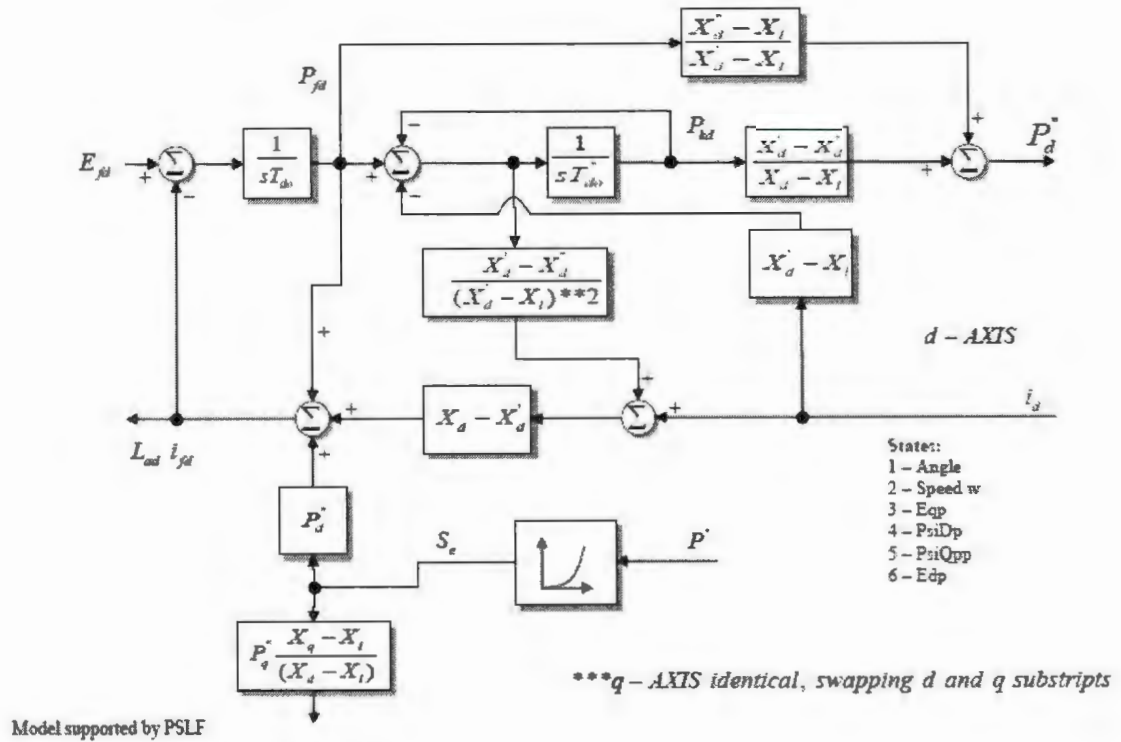


Figure 3.14 GENROU Direct Axis Model [5]

The q-axis model is identical as the direct one in Figure 3.14, substituting d by q. In the GENROU Model, the  $R_a$ , H and D are all included as the Classical Model.  $X_l$  is specified as the leakage reactance.  $X_d$  and  $X_q$  are the synchronous reactances regarding to the steady-state process;  $X'_d$  and  $X'_q$  are the transient reactances reflecting the transient process;  $X''_d$  and  $X''_q$  represent the subtransient ones, which indicate the dampers' effect in the rotor. There are four important time constants in this model: transient open circuit time constant  $T'_{d0}$  and  $T'_{q0}$ , and subtransient open circuit time constant  $T''_{d0}$  and  $T''_{q0}$ . These

time constants can be evaluated by testing the times spent by the d-axis and q-axis stator flux and the terminal voltage on responding to a field voltage change in open circuit cases [17].

Referring to Figure 3.13, the time constants  $T''_{d0}$  and  $T''_{q0}$  also reflect the initial quick changes in the subtransient period, and the time constant  $T'_{d0}$  and  $T'_{q0}$  reflect the slower changes during the transient period.

### **3.6 Case Studies**

In order to estimate the effect by the fault clearing time on the power system transient stability, different studies based on three systems are analyzed in the PowerWorld Simulator software. The three-bus system is selected as an example of a simple system, and the nine-bus system and 37-bus system are selected to exemplify larger and more complex systems. For the fast clearing scenario, a clearing time of 0.1 seconds is employed, since a typical primary fault clearing time around 6 cycles (0.1 seconds) is adopted in power systems [9].

### 3.6.1 Three-Bus System (One Machine to Infinite Bus System)

The aforementioned simple three-bus system is simulated first. The system diagram is showed in Figure 3.6. A fault is applied at 1.0 second at Bus 3, and the fault is cleared by disconnecting the switches at the two ends of the fault branch after different clearing times. The generator is modeled by the GENCL model, with  $H = 3.0$ ,  $D = 1.0$ , and  $X'_d = 0.3$  in 100 MVA base. [9]

If the fault clearing time is set to be 0.1 seconds, the system is stable as Figure 3.15 and 3.16 show. The rotor angle of the generator begins to oscillate at the instant the fault is applied. However, the oscillation decreases due to the damping torque. The voltage drops dramatically as the fault occurs, but recovers soon due to the fault clearance.

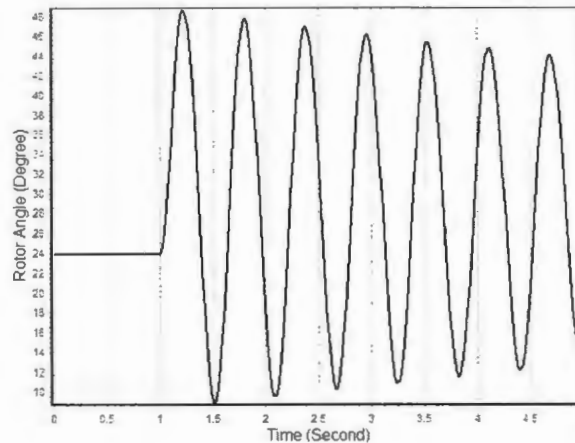


Figure 3.15 Three-Bus System Generator Rotor Angle Variations with a Fault at Bus 3 and Clearing Time

0.1 s

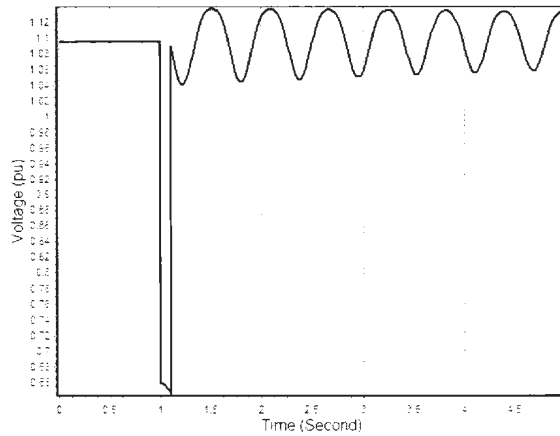


Figure 3.16 Bus 1 Voltage Variation in Three-Bus System

with a Fault at Bus 3 and Clearing Time 0.1 s

However, if the fault clearing time is adjusted to 0.4 seconds after the fault, the acceleration area for the generator in Figure 3.9 will be too large, and the deceleration area is not large enough. As a result, the system becomes unstable. The Figure 3.17 shows the rotor angle of the generator. It keeps increasing and never returns.

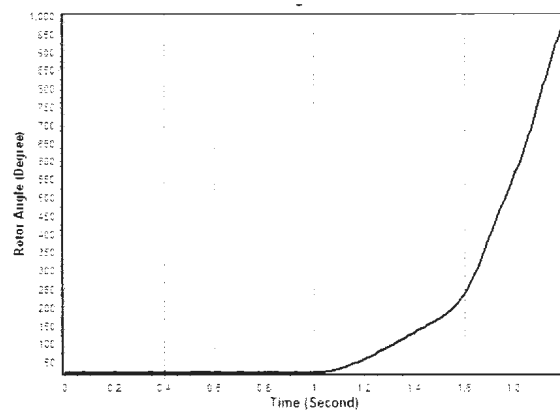


Figure 3.17 Three-Bus System Generator Rotor Angle Variations with a Fault at Bus 3 and Clearing Time

0.4 s

Compared to the Figure 3.4 and 3.5 obtained by the MATLAB software in Section 3.2, Figure 3.15 and 3.17 agree with them. Since the rotor angle of the generator increases dramatically, the voltage fluctuate up and down severely. The plot of voltage in this case obtained by the software does not convey any information.

### 3.6.2 Nine-Bus System

Fast fault clearing can also be employed in larger and more complex power systems to improve power system stability performance. A nine bus system in the following figure is introduced and analyzed. This system comes from the PowerWorld Simulator software sample systems.

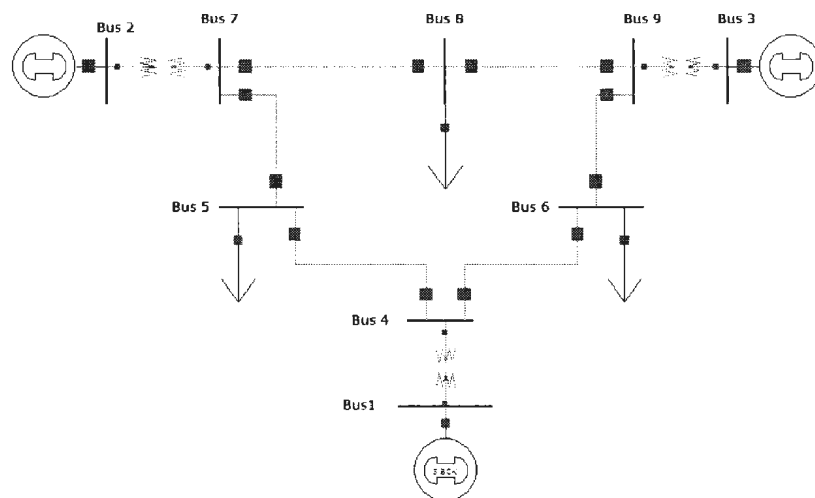


Figure 3.18 Single Line Diagram of a Nine-Bus System

After a basic power flow calculation, the load demand and the generation schedule is summarized in the table as below :

Table 3.1 Summary of the Nine-Bus System Case Information

Power System Type	Load Demand		Generation Schedule	
	Real Power (MW)	Reactive Power (MVar)	Real Power (MW)	Reactive Power (MVar)
9 Buses	315	115	320	23

A more detailed generator GENROU model is selected. Simulations are done in the PowerWorld with a three-phase-to-ground fault occurring on the transmission Line 6-9 at 1.0 second. The fault is cleared at different clearing times by disconnecting the relevant branches.

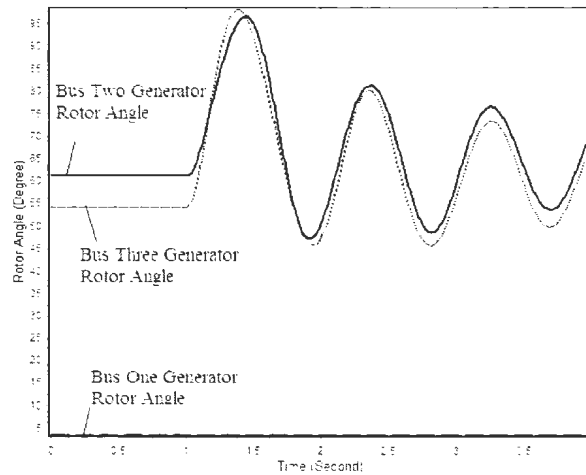


Figure 3.19 Nine-Bus System Generator Rotor Angle Variations with a Fault at Line 6-9 and Clearing Time

0.1 s

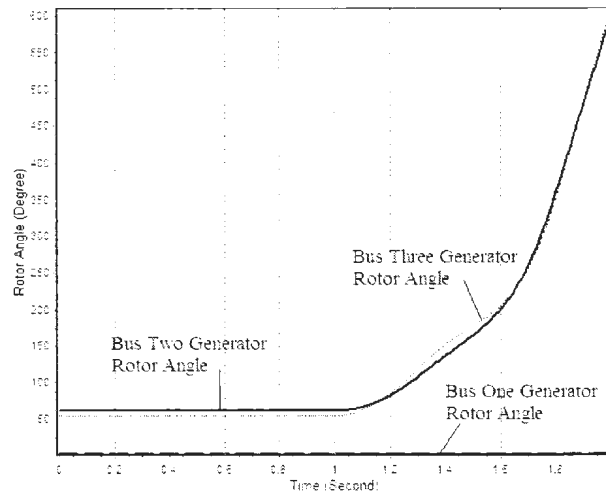


Figure 3.20 Nine-Bus System Generator Rotor Angle Variations with a Fault at Line 6-9 and Clearing Time 0.3 s

With less fault clearing time as Figure 3.19 shows, the generator rotor angles can finally return to steady-states. In Figure 3.20, the generator rotor angles keep increasing and the system loses stability because the fault is cleared too slowly. In large systems, a short fault clearing time also help the rotor angles of generators to maintain stable and enable the system to obtain more stability margins.

### 3.6.3 37 - Bus System

In order to justify that the fast fault clearing method is also suitable for large complex power systems' transient stability enhancement, the fifth study is conducted based on a 37 - bus system in PowerWorld. 9 Generators, 26 loads, 8 switched shunts and

43 transmission lines make up of this system. The system diagram is shown in Figure 3.21.

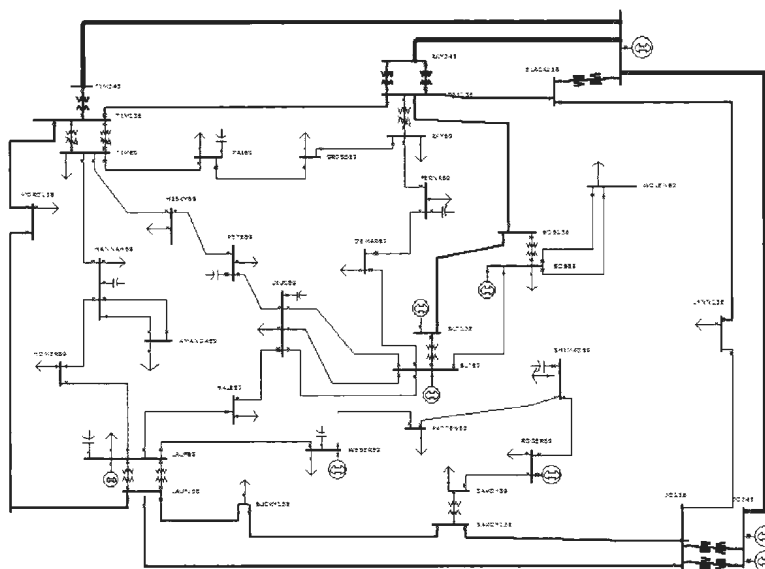


Figure 3.21 Single Line Diagram of a 37 - Bus System

The load demand and the generation schedule is summarized in Table 3.2 :

Table 3.2 Summary of the 37 - Bus Case Information

Power System Type	Load Demand		Generation Schedule	
	Real Power (MW)	Reactive Power (MVar)	Real Power (MW)	Reactive Power (MVar)
37 - Bus	808.7	283.6	818.1	110.4

GENCL models for generators are adopted in this system. A three-phase-to-ground fault case at 1.0 second on the Line Slack 345- Jo 345 is simulated in the PowerWorld

software. Different fault clearing times of 0.1 seconds, 0.6 seconds, and 2 seconds are tested.

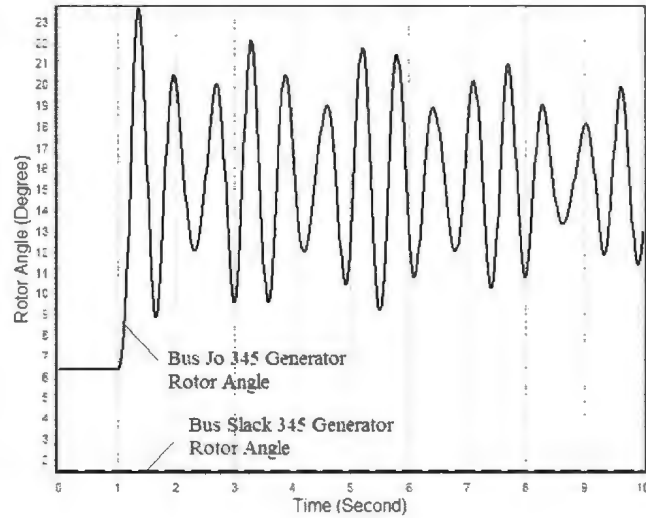


Figure 3.22 37 - Bus System Bus Jo Generator Rotor Angle Variation regarding to the Slack Bus Generator with a Fault at Line Slack 345- Jo 345 and CT = 0.1 s

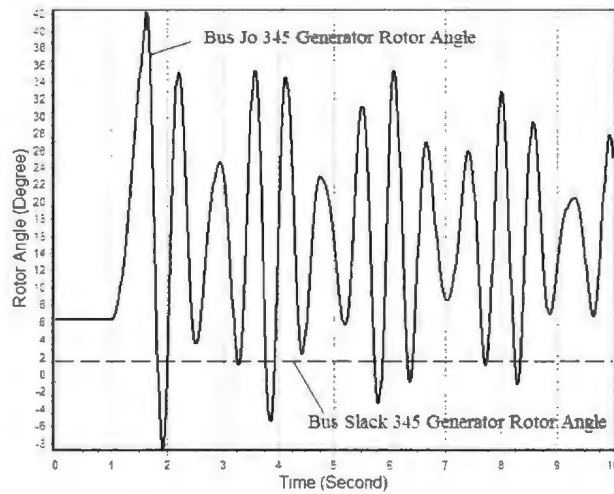


Figure 3.23 37 - Bus System Bus Jo Generator Rotor Angle Variation regarding to the Slack Bus Generator with a Fault at Line Slack 345- Jo 345 and CT = 0.6 s

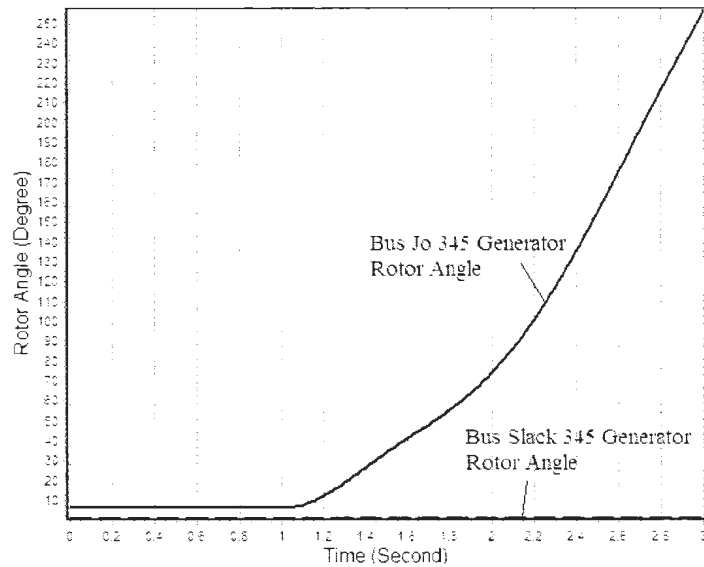


Figure 3.24 37 - Bus System Bus Jo Generator Rotor Angle Variation regarding to the Slack Bus Generator with a Fault at Line Slack 345- Jo 345 and CT = 2 s

The above three simulations and figures indicates that the Bus Jo Generator rotor angle oscillate slightly when the fault clearing time is small, and the oscillation grows larger as the fault clearing time increases. In Figure 3.24, a two seconds fault clearing time is employed, and the generator loses its transient stability by a fast growing rotor angle without boundary. A conclusion can be made that, in large power systems, the fault clearing time is also crucial to the stability maintenance. Employing a short clearing time enable the generators in the system reaching steady states with smaller oscillations and by less time. A large fault clearing time may lead to the generators' losing synchronisms and cause the whole system to become unstable. The losses of generations and loads may occur. Even a large area blackout may be triggered.

### **3.7 Conclusion**

In this chapter, the influence of the fault clearing time on the power system transient stability is discussed. From all the analysis and simulations, it is concluded that limiting the fault clearing time will help to smooth the rotor angle oscillations and provide more stability margins. The system can theoretically remain stable given a fault clearing time less than the critical clearing time (CCT). In summary, the control of the fault clearing time is an effective and direct method to enhance the power system transient stability.

## **Chapter 4**

# **Transient Stability Enhancement through High Speed Excitation**

### **4.1 Introduction**

In modern power systems, generator excitation systems are widely employed to adjust generator field currents (voltages) and to maintain generator terminal voltage levels. Automatic control instruments are adopted, and high speed responses are available because of the developments of such systems. High speed excitations are the excitation systems with small time constants in their block diagrams. For a high speed excitation, the quick response towards voltage drop contributes to the system transient performances during a large disturbance. This chapter presents details on high speed excitation systems and their effects on transient stability enhancement.

## 4.2 Typical Excitation System

For a synchronous generator which is generating electric power, the energy is transferred from the prime mover to the armature winding through the magnetic field caused by a field current. The DC (direct current) excitation creates a rotating magnetic field, which cuts the coils, and electric potential is created in the stator armature windings. In this circumstance, if the transmission lines work well and the loads are connected, electric power can be transmitted into the power grid through the armature current flow.

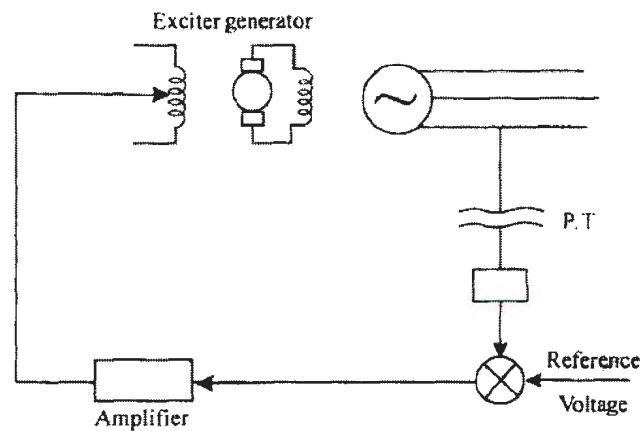


Figure 4.1 Excitation Control [18]

As Figure 4.1 shows, in order to control the generator excitation, the generator terminal voltage is monitored and compared with the reference voltage. The error signal controls the exciter generator after being amplified.

Field currents are generated and controlled by excitation systems. The values of the generator internal voltages vary with the strength of the magnetic field, as well as the field currents [19]. Therefore, providing a larger excitation current within boundaries will cause a stronger magnetic field to appear, resulting in the raise of the internal voltage level, as well as the generator terminal voltage.

In addition, a stable generator terminal voltage helps to stabilize the whole systems' voltage level. Excitation systems are crucial to the power system operation and automatic control that its main function is voltage regulation. Exciters directly provide field currents to generators, generating magnetic fields to transfer the mechanical energy from the prime mover to the electrical energy in the stator coils.

There are different types of exciters - for example, the DC exciter, the AC exciter, and the static exciter. Correspondingly, there are many types of excitation systems, and examples are explained in detail in Section 4.3. A typical excitation system contains the following main components: exciter, automatic voltage regulator (AVR), feedback stabilizer, etc. The block diagram of a typical IEEE Type I excitation system with generator [20] is shown below.

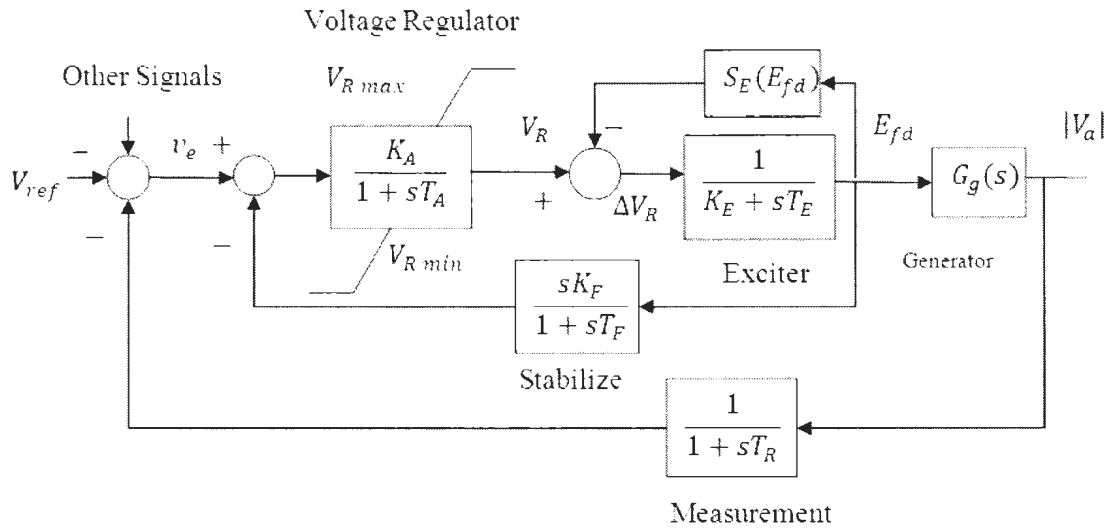


Figure 4.2 Block Diagram of Type I Excitation System and Generator [20]

The automatic voltage regulator (AVR) obtains the error signal  $v_e$  by comparing the measured generator terminal voltage and the reference voltage signal. It is the main part of the excitation system which regulates the voltage as a controller. For example, in the control part, if a higher target voltage is required, the  $V_{ref}$  can be adjusted higher, leading to a larger  $v_e$ . The voltage regulator can also be treated as an amplifier which amplifies the error signal by  $K_A$ . After the delayed amplifier,  $V_R$  is limited within a boundary.

For the exciter part, the amplified signal  $\Delta V_R$  plus the saturation compensation signal serves as the input of the exciter block. According to reference [18] and [20], considering the exciter field resistance  $R_e$  and inductance  $L_e$ , the input equals to  $\Delta V_R = R_e \Delta i_e + L_e \frac{d(\Delta V_R)}{dt} (\Delta i_e)$ . The output  $\Delta E_{fd} = K_i \Delta i_e$ , with  $K_i$  the coefficient which reflects the relationship between  $\Delta E_{fd}$  and  $\Delta i_e$ . Therefore, the exciter transfer function can be

obtained by  $\frac{\Delta E_{fd}}{\Delta V_R} = \frac{K_i \Delta i_e}{R_e \Delta i_e + L_e \frac{d(\Delta V_R)}{dt} (\Delta i_e)} = \frac{K_i}{R_e + L_e \frac{d(\Delta V_R)}{dt}}$ , and the one in the frequency domain

is

$$\frac{\Delta E_{fd}(s)}{\Delta V_R(s)} = \frac{K_i}{R_e + L_e s} = \frac{\frac{K_i}{R_e}}{1 + \frac{L_e}{R_e} s} = \frac{K_E}{1 + T_E s} \quad (4.1)$$

$K_E$  is the exciter gain, and  $T_E$  is the exciter time constant. However, in the IEEE standard diagram, this block is represented as  $\frac{1}{K_E + s T_E}$  for convenience.  $K_E = \frac{R_e}{K_i}$ , and  $T_E = \frac{L_e}{K_i}$ .

If the excitation field current is produced by a DC or an AC generator, the feedback block  $S_E(E_{fd})$  is necessary in the exciter model, representing the effect of the exciter saturation. The relationship between the exciter field current and the field voltage becomes nonlinear as the air-gap flux is saturated. The stabilizer block is also necessary to the DC and AC excitation systems in order to stabilize their dynamic performance by derivative control, which compensates the total phase lag by a leading phase component.  $T_F$  is the time constant in this stabilizer part. [17][18]

Finally, as the result of the control,  $|V_a|$  varies with the voltage regulation. For the measurement part, the  $|V_a|$  value is obtained by a sensor and goes through a feedback loop to the beginning.  $T_R$  is the measurement time constant. Since a quickly boosted terminal voltage can help with the voltage and transient stability performance, in order to speed up these procedures and make the excitation system to respond quicker, shorter

time delays in all blocks should be employed. The values of  $T_R$ ,  $T_F$ ,  $T_A$  and  $T_E$  should be very small.

The AVR has two main functions from the view of power system voltage stability: first, adjusting the generator terminal voltage to a specific value; second, helping to control the reactive power variation through the adjustment of the voltage level, which also contributes to the voltage stability enhancement, especially when the load is heavy [19]. For the transient stability enhancement, AVR also plays a significant role, due to its fast reaction to faults and disturbances in the power system. Once a sudden drop of voltage level is detected by the excitation system, the AVR can quickly receive a signal from the comparator, offer a proper voltage regulation signal to the exciter, and finally boost the terminal voltage to enhance the transient stability. A detailed analysis will be provided in Section 4.4.

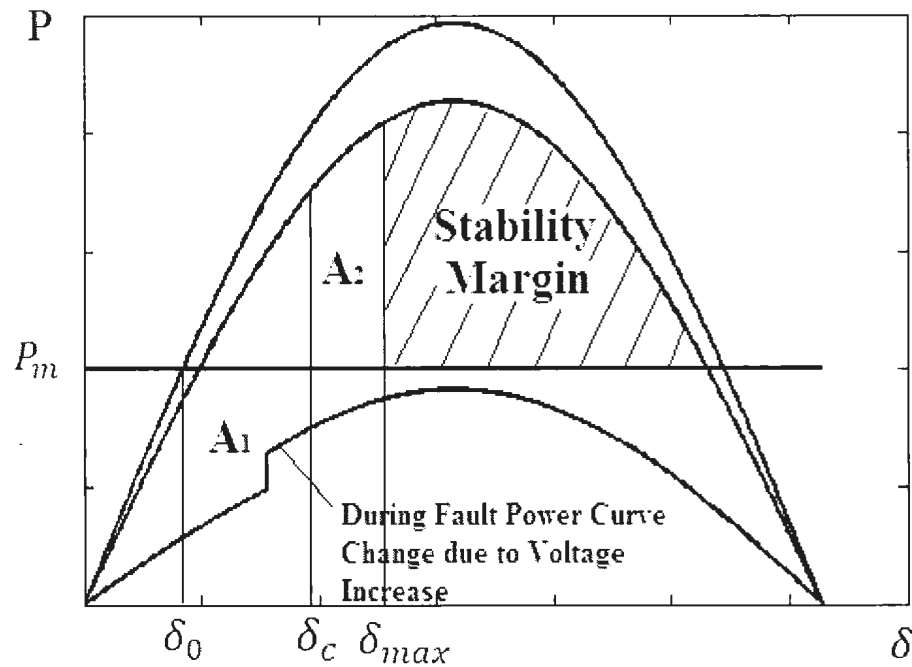


Figure 4.3 High Speed Excitation's Contribution

From the equal area criteria point of view and Figure 4.3, the during fault power curve rises as the high speed excitation system boosts the terminal voltage. The  $A_1$  acceleration area decreases, and the  $A_2$  deceleration area reduces as well ( $\delta$  stops to increase when  $A_2 = A_1$ ). Therefore, the stability margin becomes larger correspondingly with the effect of the high speed generator excitation system. More clearing time can be allowed under this circumstance, and the generator suffers less rotor angle deviation.

### 4.3 Classification of the Excitation Systems and Auxiliary Systems [17][18]

In the development history of the excitation systems, there are three types: DC excitation systems, AC excitation systems, and static excitation systems. Among those three, the DC excitation systems are the oldest type and were employed in power systems in early times. As the technology developed, they were replaced by the other two types gradually, but some early facilities are still using them.

DC excitation systems obtain the generator field current directly from a DC generator. This DC generator can be self-excited or separately excited. A DC excitation system with amplidyne voltage regulator is shown below, and it is a typical separately excited system.

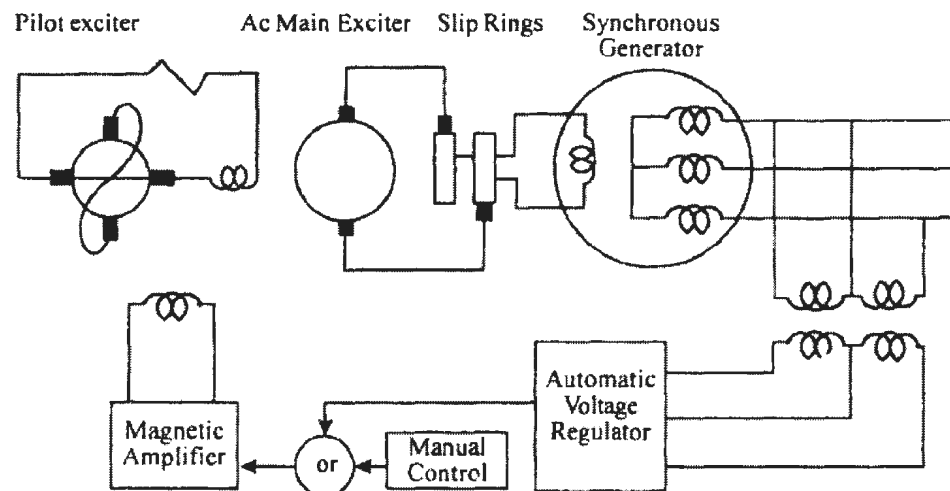


Figure 4.4 DC Excitation System with Voltage Regulator [18]

In the DC excitation system, as shown in Figure 4.4, the exciter provides DC field currents to the generator rotor through slip rings. The voltage regulator collects signals from the main generator terminal, and the control signal from it imposes on the amplidyne which serves as the field control component for the DC exciter. The amplidyne is a typical rotating amplifier, which provides the DC field current to the exciter. The amplidyne, as a “buck-boost” converter, enables the exciter field current to change. [17]

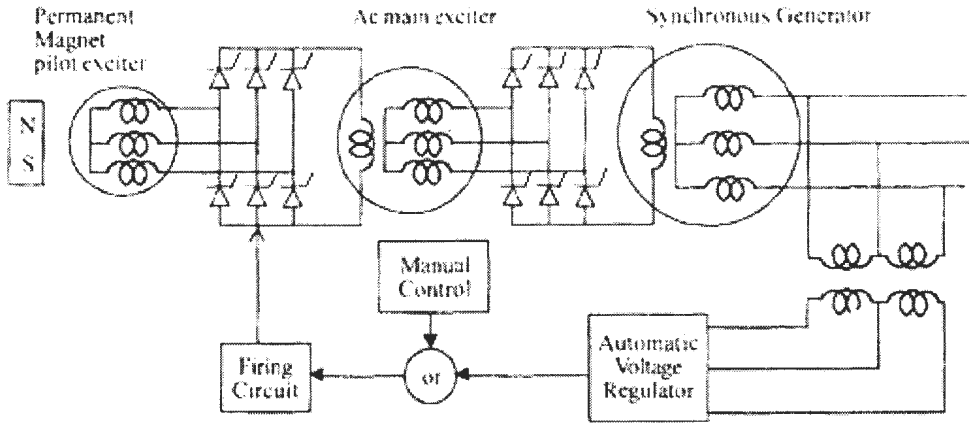


Figure 4.5 AC Alternator - Type Excitation System [18]

Figure 4.5 shows a typical AC excitation system - brushless excitation scheme. This AC excitation system usually employs an AC machine which is mounted on the same shaft with the generator rotor to generate AC power, and then transfer the alternating current into direct current by rectifiers, such as stationary diodes, and finally reach the rotor of the main generator. A permanent magnet pilot exciter is often used to provide the field current to the AC main exciter. The Automatic Voltage Regulator receives input

signals from the generator terminal, coordinates with manual control, and controls the exciter by controlling the gate pulses of the thyristors located at the terminal of the permanent magnet pilot exciter.

Though the AC excitation system does not obtain a DC field current directly as the DC excitation system does, the advantage of this design is that the exciter uses the same shaft as the main generator, which ties the system more firmly and has less time delays in the control processes than the DC excitation systems. Its responses to error changes are quicker than the DC excitation system, which contributes to the transient stability enhancement.

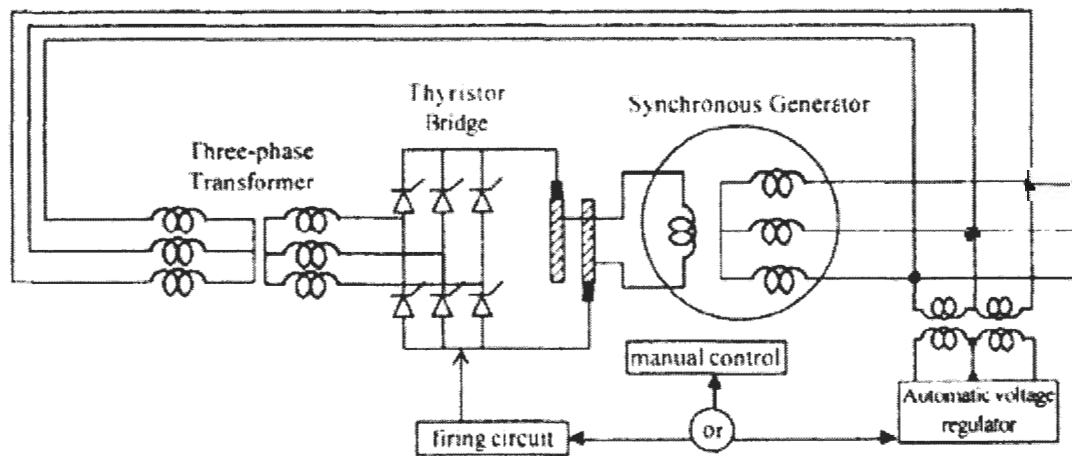


Figure 4.6 AC Static- Type Excitation Systems [18]

The static excitation system is even more advanced and better for the system transient performance improvement. As Figure 4.6 shows, the power source of the exciter

field current comes from the main generator or the station auxiliary bus, and the voltage is limited by adopting a transformer. The current rectifier is still required in order to transfer the AC current to the DC field current to create a magnetic field in the generator air gap. The exciter field is controlled by varying the thyristor firing angle. There is no individual source for the exciter. Therefore, the relationship between the exciter and the main generator can be closer, leading to an even quicker detection and response in the exciter part providing any change in the main generator part or in the system. The time constant in this type of system is quite small.

In addition, there are three common configurations of exciter control systems.

The potential-source controlled-rectifier system employs only the generator terminal voltage potential as the exciter power source after limiting it through a transformer. Therefore, once the generator terminal voltage drops due to a fault, the limitation is obvious: the field voltage will drop in the same way, which is not desirable for maintaining the transient stability. However, if it responds to voltage drop immediately, the corresponding field-forcing reaction can be taken fast.

Compared to the potential-source controlled-rectifier system, the compound-source rectifier system can perform better during a fault which leads to severe voltage drop. In its configuration, not only the main generator voltage is employed, as the generator armature current also supports the exciter. A power potential transformer (PPT) brings the voltage

from the main generator terminal, and steps it down; in the loaded condition, a saturable-current transformer (SCT) also abstracts the armature current information, and transfers it into a current component (extra power) to be added in the exciter as well as the potential component. In most fault conditions, the generator terminal voltages drop, leading to decreases in the voltage sources brought by PPT. However, the current sources inducted from the generator current still works well, providing a strong support in the exciter field-forcing reaction. A quick boost in the exciter voltage is available, which benefits the transient stability enhancement.

Like the compound-source rectifier system, the compound-controlled rectifier excitation system employs two power sources from the generator stator: the terminal voltage and the armature current. It is also capable of quickly dealing with fault conditions. In addition, it uses controlled rectifiers to further improve the performance of the exciters.

#### **4.4 Fast Acting Excitations' Contribution to Transient Stability**

From a power system stability point of view, the fast acting generator excitation system field-forcing is one of the key points that can help to improve the transient stability. The quality of dynamic criteria of excitation systems tends to influence such

stability characteristics in a crucial way. In reference [21], dynamic performances of typical excitation systems are simulated and tested by giving large and small disturbing signals. The capability of field-forcing for the generator can be evaluated by providing large signals whose results reflect the performance of the transient stability in such a power system.

According to reference [21], three significant dynamic criteria can be compared among excitation systems to decide their field-forcing effect and transient stability performances: ceiling current, ceiling voltage, and the excitation system nominal response. The ceiling current is the maximum field DC current that the excitation system can provide to the generator, and the ceiling voltage is the largest DC voltage correspondingly. The excitation system nominal response is a criterion which indicates how rapid the excitation system responds to an increase or decrease in the generator terminal voltage.

Different types of excitation systems can be estimated and compared according to the above three criteria. From the system stability point of view, all excitation systems helpful to the transient stability enhancement are expected to have a fast response character and a high ceiling voltage [18]. The static regulators perform better due to the less time delays.

#### 4.5 Power System Stabilizer (PSS)

Though the automatic voltage regulator adjusts the voltages to the target values, the amplifier gains in this closed loop may lead to even larger rotor oscillations when the load is heavy, and an unwanted instability may occur [18][22]. In order to damp large rotor oscillations, the power system stabilizer (PSS) can be employed, which is an extra input voltage signal  $V_s$  added into the exciter control diagram.

The local signal that the PSS collects and processes is the main generator rotor speed deviation  $\Delta\omega_r$ , and the purpose of PSS is damping the rotor oscillation over during various transient states [17]. The extra input signal for AVR provided by PSS is illustrated in Figure 4.7, and, with the large disturbance cases considered, the output  $V_s$  limits should also be considered.

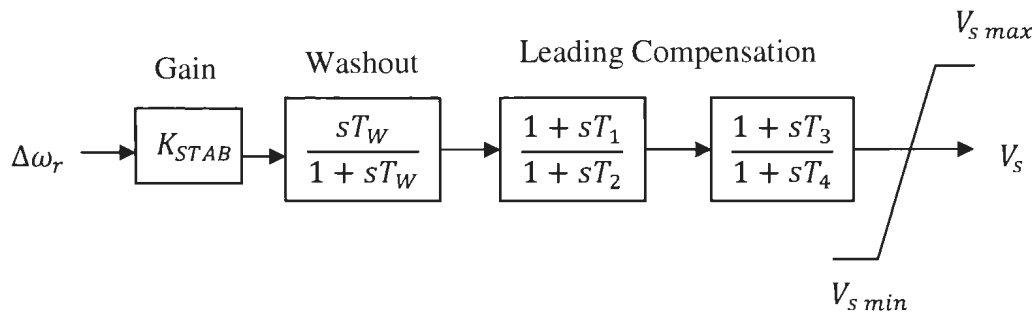


Figure 4.7 Control System of PSS [17]

As Figure 4.7 shows, the transfer function for the PSS is

$$G_{PSS}(s) = \frac{K_{STAB} s T_W}{1 + s T_W} \frac{[1 + s T_1][1 + s T_3]}{[1 + s T_2][1 + s T_4]} \quad (4.2)$$

This transfer function indicates the relationship between the speed deviation and the extra voltage signal  $V_s$  after Laplace transformation.  $s$  is the complex augment transferred from the time domain function. The gain  $K_{STAB}$  decides how much the damping is employed to eliminate the undesired oscillation, and the washout block is a high-pass filter, enabling the standard rotating speed signal  $\omega_r$  to pass and suppressing the instability [17]. The time constant  $T_W$  is chosen to be between 1 to 20 seconds to successfully pass the desired rotating speed signals as well as avoid unwanted generator terminal voltage excursions [17]. The leading compensation blocks greatly compensate the phase lags created in the original closed loop without the PSS, in which the  $T_1, T_2, T_3$ , and  $T_4$  are four time constants which are tuned to compensate the phase lag. The voltage limits prevent the  $V_s$  grows too large to lead the excitation system to saturate [18].

The PSS system connects to the main exciter control loop as shown in the following diagram.

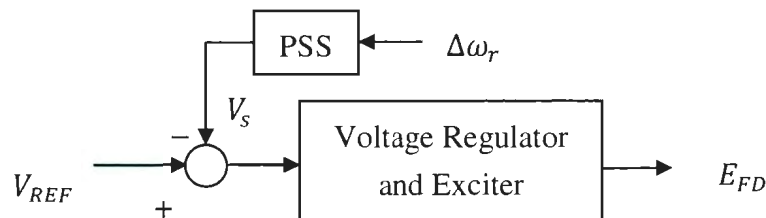


Figure 4.8 Connected Power System Stabilizer [18]

## 4.6 Case studies

In order to discuss the effect of the Automatic Voltage Regulator and the Power System Stabilizer, two systems are studied: one thermal generation station connected to an infinite bus system and the Nine-Bus system.

### 4.6.1 One Generator Connected to an Infinite Bus System

This system is taken from reference [17]. The single line diagram is shown as Figure 4.9, with four 555 MVA, 24 KV, 60 Hz generators combined together and represented by a single one. The pre-fault system condition (2220 MVA, 24 kV base) is as below:

$$P = 0.9 \text{ p.u.}, Q = 0.436 \text{ p.u.}, E_4 = 1.0 \angle 28.34^\circ \text{ p.u.}, E_2 = 0.9008 \angle 0^\circ \text{ p.u.}$$

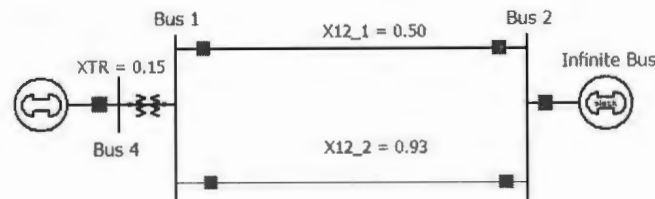


Figure 4.9 System Diagram of a Generation Station towards an Infinite Bus System

The system summary is as below:

Table 4.1 Summary of the One Generator Connected to an Infinite Bus System

Power Generation in the Station		Power Absorbed by the System		Voltage		
Real Power (MW)	Reactive Power (MVar)	Real Power (MW)	Reactive Power (MVar)	Bus One Voltage (p.u.)	Bus Two Voltage (p.u.)	Bus Four Voltage (p.u.)
1998	967.9	1998	-87.06	0.9443∠20.12°	0.9008∠0°	1.0∠28.34°

A three-phase-to-ground solid fault is applied to the end which is close to Bus 4 on the second transmission line between bus 1 and bus 2 at  $t=1.0$  second, and the fault is cleared by disconnecting the two switches at both ends of that line after a clearing time of 0.066 seconds. Three scenarios are simulated in the PowerWorld Simulator: a system with constant generator field voltage, a system with AVR only, and a system with AVR and PSS. The generator terminal voltage and the rotor angle variations are monitored.

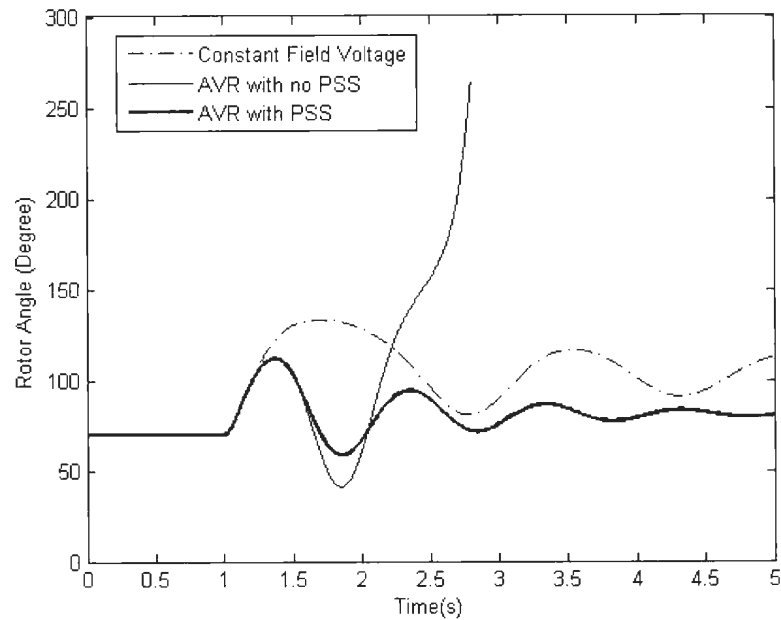


Figure 4.10 Three Scenarios of Rotor Angle Responses for One Generation Station towards an Infinite Bus System with a Fault Clearing Time 0.066 Seconds

As seen from Figure 4.10, though the voltage regulator prevents the rotor angle deviation to grow too large at the first swing, it makes the rotor angle grows to infinity at the second swing, resulting from the large oscillations introduced by the amplifier gains in the AVR closed loop, which is unacceptably unstable. This unstable case doesn't happen in every system or every fault condition. Under other circumstances, only larger oscillations may occur in generator rotor angles without going out of steps, but spending more time to damp the oscillations is inevitable. Compared to the constant field voltage case, the system with both AVR and PSS not only has more stability margin with smaller rotor angle deviations, but also damps the oscillation more quickly. Therefore, the

excitation system consisting of a voltage regulator and a power system stabilizer is helpful to enhance the transient stability performance.

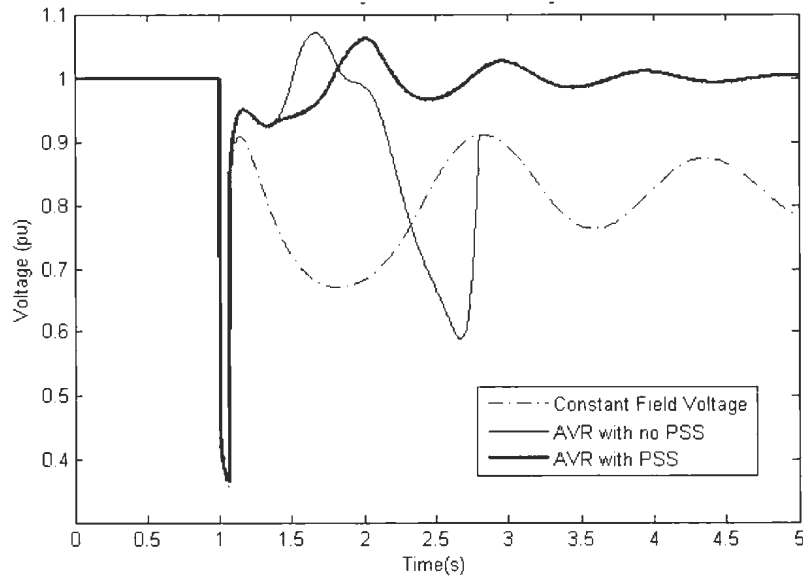


Figure 4.11 Three Scenarios of Terminal Voltages for One Generation Station towards an Infinite Bus System with a Fault Clearing Time 0.066 Seconds

From the generator terminal voltage point of view, the Figure 4.11 shows that, with the help of AVR and PSS, the terminal voltage can recover to the normal level fast after the fault clearance. Without a proper exciter, the field voltage remains constant, but large voltage dips occur after the fault clearance, which are undesirable. The trend of the dash-dot curve indicates that the voltage will return to the previous level around 1.0 per unit in this case, which severely influences the power quality and unstable voltage collapses may occur as well, because a system cannot safely operate under a low voltage level for a long

time. In a word, only when an excitation system with PSS is employed, the system remains stable given such a fault in the system and a clearing time of 0.066 seconds.

In order to better estimate the three different scenarios, the critical clearing times can also be compared. The critical clearing times for the above three scenarios are found through simulations.

Table 4.2 Critical Clearing Time and Cycle of Different Scenarios for One Generation Station towards Infinite Bus System

Scenario Description	Constant Generator Field Voltage	Generator with AVR (no PSS)	Generator with AVR and PSS
CCT (ms)	66	N/A	95
Cycle	3.96	N/A	5.7

According to Table 4.2, the generator with AVR and PSS allows a longer critical fault clearing time than the generator without AVR and PSS does. The generator with AVR without PSS cannot stay stable once a fault occurs, no matter how fast the fault is cleared. A conclusion can be drawn that the excitation system with AVR and PSS can successfully improve the system transient stability performance, and the stability margin is also enlarged. For the AVR without PSS case, the system cannot return to an equilibrium state, since the AVR amplifies the rotor angle oscillations, and the second swing is always too large no matter how much the clearing time is.

## 4.6.2 Nine-Bus System

The nine bus system studied in Section 3.6.2 is evaluated and analyzed in this chapter. Its system diagram is as Figure 4.12, and the power generation schedule is summarized in Table 3.3.

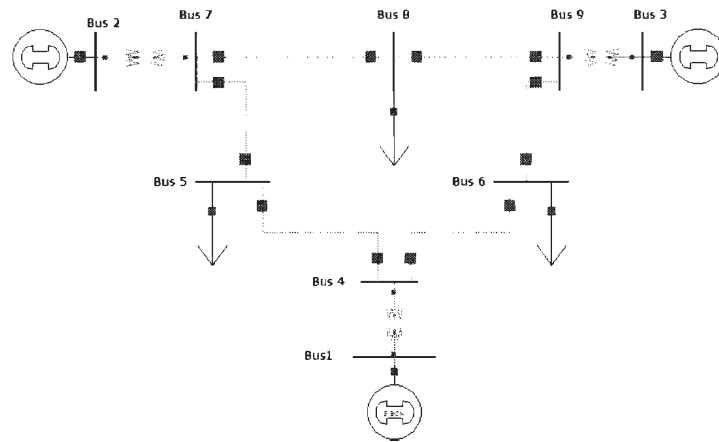


Figure 4.12 Single Line Diagram of a Nine-Bus System

A three phase to ground fault is applied to Line 7-8 at  $t=1.0$  seconds, and the fault is cleared after 0.1 seconds. For generators, a GENROU model is employed, an IEEE1 exciter is chosen, and a STAB1 stabilizer is also applied. Using PowerWorld Simulator, three scenarios are simulated: first, the generator has a constant field voltage without AVR or PSS; second, the exciter is used to regulate the terminal voltage; third, a power system stabilizer is added in this system.

The generator rotor angle variations and the terminal voltage in 10 seconds are obtained as follow.

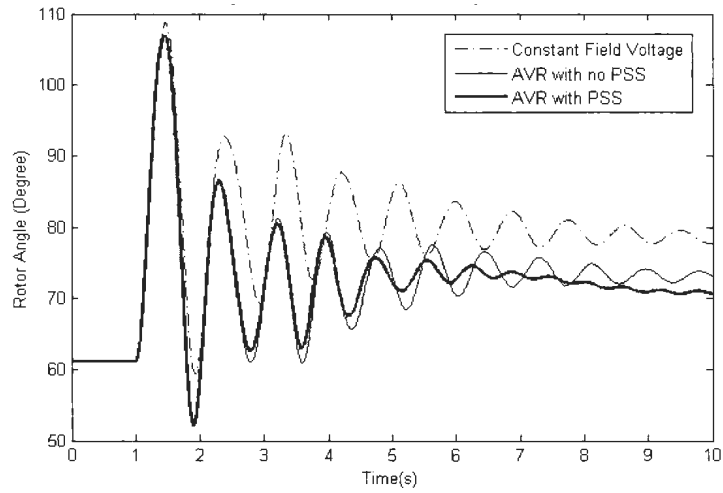


Figure 4.13 Three Scenarios of Generator Two Rotor Angle Responses for Nine-Bus System with a Fault

Clearing Time 0.1 Seconds

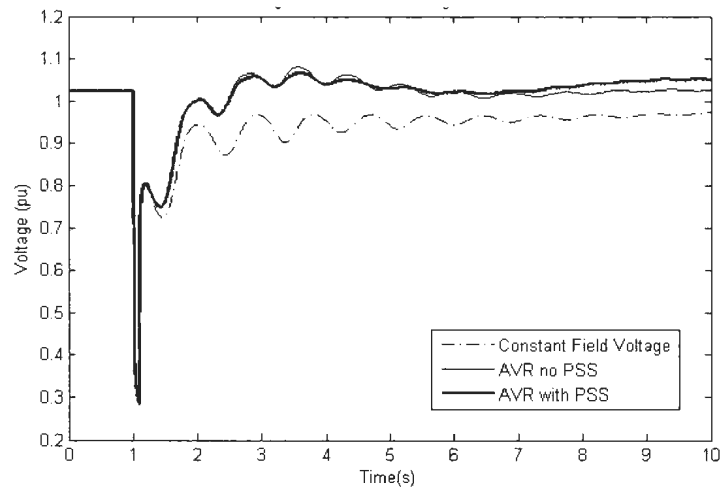


Figure 4.14 Three scenarios of Generator Two Voltage for Nine-Bus System with a Fault Clearing Time 0.1

Seconds

Similarly, through Figure 4.13, it is concluded that the application of high speed excitation system helps to reduce rotor angle deviations comparing the scenario without it. In addition, from Figure 4.14, the generator terminal voltage is greatly enhanced and regulated to the target value because of the exciter. As mentioned before, it is not safe and reliable for a power system to operate in a low voltage level. Therefore, power system exciters are necessary in this case. Moreover, it is also noticed that the PSS does not contribute much on the transient stability enhancement but is helpful to the fast damping of the rotor angle oscillation. It has its drawback as well: due to the PSS, a post fault voltage bias can occur. The terminal voltage increases a little after the voltage regulation.

The critical clearing time after the fault is also explored.

Table 4.3 Critical Clearing Time (Cycle) of Different Scenarios for Nine-Bus System

Scenario Description	Constant Generator Field Voltage	Generator with AVR (no PSS)	Generator with AVR and PSS
CCT (ms)	118	122	122
Cycle	7.08	7.32	7.32

Table 4.3 shows that the generator with AVR allows a longer fault clearing time than the one with constant field voltage does. However, in this case, the generator with AVR and PSS has the same critical fault clearing time with the one with AVR and without PSS. From the above table, it is concluded that this power system stabilizer does not contribute to the transient stability enhancement directly, because the critical clearing times are the

same between the scenarios of applying an AVR with and without a PSS. However, the generator with an excitation system indeed has more transient stability margin that a fault is allowed to be cleared more slowly than the one with constant field voltage.

In summary, the excitation system helps to improve the transient stability performance by quickly reducing the rotor angle deviation, and adjust the generator terminal voltages after faults. The function of PSS is mainly damping the rotor angle oscillations quickly in this case, but it has a side effect that it may lead to a voltage bias after the AVR works.

#### **4.7 Conclusion**

In this chapter, typical excitation systems are introduced, and the theory of the power system transient stability enhancement through high speed excitation is also explained. A fast acting excitation system helps to boost the field voltage quickly to increase the generator terminal voltage, leading to an improvement in the power system transient stability performance through raising the during-fault power transmitted. An excitation system with a power system stabilizer can also quickly damp the oscillations during transient states, contributing to the transient stability enhancement as well. Case studies are presented to illustrate the effectiveness of excitation systems and stabilizers on power

system transient stability performance. The generator and excitation system parameters in the case studies are presented in the Appendix.

# **Chapter 5**

## **Static VAR Compensator and its Contribution to Transient Stability Improvement**

### **5.1 Introduction**

The power systems have undergone changes in recent years due to the innovation of Flexible AC Transmission System (FACTS). In Chapter 5, one of the most commonly used FACTS devices – Static VAR Compensators (SVC) – are discussed. The basic theory of SVC is introduced, and its applications and advantages are explained. This chapter focuses on the contribution of SVC to the power system transient stability performance. Some power systems with and without SVCs are analyzed and evaluated.

## 5.2 Flexible AC Transmission System

The real power flow can be expressed by  $P_e = \frac{E'V\sin\delta}{x_{eq}}$  according to Section 3.3, and the power angle  $\delta$  should also be strictly controlled much less than  $90^\circ$  due to stability requirements in steady-states. Therefore, many transmission lines can transfer a relatively small amount of power compared to their thermal limit. Researchers and engineers have been thinking about how to better utilize the potential of the transmission lines to convey more power instead of uneconomically building new transmission lines in case of load demand increases. Flexible AC Transmission System (FACTS) has revolutionized power systems by introducing a power electronic and static controller based system that better controls the transmitted power flow and enlarges the transmission capability [24], [25].

Reference [25] provides a list of definitions relating to FACTS. Because of those devices, high speed and effective controls in the power systems are viable. Compared to the traditional mechanically controlled system, their capability of reacting to dynamic changes is better, too. Currently, two kinds of FACTS compensations exist: series compensations and shunt compensations. Thyristor Controlled Series Capacitor (TCSC) is a typical type of series compensation devices; Static VAR Compensators (SVC) and Static Condenser (STATCOM) are examples of shunt compensation devices.

The introduction of FACTS devices into power systems brings many merits. The series compensation can limit the equivalent system reactance  $X_{eq}$ , so the power transmission capability is enlarged according to  $P_e = \frac{E'V\sin\delta}{X_{eq}}$ . The shunt compensation supports the voltage levels, contributing more than the series compensation to stability maintenance. Reference [26] compares the scenarios of power systems improvements by employing FACTS devices and the increase of transmission line numbers. It reaches a conclusion that the FACTS devices enable the system to satisfy the “N-1” safety criteria with an economic budget close to a “N-0” system (“N-1” safety criteria: After dynamic disturbances, power systems can survive and operate in an acceptable state with only one element in the system lost. For example, one transmission line, one generation unit, or one load unit. “N-0” system: The systems survive after dynamic disturbances without losing any component). It indicates that the FACTS devices can greatly increase the stability margins and work well in the cases of heavy loads.

## 5.3 Static VAR Compensator (SVC)

### 5.3.1 Definition and Significance of SVC

In power transmission systems, the compensation of reactive power is important, especially in the cases of heavy loads. As large real power is transferred from power generation units to loads, the voltage drops in transmission lines lead to a poor voltage performance in the transmission line receiving end. Therefore, much reactive power is needed in order to maintain the voltage level in the systems, as well as to ensure stability. However, it is common that not enough reactive power is provided to power systems, especially at remote areas far from power plants. Sometimes, even adding the reactive compensation from the transmission line equivalent shunt capacitors may not be sufficient. Therefore, extra reactive power compensations are helpful if a power system operates in an overload situation, or if the voltage level needs to be adjusted, SVCs provide solutions for these problems.

SVCs were developed in 1960s, and firstly mentioned in the EPRI Journal in 1986 [24], [26]. They are most commonly used FACTS devices, and reference [25] gives the definition of SVC as following: “A *shunt-connected static VAR generator or absorber whose output is adjusted to exchange capacitive or inductive current so as to maintain or control specific parameters of the electrical power system (typically bus voltage)*”.

### 5.3.2 Configurations and Characteristics of SVC

In order to compensate reactive power, SVCs serve as reactive power generators with little real power exchange with transmission systems. They are configured with a series of special reactors and capacitors in parallel. Five types of structures exist in the modern SVC system: Thyristor-controlled reactor (TCR), Thyristor-switched capacitor (TSC), and mechanically switched capacitor (MSC), and Fixed capacitor (FC). Figure 5.1 shows three common combinations.

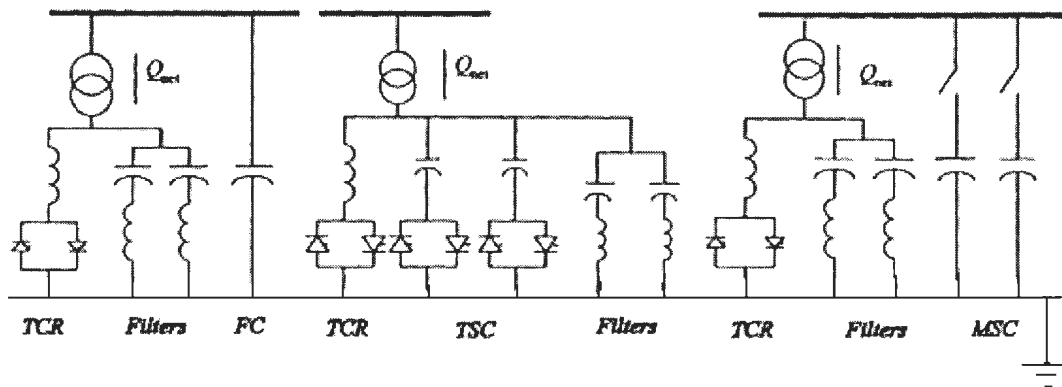


Figure 5.1 Typical Configurations of SVCs [27]

In Figure 5.1, three SVC configurations are presented: Thyristor-controlled reactors, Fixed capacitors and Filters; Thyristor-controlled reactors, Thyristor-switched capacitors, and Filters; and Thyristor-controlled reactors, Filters, and Mechanically switched capacitors. The Thyristor-controlled reactors are used to provide inductive reactive power,

with continuous values within the range available. The Fixed capacitors, Thyristor-switched capacitors and Mechanically switched capacitors are employed as capacitive reactive power sources, with only discrete values obtainable. Mechanically switched capacitors are operated only several times a day by mechanical switches, meeting the requirement of the steady-state reactive power compensation [28]. Fixed capacitors are connected to the transmission line directly without any switch. Therefore, its reactive power compensation remains at a relatively stable level. Filters are used to eliminate the harmonics injected into the power system. The sum of the inductive and capacitive reactive power gives the final reactive power compensation.

The most common SVC configuration is the TCR- TSC type. As illustrated in Figure 5.2, a TCR employs two thyristors in two opposite directions to control the time period that a reactor is connected to the system. Thyristor is a semiconductor power switch that conducts once a trigger current is given to the gate. It opens automatically when the voltage across the thyristor reverses. Part (b) of Figure 5.2 indicates that, with various firing angles  $\alpha$ , the  $i_L$  current flows have different peaks and different conducted periods, which reflects the fact that diverse inductive reactive power has been provided: with a firing angle  $\alpha$ , the conduction angle  $\sigma$  for a thyristor is  $\alpha \leq \sigma \leq \pi - \alpha$  in the positive half-cycle for the voltage; for the negative half-cycle, the angle interval becomes  $\pi + \alpha \leq \sigma \leq 2\pi - \alpha$ .

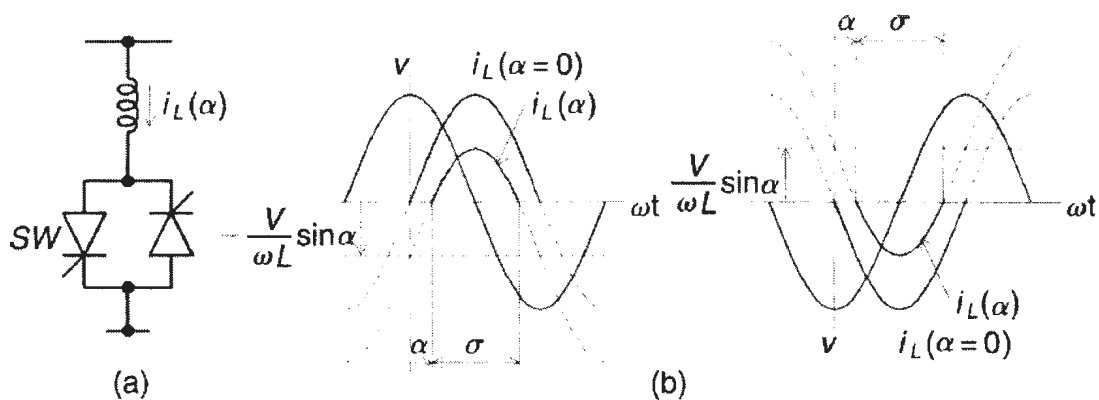


Figure 5.2 Thyristor Controlled Reactor [29]

For a TSC, the shunt capacitors can only be switched on and off, without any firing angle controls. They either connect to the grid or disconnect. The basic TSC-TCR type static VAR generator and its total VAR demand versus VAR output are shown in Figure 5.3.

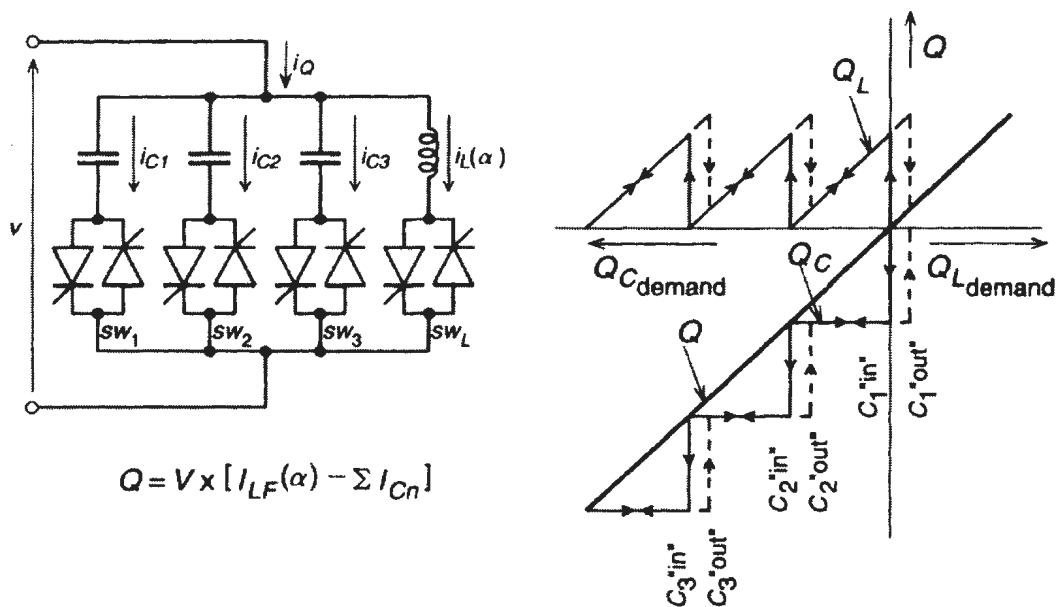


Figure 5.3 TSC-TCR SVC and Its Total VAR Demand versus VAR Output [29]

From Figure 5.3, the individual capacitors can be added to the system one by one, reflecting different reactive power output sums. The reactors serve as the adjustable part, allowing the reactive power amount to be any value within the range:  $Q = V \times [I_{LF}(\alpha) - \sum I_{Cn}]$ .  $I_{LF}$  is the variable current in the controllable reactor, and  $I_{Cn}$  is the current flowing through the connected capacitors.  $V$  represents the voltage at the terminal of this SVC.

### 5.3.3 SVC Model

There are two operation modes for a typical SVC: the voltage regulation mode and the VAR control mode [30]. Under the VAR control mode, the susceptance  $B$  remains constant at  $B_{Cmax}$  or  $B_{Lmax}$ . Under the voltage regulation mode, the terminal voltage versus current relationship is shown Figure 5.4.

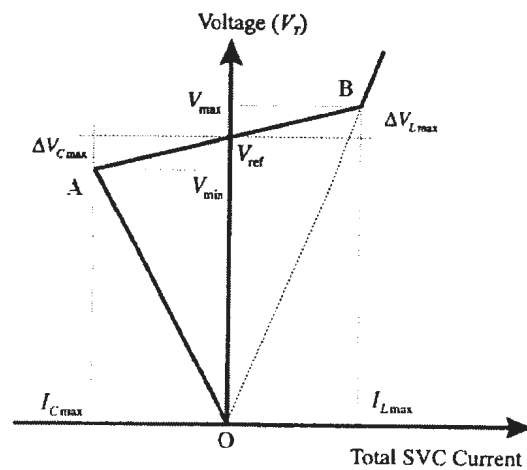


Figure 5.4 V-I Characteristic of SVC [27]

The SVC generally works within the line between point A and point B in steady state, and the slope of the line AB indicates the capability of the SVC to regulate voltages and compensate reactive power. The more the terminal voltage deviates from the reference voltage, the more real or reactive sum current will be excited in the shunt SVC branches to smooth the voltage variation. If the terminal voltage stays at the reference voltage  $V_{ref}$ , or within an acceptable range around  $V_{ref}$  in practice, there will be no current going through the SVC in a whole and no reactive power compensation [27]. If the slope of line AB is defined as a slope reactance  $X_{SL}$ , the terminal voltage during the steady state can also be derived as  $V_T = V_{ref} + X_{SL} \times I_{SVC}$  [27].

There are various SVC models and control algorithms depending on research focuses and targets in power system studies [27][29]. In this chapter, MATLAB/Simulink and Power System Toolbox based in MATLAB are used. The SVC models in these two types of software are explained as below.

### **SVC Model in MATLAB Simulink**

Figure 5.5 presents the SVC and simplified control system block diagram in MATLAB/Simulink.

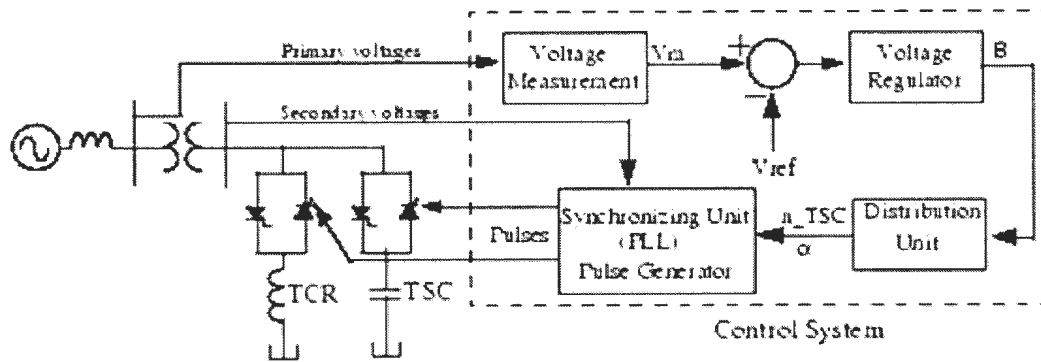


Figure 5.5 SVC and Simplified Control System Block Diagram (Phasor Type)

in MATLAB/Simulink [30]

In this model, the system primary voltage is measured to compare with the reference voltage  $V_{ref}$ , and then goes through a voltage regulator to obtain a corresponding susceptance. The control signal is sent to the distribution units to determine the appropriate number of TSCs that should be connected into the grids, and the value of the firing angle  $\alpha$  for the TCR. A phase-locked loop (PLL) connected to the secondary voltage part is used to enable the pulse generator to create pulses synchronous with the system. The control pulse signals finally reach the TCR and TSC branches' thyristors in order to control their gates.

### SVC Model in Power System Toolbox

Figure 5.6 presents the SVC Model in Power System Toolbox based on MATLAB.

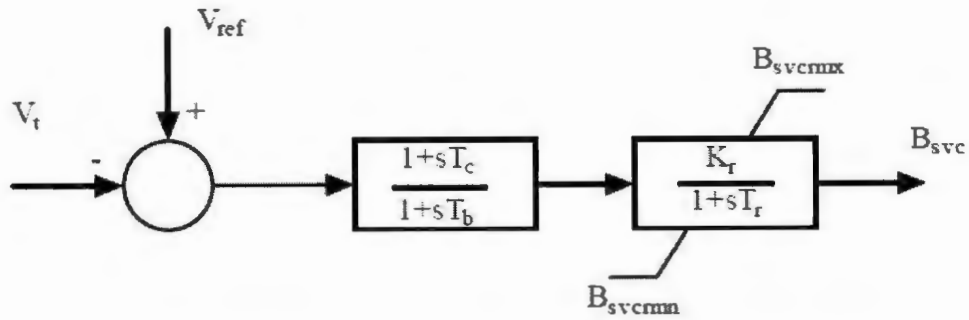


Figure 5.6 SVC Model Block Diagram in Power System Toolbox [31]

The terminal voltage is compared to the reference voltage, with an error signal generated. For the compensator control diagrams,  $T_b$  is a lag time constant, and  $T_c$  is a lead time constant.  $\frac{K_r}{1+sT_r}$  represents the voltage regulator, with the regulator gain  $K_r$  and the regulator constant  $T_r$ . The output susceptance should be standardized within a boundary:  $B_{SVCmax} \leq B_{SVC} \leq B_{SVCmin}$ .

#### 5.3.4 Effects of SVC

Since SVCs have been used in the power systems for several decades, the technologies have been improved, and SVCs have brought about many uses for power systems. As previously mentioned, SVCs enlarge the transmission capability by supporting the line voltage. Moreover, when the power systems are in their steady states, SVCs mainly eliminate the system voltage variations, smooth the effects of continuous load changes, damp oscillations, and the reactive compensation function can also help to

correct power factors to improve the power quality [18]. Furthermore, for the transient process, if systems suffer from sudden large disturbances which lead to severe voltage drops, SVCs react immediately to provide a strong reactive power support, enhancing the system voltage stability and transient stability. This point is illustrated in detail in the following two case studies.

#### 5.4 Case study: Transient Stability Enhancement with SVC

In order to estimate the transient stability enhancement function of SVC, a simple 500 kV system from MATLAB Simulink was evaluated. The system configuration is as follows:

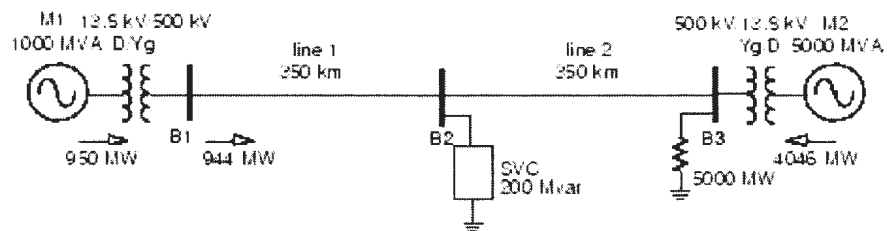


Figure 5.7 500 kV Two Generation Units Power Transmission System Diagram [30]

The system contains two power generation units M1 and M2 with rated power 1000 MVA and 5000 MVA, and 5000 MW resistive load is close to the M2 generation unit. The transmission line from M1 to the load is 700 km long, and the midpoint can be

supported by a SVC. In the steady state, the power transferred from the M1 unit to the system is 950 MW, and this value is 4046 MW for the M2 unit. Those generators are equipped with exciters and power system stabilizers.

A three phase to ground solid fault occurred at 0.1 seconds in the Line 1 (Between B1 and B2), and the fault is cleared by itself after 0.09 seconds. Two scenarios can be simulated: the system with SVC and the system without SVC. The generator rotor angle position differences  $\Delta\theta = \theta_1 - \theta_2$  and the terminal voltage of the M1 Generator were plotted as Figures 5.8 and 5.9. When the SVC is connected to the system, the reference voltage for control is set to 1.0 per unit.

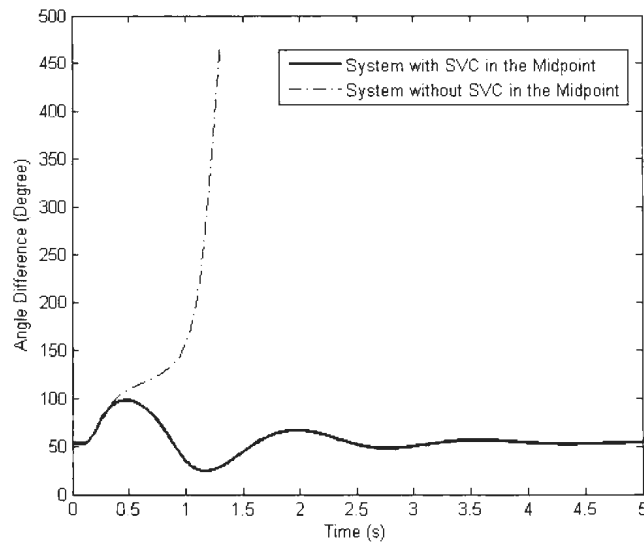


Figure 5.8 Generator One Rotor Angle Differences for 500 kV Two Generation Units Power Transmission

System with a Fault Clearing Time 0.09 Seconds

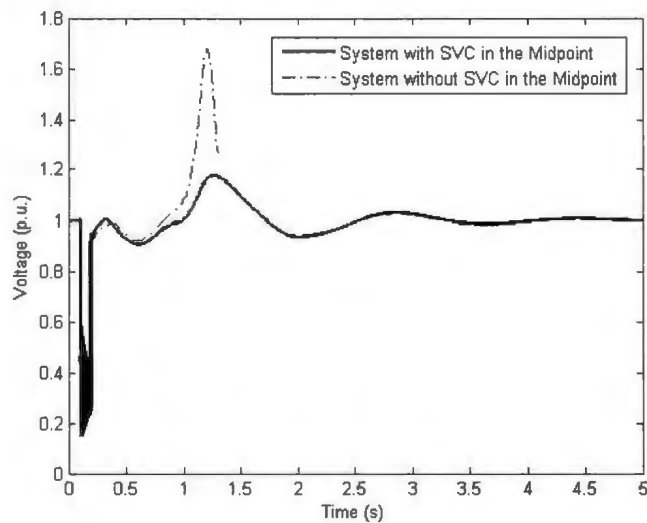


Figure 5.9 Generator One Terminal Voltages for 500 kV Two Generation Units Power Transmission

System with a Fault Clearing Time 0.09 Seconds

Figures 5.8 and 5.9 suggest that this system with a SVC in the Midpoint is beneficial to the transient stability maintenance. If the system operates without a SVC's voltage support, the two generators lose synchronism giving the same fault clearing time 0.09 seconds. Because of the reactive power compensation from the SVC, the system with SVC successfully maintains the transient stability given the 0.09 seconds clearing time after the fault, and the generator voltage is kept in an acceptable level due to the voltage regulation function of the SVC and excitation system.

The Critical Fault Clearing time is summarized in Table 5.1. It clearly shows that the system with a 200 MVAR SVC allows a longer fault clearing time, which indicates that the SVC enlarges the transient stability margin for this system.

Table 5.1 Critical Clearing Time (Cycle) Summary for 500 kV Two Generation Units Power Transmission

System

Scenario Description	System without SVC	System with 200 MVAR SVC ( $V_{ref} = 1.0$ )
CCT (ms)	87.9	101.2
Cycle	5.274	6.072

The SVC's reactive power generation limits can be further explored. Different reactive power limits were evaluated, and the results are shown in Figure 5.10. The figure suggests that the larger SVC a system owns, the better transient stability performance and more transient stability margin a system can have.

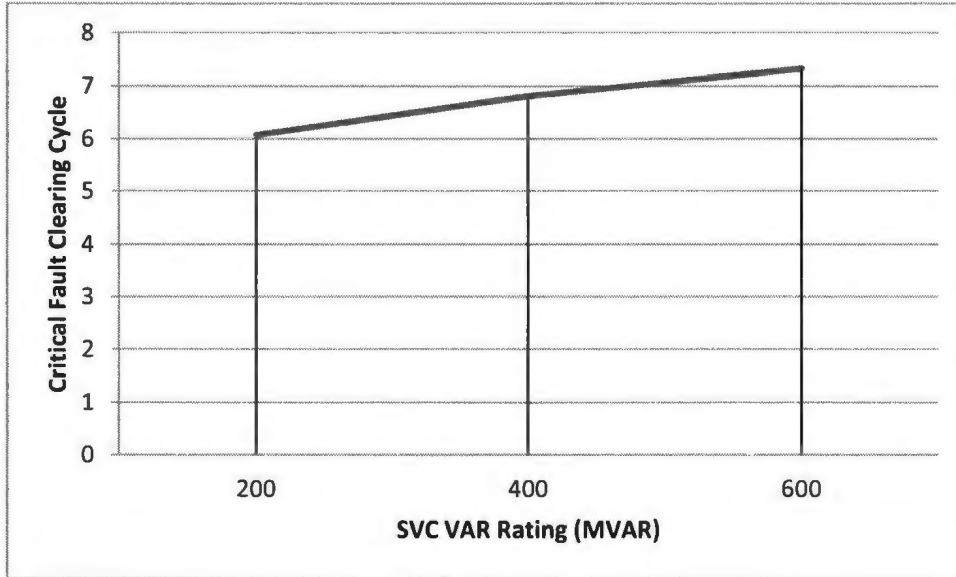


Figure 5.10 Critical Fault Clearing Cycles versus SVC VAR Ratings for 500 kV Two Generation Units

Power Transmission System

## 5.5 Case Study: Transient Stability Enhancement Evaluation in a Two Area Power System

Figure 5.11 represents a two-area with added load area system from [31]. It has five generation units included and a SVC available in Bus 21.

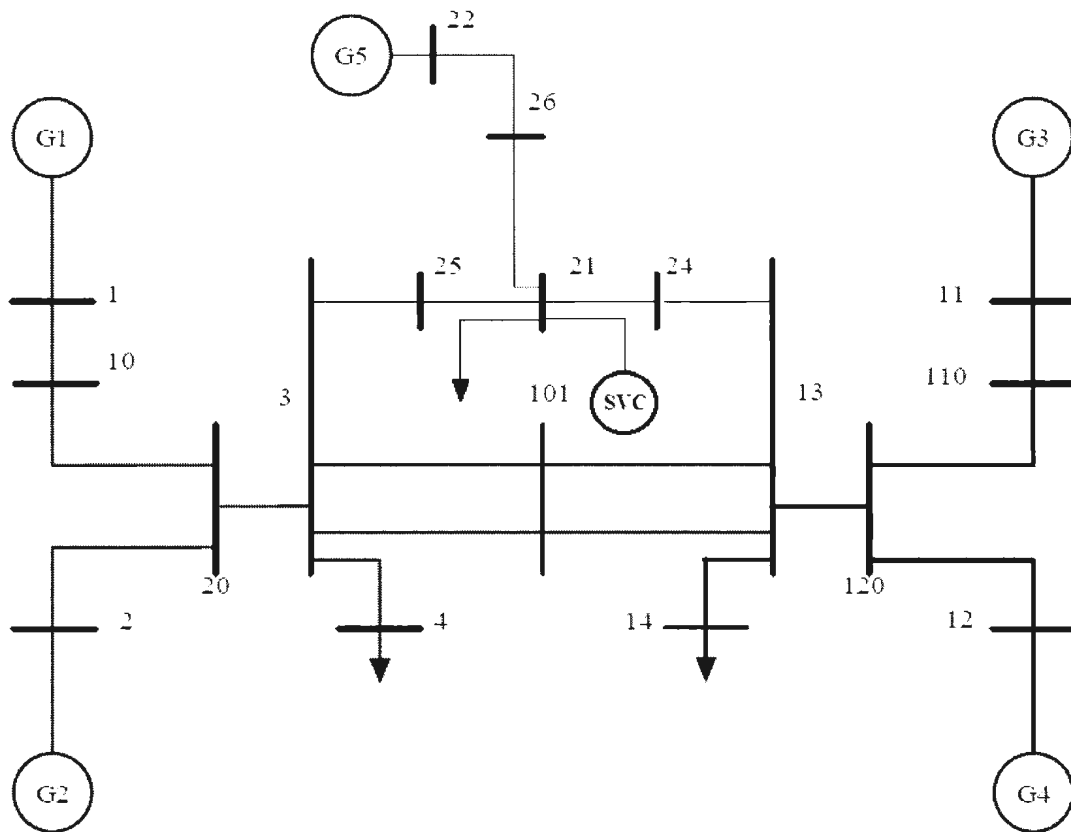


Figure 5.11 Single Line Diagram of a Two-Area with Added Load Area System [31]

The system steady state real and reactive power generations and loads are summarized in the appendix.

The Power System Toolbox based on MATLAB was used to conduct this case study. A three-phase to ground fault is assumed to occur at Bus 25 on the line 25-3 at 0.1 seconds, and the fault is cleared by itself after 0.07 seconds. The voltage at Bus 25 and the rotating speed deviation between Generator 4 and Generator 5 are monitored. (Bus 25 is the closest bus to the fault position, and the Generator 5 is the generator with the smallest inertia.) The results are presented in Figures 5.12 and 5.13.

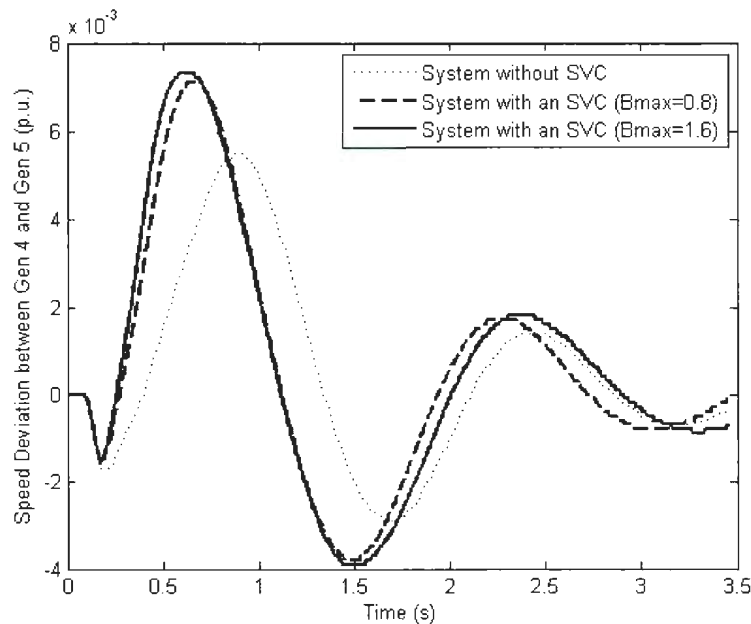


Figure 5.12 Rotating Speed Deviation between Generator 4 and Generator 5 for Two-Area with Added Load Area System with a Fault on the line 25-3 and Fault Clearing Time 0.07 seconds

Figure 5.12 indicates that, with a fault cleared after 0.07 seconds, the generator rotor speeds deviations grow larger at first, but decrease with oscillations as time grows. All the

three scenarios are stable ones. Adding an SVC enlarges the oscillation, but does not influence the rotor angle stability.

However, as Figure 5.13 shows, the voltage at Bus 25 sags severely to below 0.6 per unit after the fault is cleared if no reactive power support coming from the SVC. The Bus 25 voltage stays below 0.8 per unit for more than 0.5 seconds, indicating severe unacceptable voltage sag. It remains around 0.88 per unit even after the recovering process, leading to a quite vulnerable post-fault system. Voltage collapse and instability may occur subsequently if the voltage remains at so low a level. This instable situation can be greatly improved by some reactive compensation from a SVC at Bus 21. An SVC with the maximum susceptance 0.8 per unit (100 MVar base) reduces the voltage sag to less than 0.2 per unit. An SVC with the maximum susceptance 1.6 per unit performs even better, boosting the voltage more quickly and smoothing it better than the 0.8 per unit one. Therefore, from the above discussion, with the help of SVCs, the voltage stability and transient stability of the system have been greatly enhanced.

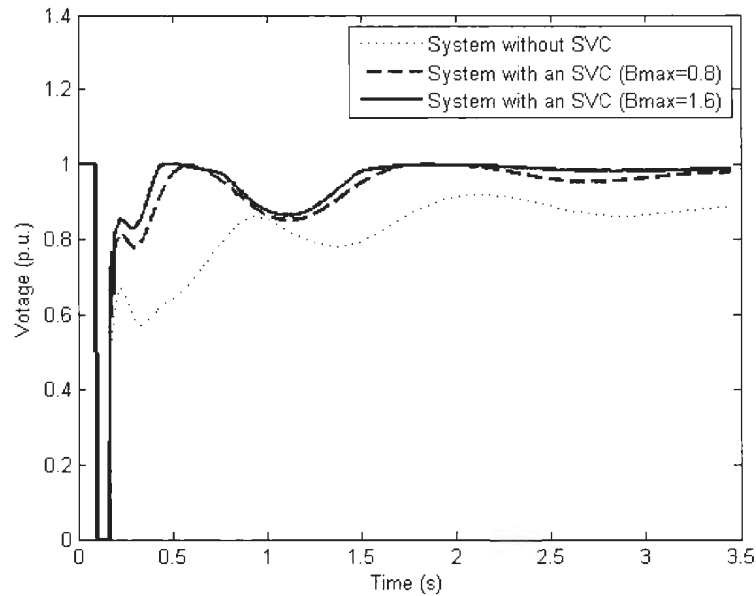


Figure 5.13 Voltage Variations at Bus 25 for Two-Area with Added Load Area System with a Fault on the Line 25-3 and Fault Clearing Time 0.07 Seconds

More evaluations can be done regarding to the critical fault clearing time. For the Power System Toolbox software, transient stability simulations are conducted assuming that all faults are cleared by themselves. The CCT values illustrate the stability margins and reflect the system stability performances under different scenarios.

Table 5.2 Critical Clearing Time Summary for Two-Area with Added Load Area System

with a fault on the line 25-3

Scenario Description	System with Excitation without SVC	System with an SVC ( $B_{SVCmax} = 0.8$ )	System with an SVC ( $B_{SVCmax} = 1.6$ )
CCT (ms)	280	390	410
Cycle	16.8	23.4	24.6

Table 5.2 illustrates how the excitation systems and the SVCs improve the power system transient stability for the Two-area with Added Load Area system. This system is hard to maintain stable, providing a three phase to ground solid fault occurs on line 25-3, without the help of the excitation systems in the generators. Though the generators may at least return to synchronism state by the voltage regulation function of the excitation systems, the post-fault voltage level at Bus 25 is quite low, which is unwanted. However, by connecting a SVC at Bus 21, the Bus 25 post-fault voltage can be greatly improved, and more time for fault clearing is allowed. In table 5.2, the system with  $B_{SVCmax} = 1.6$  SVC has the largest critical clearing time, but only 1.2 cycles larger than the one with  $B_{SVCmax} = 0.8$  SVC. Although it is obvious that a system with larger SVCs will have better transient stability performance, from the economical point of view, smaller SVCs with acceptable performance may be sufficient to tackle most of problems.

The SVC parameters are listed in Table 5.3.

Table 5.3 Summary of SVC parameters at Bus 21 for Two-Area with Added Load Area System

Bus Number	SVC Base (MVA)	Maximum Susceptance (p.u.)	Minimum Susceptance (p.u.)	Regulation Gain $K_r$ (p.u.)	Regulation Time Constant $T_r$ (p.u.)
21	100	0.8 or 1.6	0	50	0.02

## 5.6 Conclusion

This chapter has introduced the concept of Flexible AC Transmission System, and discussed the configurations, characteristics and the applications of Static Var Compensators. SVCs greatly improve the transient stability performance in power systems. Two case studies are presented to illustrate the effects of SVCs, and it is concluded that SVCs enable power systems to have larger transient stability margins and better dynamic performance.

## **Chapter 6**

# **Static VAR Compensator (SVC) Allocation and its Influence on Transient Stability Improvement**

### **6.1 Introduction**

Chapter 5 introduced the benefits of Static VAR Compensators (SVCs) to power system transient stability enhancement. In this chapter, such influence is discussed in detail. Different allocation of SVC results in varied system performance after large disturbances. For simple systems, the SVC allocation can be decided by weak buses which may lead to stability problems. For larger systems, a SVC allocation method based on simplified sensitivity analysis is studied. Two case studies are also provided using the New England 39 bus system.

## 6.2 Transient Stability Improvement Function of SVC

The adding of SVCs into power systems can enhance the power system transient stability. Chapter 5 introduced two case studies to demonstrate this by showing the increase of the system transient stability margin. Various studies have been developed to further explore ways to improve the SVCs' effect on transient stability enhancement. Reference [32] and [33] demonstrate the improvements of SVC's control algorithm: fuzzy logic controller is applied to better control the non-linear dynamic systems in order to improve transient stability performance. Reference [34] and [35] discuss how an optimized SVC allocation improves the transient stability. They mainly focus on the increase of transient stability margin and on a wider-range of fault clearing times.

A new and serious problem regarding the power system transient stability has been the focus of researchers: the transient voltage sag during the power system recovering process following a fault clearing. Many studies discuss this problem and its possible solutions. SVC is a useful tool to eliminate such voltage sag and help to enhance the power quality. The transient voltage dip/sag criteria related to the power system stability is introduced in detail in reference [36]. It emphasizes two power system stability criteria: First, the system should survive; second, the power quality should be maintained. The WECC (Western Electricity Coordinating Council) planning standard is one of the

significant standards explained in [36] to regulate the acceptable short-term voltage sag following a fault clearing. Reference [37] is the published document describing this standard specifically. Figure 6.1 shows the definition of the voltage sag/dip graphically.

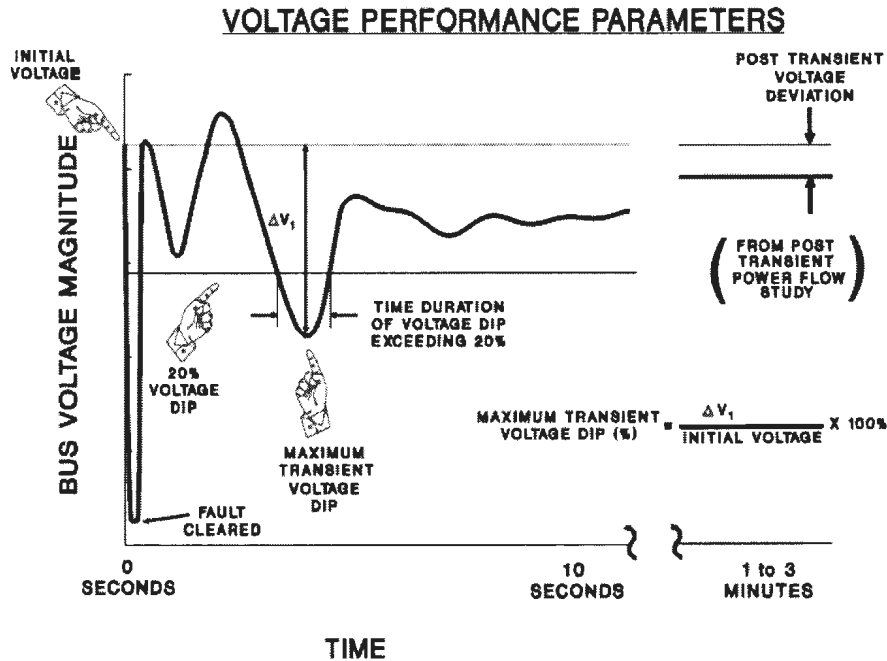


Figure 6.1 Transient Voltage Dip Definition for WECC Criteria [37]

As Figure 6.1 indicates, the maximum transient voltage dip equals the deviation between the lowest voltage value after the fault clearance and the initial voltage divided by the initial voltage.

$$\text{Maximum Transient Voltage Dip (\%)} = \frac{\Delta V_1}{\text{Initial Voltage}} \times 100\%. \quad (6.1)$$

The 20% voltage dip line shows that the voltage drops to 80% of the initial value.

These voltage sags do not appear at each bus, but load centers which are remote from generation units are generally more vulnerable and more easily to incur long time voltage sag as the generator excitation systems have less of an effect on them. The WECC Planning Standard introduced and interpreted in [36] and [37] specify that the angle stability bus voltage dip/sag following fault(s) clearing should satisfy these two main regulations:

- North American Electric Reliability Corporation (NERC) Category B: With an event or fault leading to the loss or failure of one single power system element, the non-load buses voltage dip/sag should not exceed 30%, and the dip/sag should not exceed 25% at the load buses. A voltage dip/sag must not exceed 20% for more than 20 cycles (0.33 seconds in 60 Hz system) at load buses.
- NERC Category C: With events or faults leading to the loss or failure of multiple power system elements, the voltage dip/sag should not exceed 30% at any bus, and not exceed 20% more than 40 cycles (0.67 seconds in 60 Hz system) at load buses.

These two regulation standards are widely used in research on transient bus voltage evaluations, as well as in this thesis.

The post fault voltage dip/sag problem has become a core issue for power companies and researchers, and the aforementioned standard provides a guide to improve this problem.

### 6.3 SVC Allocation

Research has demonstrated the effect of SVC on the post fault voltage performance. However, deciding where to put those SVCs is a crucial task to perform. Due to space and device requirements, SVCs can only be built in substations, which are represented as buses in the power system single line diagrams. They cannot be set in the middle of a transmission line since it requires a new substation. In addition, reactive power compensation at every bus is impossible, because the budget is limited and the maintenance is costly. Hence, the SVC allocation problem - where to put SVCs - should be decided carefully.

Reference [38] also compares two cases where SVCs are set at different buses of an 11 bus system, and it concludes that the SVCs help to improve the system transient voltage sag only at specific buses. While at other buses, setting a SVC has no effect on improving power system transient voltage sag. In other words, when aiming to eliminate post fault voltage sags during a power system planning and design, the SVC allocation plan is important.

For simple systems, the SVC allocation decision can be made by finding “weak points” in vulnerable areas where faults may lead to instability or voltage sag problems

that violate the WECC planning standard. For complex systems, systematic design algorithms are needed.

A case study on a Two-Area with Added Load Area System was conducted to explore how to set SVCs in simple systems by finding “weak points” in stability vulnerable areas. The trial and error method can be employed. However, in this chapter, the method of sensitivity analysis is emphasized. The following sections explain it in detail and exemplify it by two case studies on the New-England 39 - Bus system.

## **6.4 Allocation of SVCs by Sensitivity Analysis**

### **6.4.1 Sensitivity Analysis and its Simplification**

As discussed in Section 6.3, it is possible for a simple system to achieve a SVC design scheme by finding specific weak points and testing them. A design may be available to successfully protect the whole system from voltage sag problems and instability at every possible contingency. However, for larger systems, this becomes difficult and complex. In most cases, it is impossible to design an SVC scheme to prevent any instable case caused by every single contingency since the price for this type of design is huge. Realistically, the allocation of SVCs for transient stability enhancement

should consider many factors, such as the budget limitations and geographic conditions. Therefore, only significant contingency points should be considered instead of every spot in the power grid, and the geographic feasibility of the potential SVC positions should also be evaluated.

Much literature approaches the large system SVC allocation problems by converting them to mixed integer trajectory optimization problems [39], [40]. Those nonlinear problems require a large amount of complex calculations. For each significant contingency, sensitivity analysis is conducted to determine effective SVC positions, and the whole problem is optimized by non-linear programming method. Based on the optimization idea, reference [41] proposes that the specific power system SVC position planning can be simplified by combining the numerical approximation of sensitivity analysis and real time simulations. In this thesis, such method is applied and modified by employing a new total sensitivity index which combines both the voltage sag rate sensitivity index and the voltage sag time duration sensitivity index. It can solve the SVC optimal allocation problem faster with fewer calculations, and it also serves as an efficient way to verify the effect of the SVCs set in power grids on transient voltage sag reduction.

## 6.4.2 Calculation of Sensitivity Index

In this method, the two significant sensitivity indices required are the voltage sag rate sensitivity index and the voltage sag time duration sensitivity index. The SVC allocation decision will be made based on those indices. This method is explained in detail below.

The voltage sag duration is decided by the time that the sag begins and the time that it ends. According to the WECC planning standard and Figure 6.1, the sag beginning time is the instant that the voltage drops to below 80 % of the initial voltage. The sag ending time is the one that the voltage recovers to above 80 % of the initial voltage again. If the sag recovers slowly and does not ever rise to a more than 80 % level at the first recovery swing, the sag beginning time should adopt the fault clearing time, as Figure 6.2 shows.

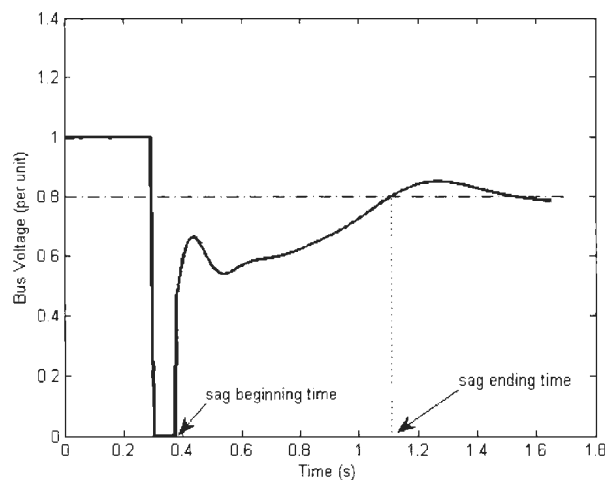


Figure 6.2 Voltage Sag Duration in Slow Recovery Case [41]

If the sag beginning time  $t_1$  and the ending time  $t_2$  are found, the sag duration, is  $t_{sag} = t_2 - t_1$ , which indicates the period that the voltage drops to less than 80% of the initial one and should be kept within 0.33 seconds according to the WECC standards. The maximum transient voltage dip/sag in Figure 6.1 is  $V_{msag} = \frac{V_0 - V_{min}}{V_0} \times 100\%$ , in which  $V_0$  is the initial voltage and the  $V_{min}$  is the voltage value at the maximum voltage sag point. If a  $V_{msag}$  value exceeds 30% for a non-load bus and 25% for a load bus, the corresponding bus transient voltage sag should be eliminated. The sensitivities of the voltage sag time duration and the maximum sag voltage towards the SVC capacitive limit are as formulae (6.1) and (6.2) [41].  $B_{SVC}$  is the susceptance of the SVC installed.  $t_{max\_sag}$  is the time when the transient voltage sag reaches its maximum value.

$$S_t \equiv \frac{\partial t_{sag}}{\partial B_{SVC}} = \frac{\partial(t_2 - t_1)}{\partial B_{SVC}} = \frac{\partial t_2 - \partial t_1}{\partial B_{SVC}}; \quad (6.1)$$

$$S_V \equiv \frac{\partial V_{msag}}{\partial B_{SVC}} = -\frac{\frac{\partial V_{min}}{\partial B_{SVC}}}{V_0} = -\left(\frac{\partial V}{\partial B_{SVC}} \Big|_{t = t_{max\_sag}}\right)/V_0. \quad (6.2)$$

$S_t$  is the voltage sag time duration sensitivity index which represents how the variation of the SVC susceptance at some bus influences the voltage sag time duration.  $S_V$  is the voltage sag sensitivity index which indicates the effect of such SVC susceptance on the bus maximum voltage sag point. The numerical approximation formulas can be obtained by replacing the partial differential calculation with the algebraic calculations which are convenient to implement. This reduces calculation complexity and saves storage space.

$$S_t = \frac{\partial t_{sag}}{\partial B_{SVC}} \approx \frac{\Delta t_{sag}}{\Delta B_{SVC}} = \left| \frac{t'_{sag}(B_{SVC} + \Delta B_{SVC}) - t_{sag}(B_{SVC})}{\Delta B_{SVC}} \right|; \quad (6.3)$$

$$S_V = \frac{\partial V_{msag}}{\partial B_{SVC}} \approx \frac{\Delta V_{msag}}{\Delta B_{SVC}} = \left| \frac{V'_{msag}(B_{SVC} + \Delta B_{SVC}) - V_{msag}(B_{SVC})}{\Delta B_{SVC}} \right|. \quad (6.4)$$

$t'_{sag}(B_{SVC} + \Delta B_{SVC})$  is the transient voltage sag duration when the susceptance of the SVC is  $(B_{SVC} + \Delta B_{SVC})$ ;  $t_{sag}(B_{SVC})$  is the corresponding value for the case that the susceptance is  $B_{SVC}$ .  $V'_{msag}(B_{SVC} + \Delta B_{SVC})$  is the maximum voltage sag for the SVC whose susceptance is equal to  $(B_{SVC} + \Delta B_{SVC})$ ; while  $V_{msag}(B_{SVC})$  is for the one with susceptance  $B_{SVC}$ . Through analyzing the sensitivity indices obtained by (6.3) and (6.4) [41], the SVCs' allocation and the capacities can be decided. Real time simulations are also employed to verify the results.

### 6.4.3 Algorithm of the Fast SVC Allocation Method based on Simplified Sensitivity Analysis

The algorithm of this fast SVC allocation method based on simplified sensitivity analysis is summarized in Figure 6.3 as a flowchart. For a specific type of SVC whose  $K_r$  and  $T_r$  are fixed and whose  $B_{SVCmax}$  can be adjusted, the following stages are to decide the SVC allocation and the minimum value of the maximum limitation  $B_{SVCmax}$ .

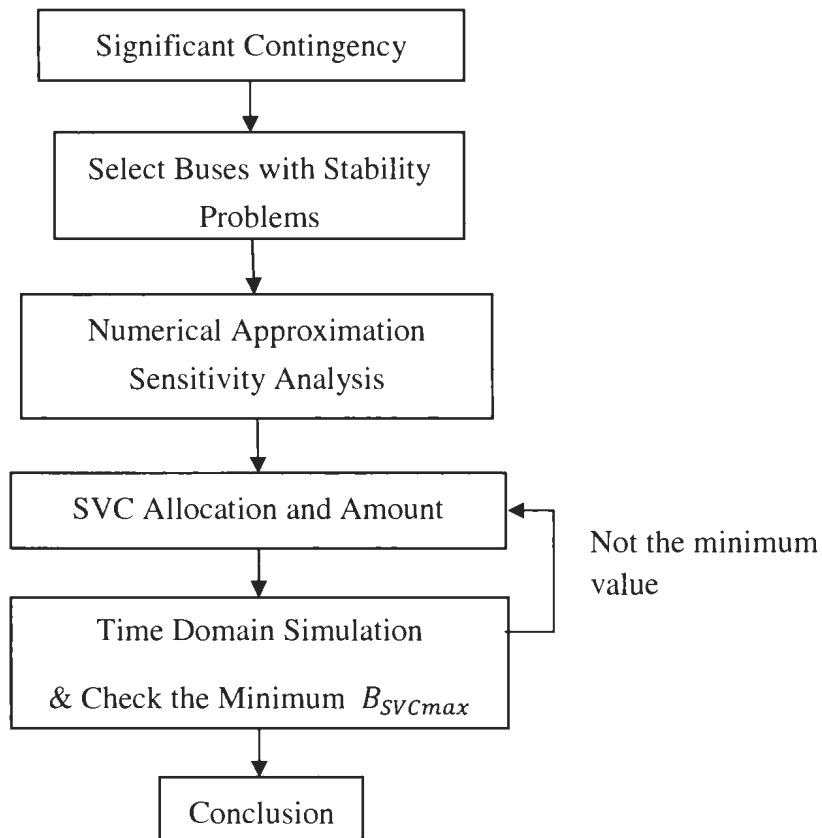


Figure 6.3 Flowchart of SVC Allocation Analysis

At the first stage, significant contingencies that cause transient voltage sag problems can be screened through simulations and analysis. Second, the weak buses with unsatisfactory voltages are picked out to conduct sensitivity analysis using the numerical approximation discussed in Section 6.4.2. Then, the SVC allocations can be primarily selected according to these results. Finally, the real time simulation is performed to test the SVCs' effect and regulate the minimum  $B_{SVCmax}$  value required. A case study on New England 39 - Bus System was conducted to illustrate this method.

## 6.5 Case Study: New – England 39 - Bus System [42]

This case study serves as an application example of the aforementioned fast SVC allocation method proposed in Section 6.4. The single line diagram of the New England 39 Bus System is presented in Figure 6.4.

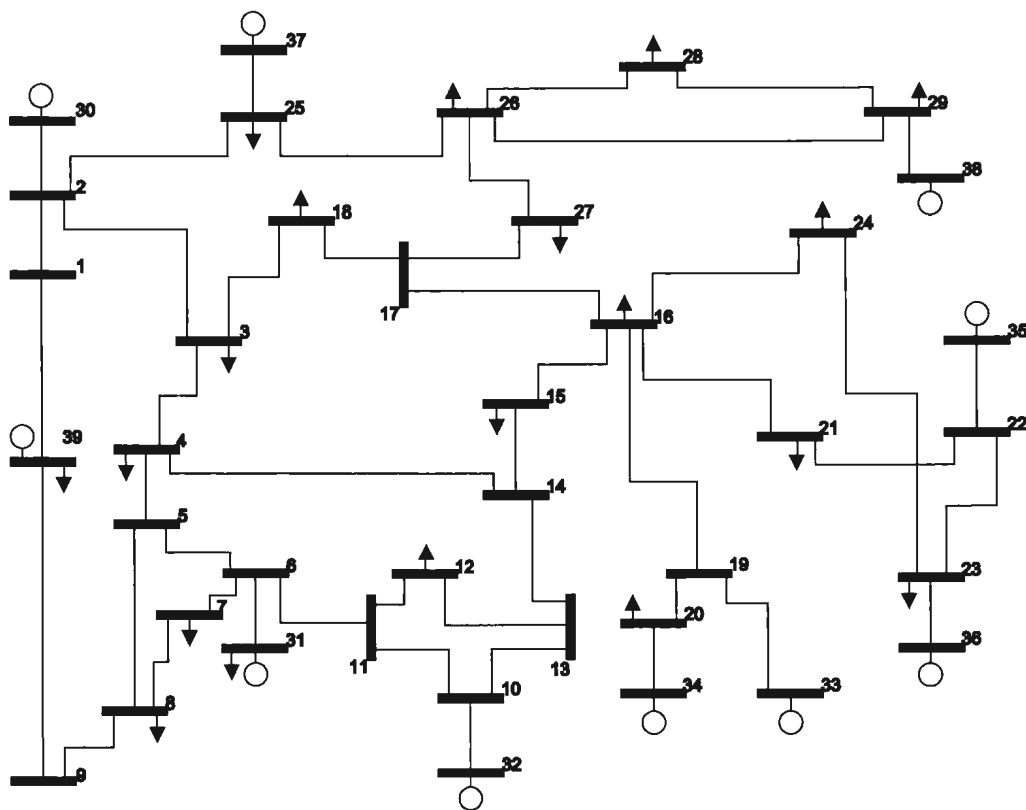


Figure 6.4 Single Line Diagram of the New England 39 Bus System

Two significant contingencies are studied: a contingency close to Bus 16 at Line 16-17, and a contingency close to Bus 21 at Line 21-22.

### 6.5.1 Contingency close to Bus 16 at Line 16-17

A typical significant contingency for this system is selected as a three-phase-to-ground solid fault close to bus 16 at line 16-17. For the contingency analysis, a typical fault clearing time of 0.1 second (6 cycles) is employed. Two typical bus voltages sags at Bus 14 and Bus 15 are shown as Figure 6.5.

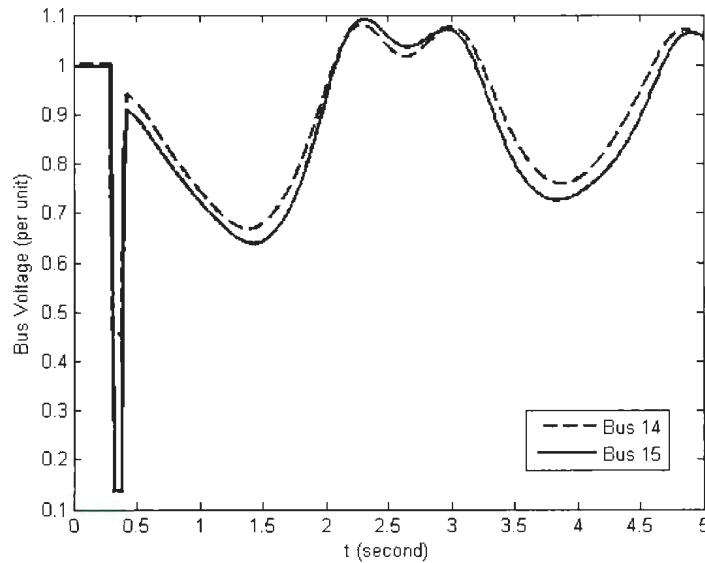


Figure 6.5 New England System without SVC Bus Voltage Sags with a Fault in Line 16-17 and Clearing Time 0.1 Seconds

Figure 6.5 shows the representatives of the bus voltage sags at Bus 14 and Bus 15 are severe. According to the simulation results, over 20% voltage sags at many buses last more than 0.33 seconds, and the bus voltages at some buses sag too much that exceed the

limits: 25% for load buses and 30% for non-load buses. The 19 buses that violate the WECC standard are Bus 4, 5, 6, 7, 8, 10, 11, 12,13,14,15, 16, 19, 20, 21,22, 24, 32, and 34. Their details and the sensitivity analysis results are listed in Table 6.1.

Table 6.1 New England System Voltage Sag and Sensitivity Index Summary  
with Contingency in Line 16 - 17

Bus Name	Voltage Sag (%)	Voltage Sag Time (s)	$S_V$	$S_t$	$S$
Bus 4 (Load Bus)	<u>28.66</u>	<u>0.85</u>	37.152	2.2	0.3469
Bus 5 (Non-load Bus)	27.86	<u>0.85</u>	34.218	1.9	0.3112
Bus 6 (Non-load Bus)	27.56	<u>0.825</u>	33.84	1.9	0.3091
Bus 7 (Non-load Bus)	27.90	<u>0.825</u>	31.482	1.8	0.2897
Bus 8 (Load Bus)	<u>27.91</u>	<u>0.825</u>	31.476	1.9	0.2962
Bus 10 (Non-load Bus)	28.68	<u>0.85</u>	42.41	2.3	0.3820
Bus 11 (Non-load Bus)	28.55	<u>0.820</u>	40.506	2.3	0.3717
Bus 12 (Load Bus)	<u>29.29</u>	<u>0.845</u>	64.148	3.4	0.5727
Bus 13	29.99	<u>0.860</u>	46.662	2.4	0.4117

(Non-load Bus)					
Bus14 (Non-load Bus)	<u>33.30</u>	<u>0.975</u>	56.246	2.5	0.4705
Bus 15 (Load Bus)	<u>35.85</u>	<u>1.105</u>	91.908	3.8	0.75
Bus 16 (Load Bus)	<u>30.87</u>	<u>1.025</u>	78.394	4.4	0.7160
Bus 19 (Non-load Bus)	25.33	<u>0.72</u>	70.348	6.5	0.8103
Bus 20 (Load Bus)	24.60	<u>0.76</u>	69.482	7.1	0.8451
Bus 21 (Load Bus)	<u>26.19</u>	<u>0.865</u>	70.972	6	0.7808
Bus 22 (Non-load Bus)	20.88	<u>0.38</u>	54.888	7.6	0.7986
Bus 24 (Load Bus)	<u>29.46</u>	<u>0.955</u>	79.834	5	0.7633
Bus 32 (Generator Bus)	21.61	<u>0.445</u>	N/A	N/A	N/A
Bus 34 (Generator Bus)	23.20	<u>0.72</u>	N/A	N/A	N/A

In this table, the data with underlines are the specific ones that fail to meet the WECC planning standard. The sensitivity indices  $S_t$  and  $S_V$  are calculated using formulae

(6.3) and (6.4) through real time simulations with a small  $\Delta B_{SVC} = 0.1$  per unit, and the total sensitivity index  $S$  combines the above two indices and is calculated by

$$S_{bus(i)} = \frac{S_{v,bus(i)}}{S_{v,maximum} \times 2} + \frac{S_{t,bus(i)}}{S_{t,maximum} \times 2}. \quad (6.5)$$

$S_{v,maximum}$  is the maximum voltage sag sensitivity index among those results.  $S_{t,maximum}$  is the maximum index regarding to voltage sag time durations.  $S_{bus(i)}$  falls into a range of [0,1]. Since the Bus 32 and Bus 34 are connected to generators, they are not included in the approach of adding SVCs to compensate reactive power. Improving the excitation systems would be a more direct and efficient way for them. Therefore, the calculation of sensitivity indices for them is meaningless, and the results in Table 6.1 for them are written as “not applicable”.

Through the sensitivity analysis, providing a contingency at line 16-17, it is noticed that the middle south part of the whole grid is weak in transient voltage. The top eight sensitive buses to SVC reactive power compensation with their total sensitivity indices are plotted from large to small in Figure 6.6.

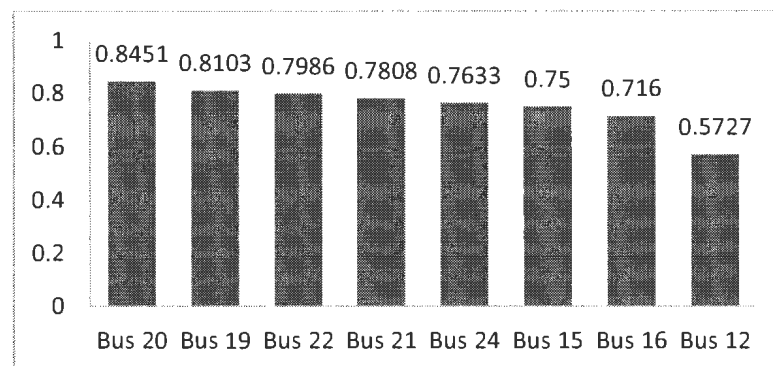


Figure 6.6 New England System Sensitive Buses with Sensitivity Indices for Fault on Line 16-17

It shows that the Bus 20, 19, 22, 21, 24, 15, 16, and 12 are the most sensitive buses to the reactive power compensation from a SVC. Therefore, these buses can be considered to set up SVCs.

Moreover, an SVC with larger susceptance will cost more, and building more SVCs in different buses needs extra investment on the site constructing. Therefore, an economical and efficient SVC allocation design should contain the least buses and use the least susceptances.

For the first design, one SVC is considered, which requires the least site constructing cost. Bus 20 with the highest total sensitivity index is chosen and the parameters are summarized as Table 6.2. The maximum susceptance is adjusted to a minimum value which can help the bus voltages just meet the standard in order to save costs.

Table 6.2 Summary of SVC Allocation Plan I for the New England System with a fault on line 16-17: One

SVC at Bus 20

Bus Number	SVC Base (MVA)	Maximum Susceptance (p.u.)	Minimum Susceptance (p.u.)	Regulation Gain $K_r$ (p.u.)	Regulation Time Constant $T_r$ (p.u.)

20	100	1.1	0	50	0.05
----	-----	-----	---	----	------

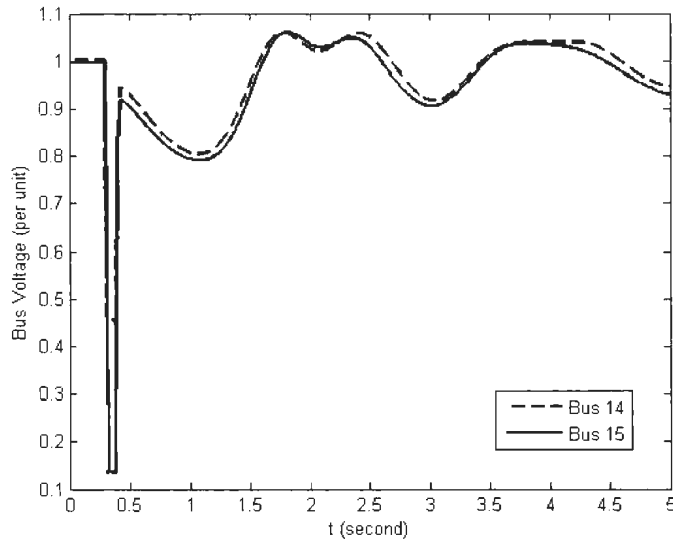


Figure 6.7 New England System with a SVC (at Bus 20) Bus Voltage Sags with a Fault in Line 16-17 and

Clearing Time 0.1 Seconds

Figure 6.7 shows the voltage curves at Bus 14 and Bus 15 after setting the SVC at Bus 20, providing the same contingency condition as before. Compared to Figure 6.5, the voltage sags are greatly improved. Simulation results also indicate that the severest transient bus voltage sag rate among those 39 buses is 20.44 % at Bus 15, and its sag time (down to less than 80%) duration is 0.325 seconds. It is also the only bus voltage that sags over 20%. All the bus voltage performances satisfy the WECC standard. Therefore, the transient voltage sag problem for this system as a fault at line 16-17 can be effectively and economically solved by setting an SVC with  $B_{max} = 1.1 p.u.$  at Bus 20.

Another design that chooses more than one SVC is also considered. In this case, if two or more SVC locations are chosen, a concept of “electrically close” should be proposed. If two buses are electrically close to each other that the reactive power compensation at one bus can also effectively support the other bus, it is unnecessary to repeat setting SVCs at all those buses, even their sensitivity indices are equally high. The SVC at one bus may be enough to benefit the electrically adjacent buses.

For this case, besides Bus 20, another SVC can be set at Bus 15, whose total sensitivity index is also high but is electrically far from Bus 20. Table 6.3 gives the best combination of maximum susceptance values for these two SVCs. The total susceptances reduce from 1.1 per unit to 0.9 per unit. However, two SVCs instead of one may need extra investment on site constructing and device setting. The “One SVC Design” may still own its merit.

Table 6.3 Summary of SVC Allocation Plan II for the New England System with a Fault in Line 16-17 and

Clearing Time 0.1 Seconds: Two SVCs at Bus 20 and 22

Bus Number	SVC Base (MVA)	Maximum Susceptance (p.u.)	Minimum Susceptance (p.u.)	Regulation Gain $K_r$ (p.u.)	Regulation Time Constant $T_r$ (p.u.)
20	100	0.7	0	50	0.05

15	100	0.2	0	50	0.05
----	-----	-----	---	----	------

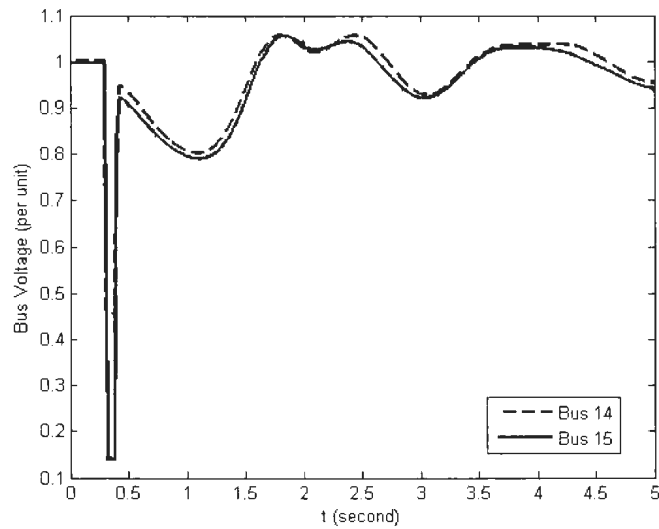


Figure 6.8 New England System with SVCs (at Bus 20 and 15) Bus Voltage Sags with a Fault in Line 16-17 and Clearing Time 0.1 Seconds

Figure 6.8 shows Bus 14 and Bus 15 voltage performances as representatives at this fault condition with SVCs at Bus 20 and 15. It indicates that the voltage sags in Figure 6.5 are also improved by this two SVC design. In this case, the only voltage sag rate over 20% is 20.49% at Bus 15 with time duration 0.33 seconds.

### 6.5.2 Contingency close to Bus 21 at Line 21-22

In order to evaluate the simplified sensitivity analysis method with more scenarios, a second contingency case can be conducted: a fault close to Bus 21 at Line 21-22. The

fault was applied at 0.3 seconds, and removed by disconnecting the Line 21-22 after 0.1 seconds (6 cycles). The Bus 21 and Bus 24 voltage curves without SVC in this system are presented in Figure 6.9.

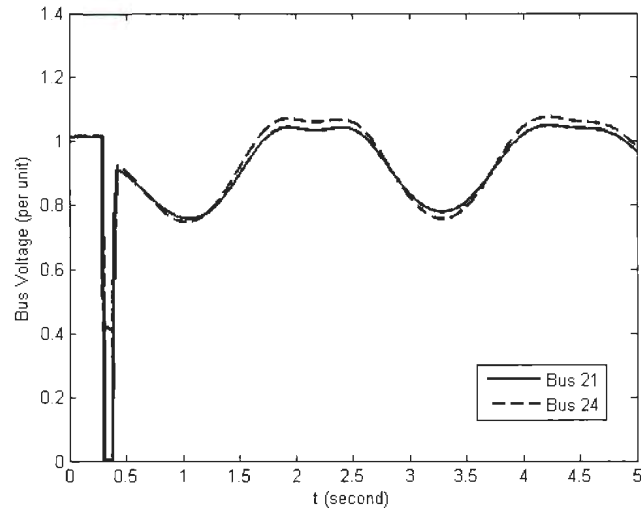


Figure 6.9 New England System without SVC Bus Voltage Sags with a Fault in Line 21-22 and Clearing  
Time 0.1 Seconds

As Figure 6.9 shows, the representative Bus 21 and Bus 24 voltages sag severely. Other buses whose voltage criteria fail to meet the WECC standards are also screened and listed with underlines below the unsatisfactory data. Those sensitivity data were evaluated by the simplified sensitivity analysis as Section 6.5.1. Table 6.4 shows the results.

Table 6.4 New England System Voltage Sag and Sensitivity Index Summary

with Contingency in Line 21-22

Bus Name	Voltage Sag (%)	Voltage Sag Time (s)	$S_V$	$S_t$	$S$
Bus 15 (Load Bus)	22.4350	<u>0.455</u>	28.002	2.2	0.6352
Bus 16 (Load Bus)	23.6402	<u>0.52</u>	27.222	1.6	0.5383
Bus 21 (Load Bus)	<u>25.2521</u>	<u>0.59</u>	39.136	2.2	0.7592
Bus 23 (Non-load Bus)	22.5933	<u>0.365</u>	44.918	3.4	1
Bus 24 (Load Bus)	<u>26.3029</u>	<u>0.585</u>	36.368	1.8	0.6695

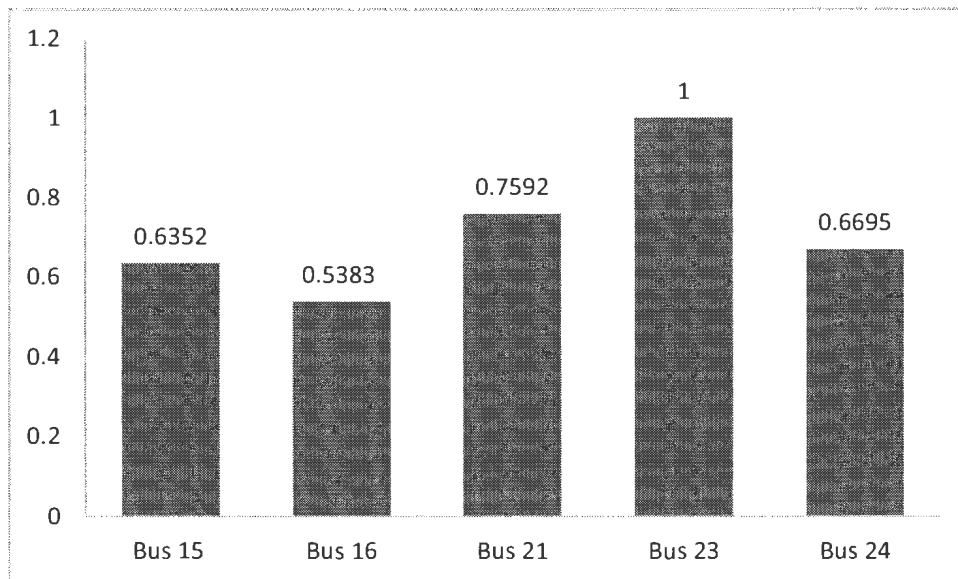


Figure 6.10 New England System Sensitive Buses with Sensitivity Indices for Fault in Line 21-22

Figure 6.10 presents all the sensitivity indices on the buses with unacceptable voltage performances after the fault. Bus 23 has the highest sensitivity index, so it should have the first priority to set an SVC. Real time simulations validate this conclusion and the minimum  $B_{SVCmax}$  can also be decided. Table 6.5 shows the most helpful and economical  $B_{SVCmax}$  in this scenario.

Table 6.5 Summary of SVC Allocation Plan for the New England System with a Fault in Line 21-22 and Clearing Time 0.1 Seconds: an SVC at Bus 23

Bus Number	SVC Base (MVA)	Maximum Susceptance (p.u.)	Minimum Susceptance (p.u.)	Regulation Gain $K_r$ (p.u.)	Regulation Time Constant $T_r$ (p.u.)
23	100	0.65	0	50	0.05

With a maximum susceptance 0.65 per unit at Bus 23, all the bus voltages in this system maintain in the acceptable boundary in this fault case.

Simulations show that if Bus 21 whose sensitivity is the second largest is selected instead of Bus 23, larger  $B_{SVCmax}$  will be needed. And extra reactive power support at Bus 24 is also unavoidable, since the SVC at Bus 23 has limited effect on the Bus 24 voltage sag improvement. Therefore, it verifies the conclusion again that the most effective and economical design is setting an SVC at Bus 23. The largest three voltage sag rates and duration times after employing an SVC at Bus 23 are plotted as Figure 6.11 and Figure 6.12.

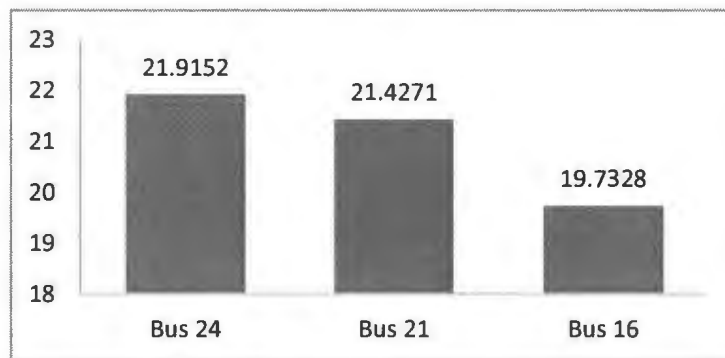


Figure 6.11 New England System Largest Bus Voltage Sag Rates with SVC at Bus 23

(Contingency in Line 21-22, Fault Clearing Time 0.1 seconds)

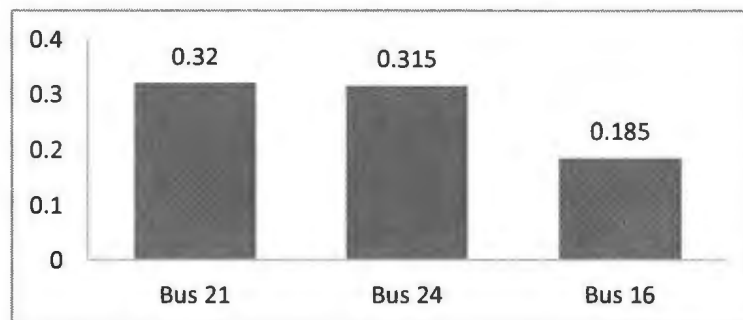


Figure 6.12 New England System Largest Bus Voltage Sag Time Durations with SVC at Bus 23

(Contingency in Line 21-22, Fault Clearing Time 0.1 Seconds)

Figure 6.11 and 6.12 both show that all the voltage sag rates are less than 25% at buses, and the voltage sag time durations are no more than 0.33 seconds, indicating the results are all satisfactory. The bus voltage performances at Bus 21 and 24 after setting the SVC are shown in Figure 6.13. It indicates that the voltage sags are eliminated by the SVC at Bus 23.

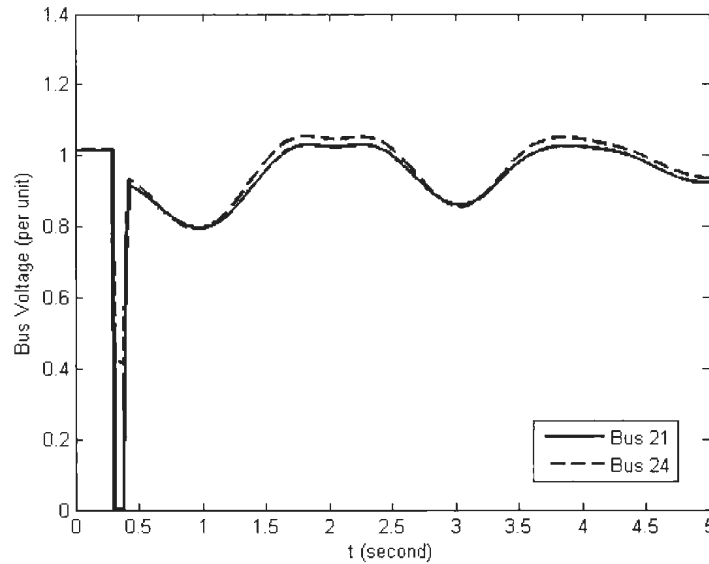


Figure 6.13 New England System with an SVC (at Bus 23) Bus Voltage Sags with a Fault in Line 21-22

and Clearing Time 0.1 Seconds

### 6.5.3 Other Severe Contingencies

In this research, the fault at Line 16-17 and Line 21-22 are selected and discussed as the above sections present. These two typical contingencies demonstrate the SVCs' contribution on the transient voltage sag problems well. Other contingencies that are also severe and serve as potential threats for this 39 - Bus power system are listed in the following table. The lines that connect the generators to the transmission grid are not included, for the faults along them cannot be simply eliminated by disconnecting the two ends of the transmission lines.

Table 6.6 Other Contingencies Threatening the New England System

with Fault Clearing Time 0.1 seconds

Contingency Position	Instability Description
1-2	unstable (Gen 10 first lose synchronism)
1-39	unstable (Gen 10 first lose synchronism)
2-25	voltage sag over time, unstable (Gen 8& 9)
25-26	Gen 9 lose synchronism
26-27	Gen 9 lose synchronism
26-28	Gen 9 lose synchronism
26-29	Gen 9 lose synchronism
28-29	Gen 9 lose synchronism

Similar analysis can be taken to design suitable SVCs to solve these problems as well. For example, the contingencies in the line 1-2 lead to the system instability, because that they cause the Generator 10 firstly lose synchronism. The Generator 10 is vulnerable and does not contain any excitation system. As faults occur close to Generator 10, the terminal voltage drop is severe and no voltage regulation is provided. The power produced in Gen 10 is much more than the power sent out, leading to the generator's fast acceleration. Finally, the generator rotor angle cannot return to the previous equivalent point or reach a new equivalent point, so the instability occurs. In order to design a SVC for this potential fault, the reactive compensation at the terminal of Gen 10 can be considered. For example, for a fault occurring close to Bus 1 in Line 1-2, an SVC at Bus 2 with minimum  $B_{SVCmax}$  can be chosen as the following table.

Table 6.7 Summary of SVC Allocation Plan for a Fault close to Bus 1

in Line 1-2 in New England System

Bus Number	SVC Base (MVA)	Maximum Susceptance (p.u.)	Minimum Susceptance (p.u.)	Regulation Gain $K_r$ (p.u.)	Regulation Time Constant $T_r$ (p.u.)
2	100	0.7	0	50	0.05

#### **6.5.4 Summary**

Two case studies based on the New England 39 - Bus System exemplify the method of allocating SVCs by simplified sensitivity analysis. This method is fast and effective. In the sensitivity index calculation, both voltage sag and voltage sag time duration sensitivities are included. The selection of SVC positions depends on the sensitivity index results and the “electrical distance” between buses: the buses with high sensitivity indices should be considered first, and selecting the buses which are electrically close to each other should also be avoided.

#### **6.6 Conclusion**

In this chapter, the allocation of SVC to improve transient voltage performance in power systems is discussed. In order to decide SVC positions for the sake of eliminating transient voltage sag problems, the simplified sensitivity analysis and a 39-bus system are explained and exemplified. For larger systems, sensitivity analysis simplified by numerical approximation gives quick answer with acceptable precision. By adding SVCs at proper positions, the transient voltage sag problems in power systems can be

successfully reduced, which also contributes to the maintenance of the power system stability.

# Chapter 7

## Conclusions and Future Work

### 7.1 Summary of the Thesis and Application of the Research

This thesis focuses on one of the threats on power systems' safety and reliability – Power system transient stability problem. It evaluates three methods to enhance it.

By clearing faults fast, more stability margins for generators to decelerate and maintain stability are available. Therefore, sensitive protection relays with less reacting time can be considered for power systems, and better sensors with well-design control algorithms are also helpful.

By applying excitation systems in generators, the generator terminal voltages can be monitored and regulated. Quickly boosting of these voltages enables the amount of electric power transmitted to increase, leading to less power imbalance in the generators. The generator acceleration processes can be mitigated. More margins are available for the fault detecting and relay reacting.

The Static Var Compensator (SVC) which belongs to the FACTS (Flexible AC Transmission System) family has good performance in improving power system transient

stability. In the remote load areas which are far from the generation units, the large disturbances such as severe faults can easily lead to voltage sag problems. SVCs are helpful to enhance the transient voltage performance for these load buses. A simplified sensitivity analysis is also presented to decide the SVC positions to fulfill this task. Simulations justify that such method is valuable with acceptable accuracy and it is also easy to implement.

The studies in this research can benefit the power system designing and planning. Ensuring the power system transient stability should be one of the targets of all the power system designing and optimization projects. It helps the power utilities to control large disturbances in power systems and avoid power outages and blackouts. The simplified sensitivity method also provides a way to decide SVC positions for the system transient stability enhancement, which serves as a quick and convenient way of SVC allocation.

## **7.2 Future Work**

Based on this research, additional work can be done for the sake of continuous studies. First, more methods can be considered and evaluated in the transient stability enhancement, such as introducing other preventive and corrective controls [43] and more FACTS devices. In addition, for the SVC allocation part, further work on exploring

methods for the large system SVC allocation design as a whole will be meaningful, and more studies on the possible lowest cost will be beneficial as well.

## References

- [1] C. P. Steinmetz, "Power control and stability of electric generating stations", *AIEE Trans.*, Vol. XXXIX, Part II, pp. 1215–1287, July 1920.
- [2] AIEE Subcommittee on Interconnections and Stability Factors, "First report of power system stability", *AIEE Trans.*, pp. 51–80, 1926.
- [3] P.Kundur, J.Paserba, V.Ajjarapu, G.Andersson, A. Bose, C.Canizares, N.Hatziargyriou, D. Hill, A.Stankovic, C. Taylor, T.V.Cutsem, and V.Vittal, "Definition and Classification of Power System StabilityIEEE/CIGRE joint task force on stability terms and definitions", *IEEE Trans. on Power Systems*, Vol.19, No.2, pp. 1387–1401, May 2004.
- [4] G. Andersson, P. Donalek, R. Farmer, N. Hatziargyriou, I. Kamwa, P. Kundur, N. Martins, J. Paserba, P. Pourbeik, J. Sanchez-Gasca, R. Schulz, A. Stankovic, C. Taylor, and V. Vittal, "Causes of the 2003 Major Grid Blackouts in North America and Europe, and Recommended Means to Improve System Dynamic Performance", *IEEE Trans. on Power Systems*, Vol.20, No.4, pp. 1922–1928, November 2005.
- [5] PowerWorld Simulator, Version 15, PowerWorld Corporation, Champaign, IL, USA, March 2011.
- [6] MATLAB, Version 7.10.0.499, Mathworks, Inc., USA, 2010.

- [7] Power System Toolbox (PST), Version 3.0, Joe Chow and Graham Rogers,  
Rensselaer Polytechnic Institute, USA.
- [8] G. W. Stagg and A. H. El-Abiad, *Computer methods in Power Systems*, New York:  
McGraw-Hill, 1968.
- [9] J. D. Glover, M. S. Sarma, T. J. Overbye, *Power System Analysis and Design*, 5<sup>th</sup> ed.  
Global Engineering, 2011.
- [10] I. Elgerd, *Electric Energy Systems Theory*, 2<sup>nd</sup> ed. New York: McGraw-Hill, 1982.
- [11] V. Vittal. “Transient Stability and Control of Large Scale Power Systems”, PSERC  
Background Paper, September, 2003.
- [12] R.Schainker, P. Miller, W. Dubbelday, P. Hirsch and G. Zhang. “Real-time dynamic  
security assessment: fast simulation and modeling applied to emergency outage  
security of the electric grid”, *IEEE Power and Energy*, Vol.4, No.2, pp. 51–58,  
March/April 2006.
- [13] T. Miki, D. Okitsu, E. Takashima, Y. Abe and M. Tano, “Power System Transient  
Stability Assessment Using Critical Fault Clearing Time Functions”, Transmission  
and Distribution Conference and Exhibition 2002: Asia Pacific. IEEE/PES, Vol.3, pp.  
1514–1517, October 2002.
- [14] PSCAD Webpage. Available at: <https://pscad.com/products>.
- [15] Power System Analysis Toolbox (PSAT) Webpage. Available at:  
<http://www.uclm.edu/area/gsee/Web/Federico/psat.html>.

- [16] Power System Toolbox Webpage. Available at:  
<http://www.ecse.rpi.edu/pst/PST.html>.
- [17] P. Kundur, *Power System Stability and Control*. New York: McGraw-Hill, 1994.
- [18] P. S. R. Murty, *Operation and Control in Power Systems*, 2<sup>nd</sup> ed. BS Publications, 2009.
- [19] S. Small, An application of Automatic Voltage Regulators to Transient Stability Study, ENGI 9847 Project Report, Memorial University of Newfoundland, 2007.
- [20] A. R. Bergen, V. Vittal, *Power System Analysis*, 2<sup>nd</sup> ed. Prentice Hall, 2000.
- [21] *IEEE Guide for Identification, Testing, and Evaluation of the Dynamic Performance of Excitation Control Systems*, IEEE Standard 421.2–1990.
- [22] R.C. Dorf, R. H. Bishop, *Modern Control Systems*, Upper Saddle River, NJ: Prentice Hall, 2005.
- [23] IEEE Committee Report, “Excitation System Models for Power System Stability Studies,” *IEEE Transactions of Power Apparatus and Systems*, vol. PAS-100, pp. 494–509, 1981.
- [24] N. G. Hingorani, “FACTS – Flexible AC Transmission System”, International Conference on AC and DC Power Transmission 1991, London, UK, pp. 1–7. Sept. 17–20, 1991.
- [25] A.-A. Edris, R. Adapa, M. H. Baker, L. Bohmann, K. Clark, K. Habashi, L. Gyugyi, J. Lemay, A. S. Mehraban, A. K. Myers, J. Reeve, F. Sener, D. R. Torgerson, and R.

- R. Eood, "Proposed terms and definitions for flexible AC transmission system (FACTS)," IEEE Trans. on Power Delivery, vol. 12, no. 4, pp. 1848–1853, Oct., 1997.
- [26] S. Chatzivasileiadis, T. Krause, and G. Andersson, "Flexible AC Transmission Systems (FACTS) and Power System Security – A Valuation Framework", Power and Energy Society General Meeting, 2011 IEEE, pp. 1–8, July 24–29, 2011.
- [27] M. Noroozian, Modeling of SVC in Power System Studies, ABB Inc., Sweden.
- [28] ABB Review, 5/1999, ABB Inc, Sweden .
- [29] N. G. Hingorani and L. Gyugyi, *Understanding Facts - Concepts and Technology of Flexible AC Transmission Systems*, 1<sup>st</sup> ed. Wiley-IEEE Press, 1999.
- [30] MATLAB Simulink SimPowerSystems Documentation, Version 2011b, Hydro Quebec, Quebec, Canada.
- [31] K. W. Cheung, J. Chow, and G. Rogers, Power System Toolbox Manual, Version 3.0, 2008.
- [32] T. Abdelazim, "Intelligent SVC control for transient stability enhancement", Power Engineering Society General Meeting, vol.2, pp. 1701–1707, 12–16 June 2005.
- [33] I. Mansour, D. O. Abdeslam, P. Wira, J. Merckle, "Fuzzy logic control of a SVC to improve the transient stability of ac power systems", Industrial Electronics IECON '09. 35th Annual Conference of IEEE, pp.3240–3245, 2009.

- [34] F. Qian, G. Tang, Z. He, "Optimal Location and Capability of FACTS Devices in a Power System by Means of Sensitivity Analysis and EEAC", Third International Conference on Electric Utility Deregulation and Restructuring and Power Technologies, pp. 2100–2104, 2008.
- [35] E. A. Zamora-Cardenas, C. R. Fuerte-Esquivel, L. Contreras-Aguilar, "Application of dynamic sensitivity theory to assess the thyristor-based FACTS controllers' effect on the transient stability of power systems", 2009 IEEE Bucharest PowerTech, pp. 1 – 7, 2009.
- [36] D. J. Shoup, J. J. Paserba, C. W. Taylor, "A Survey of Current Practices for Transient Voltage Dip/Sag Criteria Related to Power System Stability", IEEE PES Power Systems Conference and Exposition, vol.2, pp. 1140–1147, 2004.
- [37] NERC/WECC, "Planning Standards", April 10, 2003. Available at:  
<http://www.wecc.biz/library/Library/Planning%20Committee%20Handbook/WECC-NEERC%20Planning%20Standards.pdf>
- [38] L. Weng, B. Jeyasurya, "Effectiveness of VAR Sources for Power System Performance Enhancement", 2011 IEEE Electrical Power and Energy Conference (EPEC), pp. 368–373, 2011.
- [39] A. Tiwari, V. Ajjarapu, "Optimal Allocation of Dynamic VAR Support Using Mixed Integer Dynamic Optimization", IEEE Transactions on Power Systems, vol. 26, no.1, pp. 305–314, 2011.

- [40] A. Tiwari, V. Ajjarapu, “Optimal Allocation of Dynamic VAR for Enhancing Stability and Power Quality”, IEEE Power and Energy Society General Meeting - Conversion and Delivery of Electrical Energy in the 21st Century, pp. 1–7, 2008.
- [41] H. Liu, “Planning reactive power control for transmission enhancement”, PhD thesis, Iowa State University, 2007.
- [42] X. Lu and B. Jeyasurya, “Static VAR Compensator Allocation by Simplified Sensitivity Analysis and its Influence on Transient Voltage Performance Improvement”, 44th North American Power Symposium, September 9–11, 2012.
- [43] I. Genc, R. Diao, V. Vittal, S. Kolluri, and S. Mandal. “Decision tree-based preventive and corrective control applications for dynamic security enhancement in power systems”, *IEEE Trans. on Power Systems*, Vol.25, No.3, August, 2010, pp.1611–1619.

## Appendix A: One Generation Station towards Infinite Bus System Data

[17]

The generator model is a GENROU model whose base is 2220 MVA, with the following parameters:

$$X_d = 1.81, X_q = 1.76, X'_d = 0.3, X'_q = 0.65, X''_d = 0.23, X''_q = 0.25, X_l = 0.15,$$

$$R_a = 0.003, T'_{d0} = 8.0 \text{ s}, T'_{q0} = 1.0 \text{ s}, T''_{d0} = 0.03 \text{ s}, T''_{q0} = 0.07 \text{ s}, H = 3.5, K_D = 0.$$

An IEEE Type ESAC4A Exciter model is chosen, and a STAB1 Stabilizer is employed, with parameters as below:

$$K_A = 200, T_R = 0.015 \text{ s}, T_A = 0.015 \text{ s}, V_{rmax} = 7.0, V_{rmin} = -6.4;$$

$$\frac{K}{T} = 9.5, T = 1.41 \text{ s}, T_1 = 0.154 \text{ s}, T_3 = 0.033 \text{ s}, H_{LIM} = 0.2.$$

## Appendix B: Nine - Bus System Data [5]

The generator model is a GENROU model whose base is 2220 MVA, with the following parameters:

$$X_d = 2.2395, X_q = 2.161, X'_d = 0.2995, X'_q = 0.4922, X''_d = 0.225, X''_q = 0.225,$$

$$X_l = 0.15, R_a = 0, T'_{d0} = 6.0 \text{ s}, T'_{q0} = 0.535 \text{ s}, T''_{d0} = 0.03 \text{ s}, T''_{q0} = 0.05 \text{ s},$$

$$H = 2.56, K_D = 0.$$

An IEEE1 Exciter model is chosen, and a STAB1 Stabilizer is employed, with parameters as below:

$$K_A = 20, T_R = 0 \text{ s}, T_A = 0.2 \text{ s}, V_{rmax} = 3.0, V_{rmin} = -3.0;$$

$$K_e = 1.0, T_e = 0.314, K_f = 0.063, T_f = 0.35, E_1 = 2.8, SE(E_1) = 0.3034,$$

$$E_2 = 3.73, SE(E_2) = 1.2884$$

$$\frac{K}{T} = 20, T = 1.4, \frac{T_1}{T_3} = 7, T_3 = 0.1, \frac{T_2}{T_4} = 35, T_4 = 0.02, H_{lim} = 0.1$$

## Appendix C: 500 kV Transmission System with Two Generation Units

### Data [6]

Generator 1 and Generator 2:

$$X_d = 1.305; X'_d = 0.296; X''_d = 0.252; X_q = 0.474; X'_q = 0.243; X_l = 0.18;$$

$$T'_d = 1.01; T''_d = 0.053; T''_{do} = 0.1; H = 3.7$$

SVC:  $X_s = 0.03$ ;  $K_i = 300$ ;

## Appendix D: Two - Area with Added Load Area System Data [7]

Loads:

Table: Summary of the Power in Two-Area with Added Load Area System

Power Generation in the Stations			Power Absorbed by the System		
Real Power (MW)	Reactive Power (MVar)		Real Power (MW)	Reactive Power (MVar)	
3098.81	1808.6		3000	400	

Generator 1, 2, 3, 4:  $S_{base} = 1000 \text{ MVA}$ ,  $R_a = 0.0025$ ;  $X_d = 1.8$ ;  $X'_d = 0.3$ ;  $X''_d = 0.25$ ;  $X_q = 1.7$ ;  $X''_q = 0.25$ ;  $X_l = 0.2$ ;

$T_{do}' = 8 \text{ s}$ ;  $T''_{do} = 0.03 \text{ s}$ ;  $T'_{q0} = 0.4 \text{ s}$ ;  $T''_{q0} = 0.05 \text{ s}$ ;  $H = 6.5 \text{ s}$

Generator 5:  $S_{base} = 1000 \text{ MV}$ ,  $R_a = 0.0025$ ;  $X_d = 1.8$ ;  $X'_d = 0.3$ ;  $X''_d = 0.25$ ;  $X_q = 1.7$ ;  $X''_q = 0.25$ ;  $X_l = 0.2$ ;

$T_{do}' = 5.0 \text{ s}$ ;  $T''_{do} = 0.03 \text{ s}$ ;  $T'_{q0} = 0.4 \text{ s}$ ;  $T''_{q0} = 0.05 \text{ s}$ ;  $H = 5.0 \text{ s}$

## Appendix E: New England 39 - Bus System Data [7]

Table 1 Characteristics of the 10-Generator, 39-Bus System

Numbers of Buses	39
Numbers of Lines	46
Numbers of Generators	10

Table 2 Generation Unit Summary

Generator Number	Inertia Constant H (s)	Real Power Generation (MW)	Reactive Power Generation (MVar)	Excitation System
1	4.2	250.0	167.07	DC Excitation
2	3.03	572.93	771.31	DC Excitation
3	3.58	650.0	241.84	DC Excitation
4	2.86	632.0	168.51	DC Excitation
5	2.6	508.0	194.59	DC Excitation
6	3.48	650.0	278.01	DC Excitation
7	2.64	560.0	138.38	DC Excitation
8	2.43	540.0	16.13	DC Excitation
9	3.45	830.0	19.26	DC Excitation
10	50.0	1005.29	162.53	No Excitation

Table 3 Load Summary

Bus Number	Real Power (MW)	Reactive Power (MVar)
------------	-----------------	-----------------------

3	322.0	2.4
4	500.0	184.0
7	233.8	840.0
8	522.0	176.0
12	8.5	88.0
15	320.0	153.0
16	329.4	323.0
18	158.0	30.0
20	680.0	103.0
21	274.0	115.0
23	247.5	84.6
24	308.6	-92.2
25	224.0	47.2
26	139.0	17.0
27	281.0	75.5
28	206.0	27.6
29	283.5	126.9
31	9.2	4.6
39	1104.0	250.0

### **Research Papers Presented during the M.Eng. Program**

[1] X. Lu and T. Iqbal, "Dynamic Modeling and Simulation of a 10kW Wind Turbine with Pumped Hydro Energy Storage", Newfoundland Electrical and Computer Engineering Conference, St.John's, NL, Canada, November 1, 2011

[2] X. Lu and B. Jeyasurya, "Static VAR Compensator Allocation by Simplified Sensitivity Analysis and its Influence on Transient Voltage Performance Improvement", 44th North American Power Symposium, Urbana-Champaign, IL, the USA, September 9-11, 2012.

